# STIRRED WELL FILTRATION AS A HIGH-THROUGHPUT TECHNIQUE

# DEVELOPMENT OF STIRRED WELL FILTRATION AS A HIGH-THROUGHPUT TECHNIQUE FOR DOWNSTREAM BIOPROCESSING

By

AMIR SADEGH KAZEMI, B.Sc.

A Thesis Submitted to the School of Graduate Studies in Partial Fulfillment of the

Requirements for the Degree Master of Applied Science

**Descriptive Notes**

MASTER OF APPLIED SCIENCE (2014) McMaster University

(Chemical Engineering) Hamilton, Ontario

TITLE: DEVELOPMENT OF STIRRED WELL FILTRATION AS A HIGH-THROUGHPUT TECHNIQUE FOR DOWNSTREAM BIOPROCESSING

AUTHOR: Amir S. Kazemi, B.Sc. (Amirkabir University of Technology)

SUPERVISOR: Dr. David R. Latulippe

NUMBER OF PAGES: *CXI*, 111

## Abstract

Micro-scale processing (MSP) techniques are miniaturized version of upstream and downstream conventional unit operations that are designed to accelerate the pace of bioprocess design and development. Previous 'dead end' filtration studies have demonstrated the usefulness of this concept for membrane filtration processes. However, these experiments were performed without stirring which is the most common strategy to control the effects of concentration polarization and fouling on filtration performance.

In this work, the pressure-driven stirred conditions of a conventional stirred-cell module were integrated with a 96-well filter plate to develop a high throughput technique called 'stirred-well filtration' (SWF). The design allowed for up to eight constant flux filtration experiments to be conducted at once using a multi-rack programmable syringe pump and a magnetic lateral tumble stirrer. An array of pressure transducers was used to monitor the transmembrane pressure (TMP) in each well. The protein sieving behavior and fouling propensity of Omega™ ultrafiltration membranes were assessed via a combination of hydraulic permeability measurements and protein sieving tests in constant filtrate flux mode. The TMP profile during filtration of bovine serum albumin (BSA) solution was strongly dependent on the stirring conditions – for example the maximum TMP in the stirred wells were an average of 7.5, 3.8, and 2.6 times lower than those in the unstirred wells at filtrate fluxes of 12, 36, and 60 LMH (5, 15, and 25 μL/min) respectively. The consistency of the data across different wells for the same stirring condition was very good. To demonstrate the effectiveness of the SWF technique, the eight tests for a simple $2^2$ factorial design-of-experiments (DOE) test with duplicates was run to evaluate the effect of solution pH and salt concentration on protein filtration. The combination of SWF with statistical methods such

as DOE is shown to be an effective strategy for high-throughput optimization of membrane filtration processes.

In Memory of

Alireza Tohidi Gol

**Acknowledgments**

First and foremost, I would like to express my sincere gratitude to my supervisor, Dr. David Latulippe, for his continuous support and encouragement throughout my studies at McMaster University. I would like to thank Dr. Raja Ghosh for his aspiring guidance in the course of my project. I appreciate the help of my course instructors Dr. Younggy Kim, Dr. Raja Ghosh, Dr. Sarah Dickson and Mr. Kevin Dunn for their directions.

From the Department of Chemical Engineering, I would like to acknowledge all the administrative staff, especially Kathy Goodram, Lynn Falkiner, Cathie Roberts and Melissa Vasil for supporting me even prior to my arrival at McMaster University. I am thankful to Doug Keller and Justyna Derkach for their continuous efforts to provide a safe environment for my research. Many thanks to Paul Gatt and Dan Wright without whose involvement in the manufacture and setup of the experimental system completion of this work would have been difficult. Finally, I must acknowledge Prof. Singh and Dr. Eric Seidlitz from Faculty of Health Sciences for allowing me to use the BioTek PowerWave microplate reader for protein and volume measurements of this work.

The completion of this project would not have been possible without the help and support of my fellow researchers, colleagues and friends during the past 20 months. Special thanks to Hajir Mokhtari, Caroline Shang, Roozbeh Mafi, Pedram Madadkar, Ali Mohammad Rabea, Rahul Sadavarte, Jeff Cobbledick, Maryam Emami and Maryam Badv for their friendship, encouragement, and invaluable advice.

Last but not least, I would like to thank my parents, Maryam & Hamid, and my dear sister, Kimia, for their endless support and unconditional love throughout my life. I would also

like to express my gratitude to my aunt and uncle (Minou & Mahmoud), cousins (Rouzbeh, Sara, & Ali) and all my friends and relatives in the Greater Toronto and Hamilton Area who have been with me through thick and thin.

# Contents

# List of Figures

# List of Tables

# List of acronyms

ATPS: Aqueous two-phase system

CFD: Computational fluid dynamics

DAQ: Data acquisition board

DBC: Dynamic binding capacity

DMAC: Dimethylacetamide

DMF: Dimethylformamide

DMSO: Dimethylsulfoxide

DNA: Deoxyribonucleic acid

DO: Dissolved oxygen

DOE: Design of experiments

ELISA: Enzyme-linked immunosorbent assay

GA: Genetic algorithm

HCP: Host cell protein

HPLC: High performance liquid chromatography

HPLC-MS: High performance liquid chromatography–mass spectrometry

HT: High-throughput

LC-MS: Liquid chromatography–mass spectrometry

LMH: $\frac{\mathrm{L}}{\mathrm{m^2 hr}}$

mAb: Monoclonal antibodies

MF: Microfiltration

MSP: Micro-scale processing

NF: Nanofiltration

NOM: Natural organic matter

OD: Optical density

PA: Polyamides

PB: Phosphate buffer

PBS: Phosphate buffered saline

PCR: Polymerase chain reaction

PDMS: Polydimethylsiloxane

pDNA: Plasmid deoxyribonucleic acid

PEG: Polyethylene glycol

PES: Polyethersulfone

PS: Polysulfone

PTFE: Polytetrafluoroethylene

PVDF: Polyvinylidene fluoride

PVP: Polyvinylpyrrolidone

RNA: Ribonucleic acid

RO: Reverse osmosis

RSM: Response surface modeling

SWF: Stirred well filtration

UF: Ultrafiltration

WR: Working reagent

**Declaration of academic achievement:** The majority of this work will be published in an upcoming issue of the Journal of Membrane Science (A.S. Kazemi, D.R. Latulippe / Journal of Membrane Science 470 (2014) 30–39).

## Chapter 1. Introduction: Micro-scale processes

Recent advances in biotechnology and genetic engineering have offered many new technologies to produce bio-products such as therapeutic proteins which are capable of addressing illnesses with poor conventional treatments [1]. Such developments have generated new challenges in the field of purification of biological products to assure that the quality specifications as determined by regulatory agencies are met. The purification process should be developed considering both the economical restrictions and society requirements for production of new therapeutic products. In general, the complexities of real biological products makes it very difficult to predict the behavior of the product without empirical assessments of different process variables such as solution chemistry and hydrodynamic conditions. The main challenge associated with empirical assessment is the number of experiments needed to evaluate variable effects and their interaction under various circumstances. Performing multiple experiments could be costly, laborious and waste a lot of resources. Hence, there is a great interest in devising new high-throughput (HT) methods in order to speed-up the development of such purification processes [1–3].

Therapeutic proteins (e.g. recombinant Erythropoietin which helps the body to create more red blood cells) have been grown to a costly sector ($40 billion per annum) in the recent decades [1]. The conventional work-flow for development of these products is to perform large scale pilot experiments to evaluate the process and identify any changes required prior moving to a full-scale system. Such pilot-scale activities are very expensive and will generally delay the process

significantly, especially considering the existing complexities in downstream bioprocessing techniques [1,2]. Thus, extreme scale-down of such processes can be considered as an efficient solution to expedite the development of different products. Extreme scale-down can be defined as the use of devices which have a much smaller size than larger laboratory or industrial equipment but can represent these units at lower cost.

Micro-scale bioprocessing techniques are miniaturized version of upstream and downstream conventional unit operations which could be scalable to actual production conditions. There is considerable interest in the use of micro-scale processing (MSP) techniques for the development and optimization of biological processes [1,2,4] as well as chemical processes such as chemical reactions [5]. There are several advantages in developing MSP techniques. First, it reduces the material costs associated with running a large number of lab-scale or full-scale experiments especially in case of expensive materials such as pharmaceutical products. Second, MSP techniques could speed-up bioprocess development by doing parallel experiments which are ideally suited for HT screening and statistical methodologies such as design of experiments (DOE) for process optimization. This approach has been proven to be more efficient than the traditional sequential approach to process optimization. Third, it can be integrated with instrumentation for real-time monitoring of process performance and automated systems. Chhatre and Titchener-Hooker [2] outlined the drivers for micro-scale bioprocess engineering development as (1) financial and (2) process-related and regulatory. In terms of financial issues, micro-scale bioprocess engineering systems are usually considered to reduce the high resources needed for traditional development of a product when using laboratory and pilot-scale systems. It can also reduce the time needed for a product to enter the market as well as the financial penalty for the products which fail to enter the market. Regarding process-related and regulatory concerns, micro-

scale techniques can achieve rapid process understanding in the very early stages of process development to enhance the design and reduce the risk of the next phases of the development.

Recent advances in micro-fluidics and automation fields have offered an exceptional opportunity to minimize or even possibly eliminate the challenges associated with human intervention and manpower costs from bioprocessing development. Micro-scale studies can also be accompanied by mass transfer and flow regime analysis such as computational fluid dynamics (CFD) to evaluate the effect of extreme scale-down on product stability. It must be emphasized that such studies will not rule out the necessity of larger-scale studies because the micro-scale studies result along with regime analysis will need to be adjusted and the fluid flow and mass transport characteristics should be verified.

A brief description of upstream and downstream MSP techniques for bioprocessing development is outlined through the next two sections. The upstream bioprocess refers to the first stage of the bioprocess in which the bio-reaction takes place or the cells are grown. On the other hand, the downstream part of a bioprocess indicates the stage where the product from the upstream are processed and purified to meet the quality requirements. Then an overview of the main objectives of this work is presented.

### 1.1. Upstream bioprocessing

Numerous studies have used micro-well plates which are flat plates with multiple "wells" (typically between 6 to 1536 wells) as small test vessels. These plates have become a standard tool in analytical research especially in bioprocessing field. Micro-well plates have been used for the development or optimization of a variety of upstream bio-processes including microbial

fermentation [4,6–8], tissue engineering applications [9], bioreactors [3,10], and mammalian cell culture [11,12]. These studies typically focus on the effect of various process parameters such as well geometry, fill volume, solution conditions, and mixing conditions on process performance. A select number of studies are described in detail below; for additional details, the reader is encouraged to read an excellent review of this field prepared by Lye and colleagues [13].

Zanzotto et al. [6] fabricated a micro-scale bioreactor for monitoring the growth kinetics of bacteria. It featured polydimethylsiloxane (PDMS), glass, gas-permeable PDMS membrane aeration and integrated sensors for measuring optical density (OD), dissolved oxygen (DO), and pH. It was shown that the behavior of the bacteria in the micro-scale bioreactor was similar to that in the 500 ml bioreactor in terms of growth kinetics, DO profile within the vessel over time, pH profile over time, final number of cells, and cell morphology. Moreover, it was demonstrated that the sensitivity and reproducibility of the micro-scale bioreactor system are such that statistically significant differences in the time evolution of the OD, DO, and pH can be used to distinguish between different physiological states.

Fernandes and Cabral [10] prepared a thorough review on micro-scale shaken bioreactors (including Erlenmeyer flasks, test-tubes, and micro-well plates) with an analysis of the engineering features as well as monitoring and process control aspects. Barrett et al. [12] have characterized the growth of murine hybridoma cells producing IgG1 in 24-well plates in terms of energy dissipation ($P/V$) via CFD analysis, fluid flow, mixing and oxygen transfer rate as a function of shaking frequency and liquid fill volume. The cell growth kinetics and antibody titer data were similar to those obtained in 250 mL shake flasks. CFD simulations of the shear rate revealed that hydrodynamic forces do not have a negative impact on cells. In contrast, high shaking speeds were shown to have undesirable effect on cell growth and a combination of low shaking speed and high

well fill volume were found to lead to oxygen limited conditions. These findings were used for conducting an engineering comparison of cell culture kinetics in micro-scale and shake flask formats. The presented results were reproducible and scalable in both formats. Khademhosseini et al. [9] have provided a review on micro-scale technologies applications in tissue engineering such as spatially regulated hydrogels and scaffolds, cell assembly for tissue engineering, controlling the cellular microenvironment *in vitro* and patterned co-cultures for controlling cell–cell interactions.

Recent work has reported on the use of MSP techniques for bio-molecule modifications. Maiser et al. [14] developed a micro-plate-based HT technique for optimizing the relevant reaction conditions for the preparation of PEGylated proteins. PEGylation involves the covalent attachment of polyethylene glycol (PEG) polymer chains to another molecule (e.g. protein) and has gained widespread use in the bio-pharmaceutical industry. There are several advantages associated with PEGylation such as prolonging the residence time of a drug in body by increasing its hydrodynamic size. There have been a number of review articles summarizing various concepts of PEGylation [3,15–17].

### 1.2. Downstream bioprocessing

Development of more efficient downstream bioprocesses for biopharmaceuticals has been motivated by the significant recent advances in cell culture titers, the emergence of biosimilars, product quality controls, and new regulatory initiatives [18]. In order to profit from the improvements in upstream side of micro-scale bioprocessing techniques, downstream processing requires an increasing attention of the micro-scale bioprocess development efforts. Furthermore, downstream processing can account for over 85% of total production costs [19]. Meanwhile, downstream processes must be optimized for process performance. This can be a formidable

challenge to achieve by conventional strategies because either the nature of the process is poorly understood or there are a very large number of conditions that need to be screened. For all of these reasons, various purification technologies have been adapted to the MSP level. Thus, MSP development must be performed for downstream processes in parallel with upstream processes.

### 1.2.1. Aqueous two-phase systems

Bensch et al. [20] merged a HT screening approach using deep-well micro-plates and a Tecan Freedom Evo 200 robotic instrument to measure the protein partitioning behavior in a polymer-salt aqueous two-phase system (ATPS) in a rapid manner (approximately six hundred samples per day). Parallel and automated quantification of protein content and measurement of partition coefficients and yields offers the possibility to design ATPS by screening a broad range of variables. The authors suggested that the same system could be used for the determination of cell debris and enzyme-linked immunosorbent assay (ELISA; an immunological assay technique making use of an enzyme bonded to a particular antibody or antigen) or activity assays for specific protein determination.

The ATPS method in combination with statistical evaluation were adapted by Oelmeier et al. [21], to evaluate the separation of monoclonal antibodies (mAbs) from host cell protein (HCP) mixtures. PEG4000–$PO_4$ binodal curves[1] were measured both automatically and manually and were found to be identical within reasonable error. The influence of pH, NaCl addition, and tie

[1] The binodal is defined as the condition at which two distinct phases may coexist. Generally, the bimodal curve is defined by the condition at which the chemical potential of all solution components is equal in each phase. The phase equilibrium for an ATPS can be represented as a binodial curve relating the phosphate and PEG concentrations, for example. Typically, phase plane could be divided into three regions according to binodal curve. Asenjo and Andrews have presented a valuable review in this regard [100].

line length was investigated in a model system that contained lysozyme, two mAbs, and a HCP pool. The selected model system provided a reduction of up to 50% of HCP with a recovery of greater than 95% of the target proteins.

Another HT study for ATPS was performed by Wiendahl et al. [22] who demonstrated an automated, miniaturized screening approach for the separation of plasmid DNA (pDNA) and RNA using two different optimization approaches: response surface modeling (RSM) and genetic algorithm (GA). Their results were reported to be identical to those from previous studies. The strategy was able to speed-up the process development as well as reducing the necessary sample amount. The results suggest that this approach is ideally suited for the development of pDNA purification processes.

### 1.2.2. Adsorption

Welch et al. [23] developed a micro-well system to identify the appropriate adsorbents and conditions for removing process impurities (e.g. metal ion contaminants) from pharmaceutical intermediate products. This method enabled the rapid identification of a simple and economically feasible solution to the purification challenge. The authors claimed to screen all of the intended adsorbent materials in terms of their selectivity for metal contaminants in just two days. This approach were combined with a rapid analysis system that used liquid chromatography–mass spectrometry (LC-MS), colorimetric indicators, or a combination of both. An alternative technique using micro-plate and micro-tube screening was found to be simple and convenient for the evaluation of the selective adsorption of metal impurities from pharmaceutical process streams using a variety of commercially available process adsorbents (95 different adsorbents such as

Sepabeads SP207SS, Merrifield Polymer, Amberlite XE-305, Ecosorb C-941, Methyl Cellulose, Diaion PA308, and Chiralpak AS) [24]. The protocol involved adding a sample solution to each tube using a multi-channel pipette, plate agitation, and centrifugation. Different analyses were performed to measure the concentration of product and impurity, which can be used to estimate the selectivity of the adsorption of product and the remaining impurity. Unlike the previous study [23], colorimetric methods were not found to be effective and high performance liquid chromatography (HPLC) or high performance liquid chromatography–mass spectrometry (HPLC-MS) were conducted instead [24].

### 1.2.3. Chromatography

Chromatography is the workhorse of the downstream processing industry. In general, micro-scale chromatography processes involve either resin screening, ligand screening, or column screening [25]. For example, a large number of commercial ion exchange and affinity resins are available from different vendors (e.g. Pall, GE, and Life Technologies). MSP techniques are ideally suited to be used for the chromatography processes because of the wide variety of chromatography media and operating conditions. Typical columns for conventional chromatography processes such as HPLC are commercially available with an internal diameter (ID) of between 1 mm and 5 mm and a height of 3 cm to 25 cm; for example, columns between 3 cm × 2.1 mm (height × ID) and 15 cm × 4.6 mm (height × ID) are available from Sigma Aldrich. However, as reported by Chhatre et al., [26] there are three common formats for micro-scale chromatography studies that feature the use of small volumes of resin material:

### *I. The microliter batch incubation approach*

Standard batch chromatography experiments for kinetic and thermodynamic data gathering have been performed using resins in small tubes for many years. However, using a micro-well plate based approach has been shown to be a feasible solution to speed-up process development and reduce sample consumption. In particular, filter plates (membrane-bottom micro-plates) have been found as valuable tools for chromatography development studies. In this format, the feed material and resin are mixed together in a suspension, then the liquid phase is removed by either centrifugation or vacuum filtration. The use of such plates is particularly amenable to the use of robotic systems; several studies have demonstrated the usefulness of this approach. For example, Coffman et al. [27] developed a batch binding system that used between 50 and 100µL of resin per well in a 96-well filter plate in order to assess the binding behaviour of different chromatographic media using two impure feed streams containing a mAb and an Fc fusion protein[2]. Results were compared with conventional studies and although clear dissimilarities were observed, the micro-scale format gave a reasonably good prediction of recoveries and purities.

### *II. Micropipette chromatography tips*

The second format for HT development of chromatography processes is forming micro-columns by usage of packed chromatography pipette tips. Although there are custom technologies available for this approach, one of the suppliers of micropipette chromatography tips is PhyNexus (San Jose, CA). The reusable PhyNexus tips are produced by drawing resin into the bottom under

[2] Fc-based fusion proteins are composed of an immunoglobin Fc domain that is directly linked to another peptide. For more information refer to [101].

vacuum and then sealing into place with screens above and below the packed bed. Feed samples and buffers are held in a multi-well plate and are aspirated and dispensed repeatedly for the required total residence time. These pipette tips have been used in a number of studies featuring a series of equilibrating, loading, washing, eluting and cleaning steps to achieve elimination of impurities and recovery of the desired product species. The steps are done to identically match the conventional chromatography process. For example, Wenger et al. [28], have used pipette tip method for the purification of virus-like particles from yeast cultures. Both PhyNexus and custom tips were shown to provide good separation in this micro-scale chromatography format.

*III. Miniature packed bed columns.*

Unlike the two previously mentioned chromatography formats, packed micro columns (are similar to conventional chromatography columns in terms of geometry. This format can be used with robotic systems to obtain high throughput and consistency and are useful for determining the effect of flow rate through repeated loading cycles. However, the residence time cannot be high enough to compare very low-volume columns with conventional format by using robotic systems.

For example, Britsch et al. [29] have investigated the ability of miniature robotic columns (~ 200 μL of resin) for protein separation from an industrially relevant feedstock. The use of an automated protein A micro-column system not only provided a rapid purification step but it also enabled the capability of rapid testing for this process. The authors also reported that the micro-column results were comparable with conventional columns in the case of cation exchange columns.

There has been significant work in the development of HT chromatography processes in different formats. For instance, Bergander et al. [30] developed a HT approach based on implementing the batch uptake principle into micro-well plates for chromatography application. This approach could be used as either qualitative or quantitative estimation of dynamic binding capacity (DBC) as a function of residence time with minor modifications. For example, dynamic binding capacities of human polyclonal IgG on MabSelect SuRe resin (GE) were given as an illustration of quantitative estimation. The proposed micro-scale technique significantly reduced the time and sample consumption compared to a traditional method utilizing packed chromatography columns. The same authors also used microliter filter plates filled with a specific volume of resin to estimate the residence time. This technique reduced the number of required experiments and the cost. A HT mixed-mode cation exchange chromatography technique for polyclonal antibodies recovery from ovine sera was developed by Chhatre et al. [31], to reduce the optimization costs of the process. $2^3$ factorial design[3] was applied as an optimization method to assess the effect of loading buffer, salt concentration and pH (operated by 20 ul packed pipette tips) on response variables of purity, capacity and yield. Duplicating two of the conditions in 10mL packed bed showed the scalability of the method. Chhatre et al., [26] have presented a thorough review describing different aspects of HT chromatography development for pharmaceutical applications.

[3] An experimental design which consists of 3 factors and their interactions. More details described in section 4.4.

### 1.2.4. Membrane filtration

Previous studies have demonstrated the concept of HT screening for membrane filtration processes. Chandler and Zydney [32] assessed the performance of numerous microfiltration (MF) modules including 96-well filter plates, syringe filters, and unstirred filtration cells, using a combination of both pressure and vacuum driven processes, to find the optimal operational conditions for the harvesting of yeast cells. The hydraulic and specific cake resistances of the membranes were compared both within the same filter plate and also across different filter formats. The results were very consistent for Millipore polyvinylidenefluoride (PVDF) and mixed cellulose ester membranes except for the XL-2 pleated cartridge format. More variability was observed among a single plate and different membrane formats when using Pall membranes; this result was attributed to sealing issues.

Subsequent studies have exclusively used vacuum-driven filtration processes because of the ease of setup and operation using commercially available vacuum manifolds. However, the disadvantage of these studies is that there is no reservoir for continuous feed introduction and thus the amount of filtrate that can be processed is limited to the volume within each well of a filter plate. The performance of both 96-well filter plates and a custom designed plate fitted with centrifugal filter units for the processing of fermentation broth were studied by Jackson et al. [33]. Parallel evaluation of the effects of broth harvest time, buffer composition, and growth media composition were performed using an automated vacuum filtration manifold. The results were compared to those found with a conventional unstirred membrane cell and shown to be identical in terms of membrane resistance and specific cake resistance. Zhou and colleagues [34,35] developed a HT technique that used photo-induced graft polymerization [36,37] of a monomer library onto 96-well filter plates to screen for the fouling propensity of the modified membranes

towards natural organic matter (NOM) [34] and protein solutions [35]. The same vacuum filtration setup was used for both the surface modification step and fouling studies. The results have been verified using bench-scale setup for selected monomers. The results were found to be both scalable and reproducible especially in case of NOM filtration. Kong et al. [38] have introduced an automated technique for membrane unstirred filtration of plasmid DNA in sterile conditions in multi-well format with a filtration area of 0.28 $cm^2$ per well. This setup allows for performing eight parallel experiments to assess the effect of transmembrane pressure (TMP), plasmid size, and membrane type using low DNA volumes. The scalability of the method in terms of the filtration capacity was verified by conducting identical experiments in conventional unstirred cell filtration experiments. It is worth mentioning that HT-membrane filtration modules have also been adapted to other applications such as gas separation [39] and membrane bioreactors [40].

In all five of these works [32–35,38], the experiments were conducted in the so-called ‘dead end’ filtration mode and in the absence of any stirring above the membrane.

To sum up, Fig. 1.1 demonstrates a summary of MSPs as introduced in sections 1.1 and 1.2 while Table 1.1 summarizes the presented formats of different micro-scale downstream bioprocessing studies.

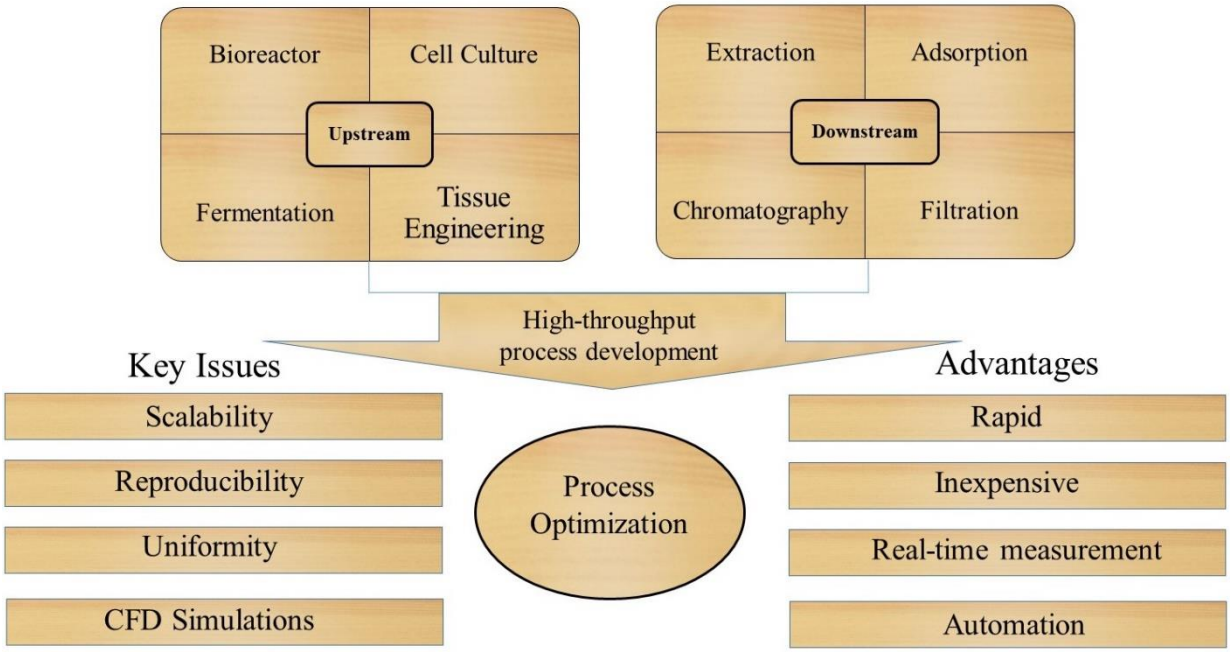


Figure 1.1. Summary of micro-scale bioprocessing techniques.

Table 1.1. Summary of previous micro-scale downstream bioprocessing formats.

| **Process** | **Available Formats** | **References** |
|---|---|---|
| Extraction | Micro-plates | [20–22] |
| Adsorption | Micro-plates and Micro-tubes | [23,24] |
| Chromatography | Micro-plates, Micro columns, Pipette tips, and Microfluidic devices | [25–31] |
| Filtration | Multi-well filter plates and Microfluidic devices | [32–35,38–41] |

## 1.3. Objectives

The previous sections were dedicated to describe the concept of micro-scale processing and its applications with emphasis on bio-industries. It was declared that HT testing is considered

as a requirement for rapid development of different processes including upstream and downstream bioprocesses for process optimization.

Among downstream bioprocessing techniques, there has been relatively little work on development of a HT filtration testing system with identical characteristics of the conventional filtration formats. Like other HT downstream processes, micro-scale membrane filtration processes should be designed to address three key issues: (1) the scalability of the data between the micro-scale module and conventional modules; (2) the reproducibility of the data obtained at the very small scales; (3) the ability to maintain uniform operational conditions. For these issues to be addressed the technique should not only have a flawless experiment condition, but it should also be capable of providing most of the components available in the conventional-scale modules in micro format.

It is widely established that the accumulation of solutes at the membrane surface can severely change the process performance in dead-end filtration [42]. Introduction of a mixing method near the membrane surface is one of the simplest approaches to limit the effects of this polarization phenomenon. Fane and colleagues [43,44] have established some of the earliest work in the field of concentration polarization and membrane fouling. They have shown that during constant pressure ultrafiltration (UF) of a colloidal silica suspension a higher filtration rate was obtained with stirring compared to unstirred configuration. It was also demonstrated that the dynamics of polarization varied with stirring conditions during the filtration of protein and polysaccharide solutions. Katsoufidou et al. [45] investigated the effects of stirring and solution conditions on the UF of sodium alginate, a model polysaccharide using flat-sheet UF membranes. They observed that the normalized solution flux decreased more rapidly without stirring and attributed this observation to the formation of a concentrated layer near the membrane surface

which is strongly influenced by the local hydrodynamic conditions.. More recently, Chhaya et al. [46], observed the similar phenomenon (effect of stirring conditions on solution flux decline) when performing filtration experiments with the Stevia extracts through UF membranes. In all of these works, the experiments were conducted using a stirred cell filtration device ('dead end' filtration format) that accommodates a single membrane. It appears that the ability to control the stirring conditions in a HT membrane filtration test could be a decisive factor in process optimization.

To date, Vandezande et al.[41] have presented the only work which allows for stirred membrane filtration tests to be conducted in a HT format. They evaluated the performance of flat-sheet nanofiltration (NF) membranes using a module that featured sixteen individual stirred cells, as well as temperature control and automated permeate collection. Although their technique does allow for HT screening of pressure-driven membrane processes with stirring, the experimental design itself was custom made with expensive components and required that the various equipment pieces be dedicated exclusively to it. Furthermore, unlike large-scale filtration operations, their work used a constant pressure filtration setup.

It is believed that the mentioned dissimilarities may affect the results obtained from HT studies and in absence of identical features, the results from HT filtration testing are not representative of what is normally done in conventional formats. Furthermore, most of the developed HT filtration testing systems in previous studies have required a number of costly equipment to be dedicated for their operation. The main objective of this research was to integrate the pressure-driven stirred conditions of conventional stirred-cell modules and 96-well filter plates for rapid screening of filtration operating conditions including, but not limited to, membrane pore size, filtrate flux, stirring conditions, and solution conditions (e.g. pH, ionic strength). This work was developed as the first ever HT filtration setup that uses 96-well filter plates and incorporates

mixing of the feed solution directly above the membrane surface akin to the stirred-cell filtration device – this design is hereafter referred to as 'stirred-well filtration' (SWF). The stirring was achieved using a lateral tumble stirrer which uses one drive magnetic field to simultaneously stir a multiple number of vessels. A programmable syringe pump was used to conduct filtration experiments in constant filtrate flux mode. 96-well filter plates were chosen for this work because they are manufactured in standard dimensions, are available from a number of suppliers with various UF and MF membranes, and are directly compatible with other micro-plate formats (e.g. 384-, or 1536-well) for sample collection and analysis.

The overall goals of different parts of this work presented in following chapters were (1) to pre-design, design, develop and test the SWF technique as a HT method; (2) to show the reproducibility, scalability, and uniformity of the data for common membrane filtration experiments such as hydraulic permeability and sieving experiments in SWF module; (3) to demonstrate the effect of stirring on filtration performance as well as uniformity and reproducibility of the data; (4) to prove the usefulness of the SWF technique for filtration process optimization by means of DOE concept. Figure 1.2 demonstrates the summary of this research.

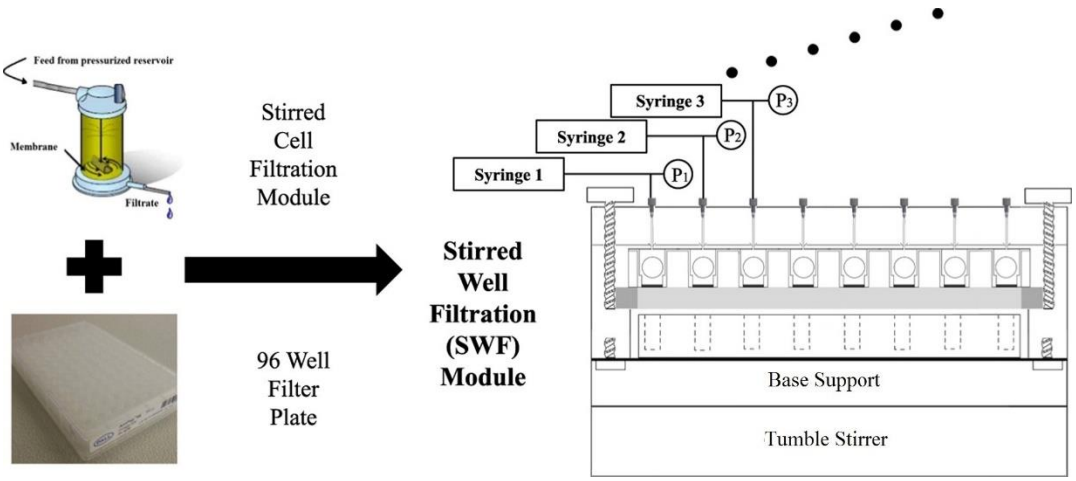


Figure 1.2. Research graphical summary.

## Chapter 2. Membrane processes and stirred well filtration (SWF) design and development

In terms of separation processes, a membrane is defined as a thin barrier or film through which solvent and solutes are selectively transported. Membrane processes have been developed for several separation applications in the pharmaceutical, environmental, and food processing industries over the past 50 years. The opportunities for using membrane processes in different industries are growing due to enhancements in the chemical, thermal and mechanical properties of the membranes as well as the design of new process configurations that enhance the filtration performance. Synthetic membranes can be classified according to the membrane material, morphology, geometry, and/or manufacturing methods. For example, membranes can be classified as flat sheet, tubular or hollow fiber according to geometry, organic (polymeric) or inorganic in terms of the nature of the membrane material, homogenous/heterogeneous, porous/dense and symmetric/asymmetric in structure.

Membrane modules are designed as a core element to facilitate the application in practice. Hollow fiber, spiral wound, tubular, and flat sheet are a few examples of the common module configurations widely used for different applications (Fig. 2.1).

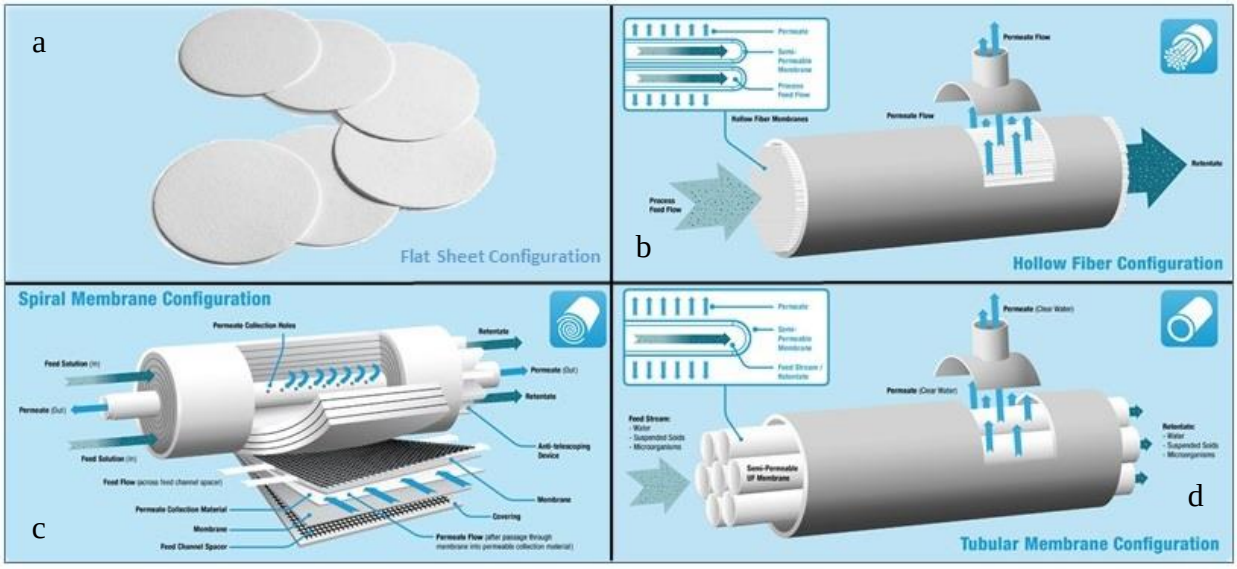


Figure 2.1. Module configurations: a. flat sheet membrane (adapted from Sartorius) b. hollow fiber membrane (credits Koch Membrane Systems); c. spiral wound membrane (credits Koch Membrane Systems); d. tubular membrane (credits Koch Membrane Systems).

As shown in Fig 2.2, there are basically two modes of operation for membrane filtration processes. In the dead-end configuration, the feed flow is oriented perpendicular to the membrane surface and hence any retained particles accumulate and deposit on the membrane surface. In the cross-flow operation, the feed flow is oriented parallel to the membrane surface. Cross-flow operation can have a much higher permeation rate but it needs more complex equipment to operate and costs more energy [47]. Note that in membrane filtration terminology filtrate or permeate stream is defined as the liquid that passes through the membrane while retentate is liquid that does not flow through the membrane and is retained.

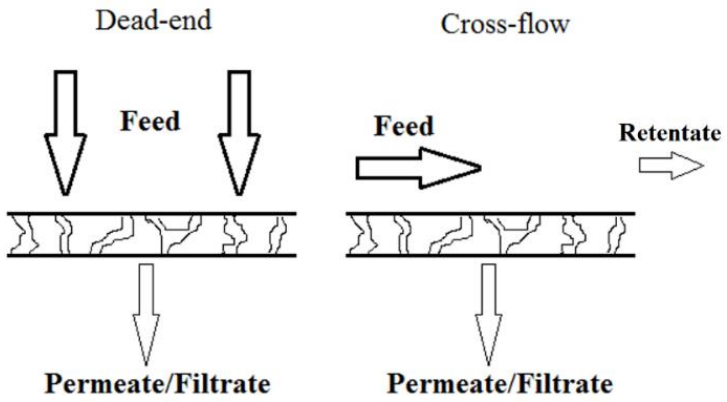


Figure 2.2. Modes of operation in membrane filtration processes

## 2.1. Membrane classification

Membrane processes can be grouped according to the driving force as well. Pressure-driven processes for liquid separations include reverse osmosis (RO), nanofiltration (NF), ultrafiltration (UF), and microfiltration (MF); see Fig 2.3 for a schematic of the different pore size characteristics and filtration properties of these four processes. Other membrane processes use concentration gradients (e.g. dialysis), temperature (e.g. membrane distillation), or electrical potential gradients (e.g. electrodialysis). UF and MF processes are used in a wide number of applications in the bio-processing field and thus are the focus of this study. For example, membrane UF is one of the common methods for protein fractionation and concentration [48–54] while MF process has been used for applications such as yeast cell harvesting filtration [32] and filtration of Escherichia coli fermentation broths [33].

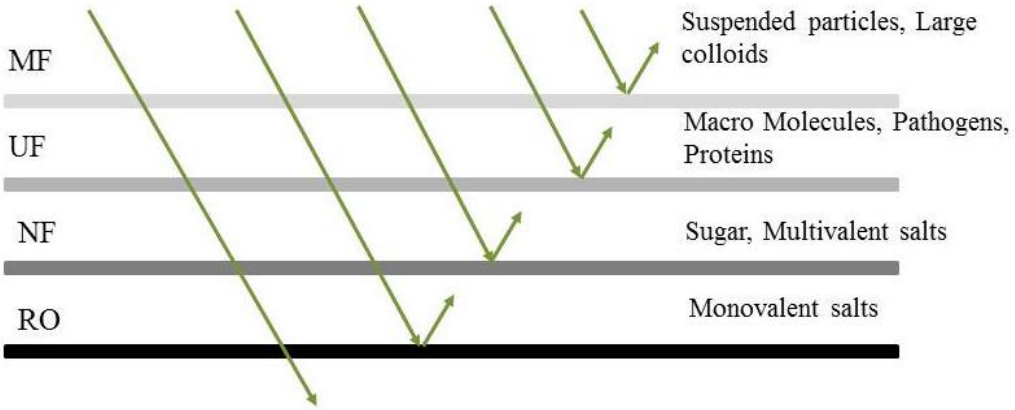


Figure 2.3. Membrane classification according to pore size (adapted and modified from [55]). The permeate of the MF process becomes the feed to the UF process; the permeate of the UF process becomes the feed to the NF process; the permeate of NF process becomes the feed to RO process.

### 2.1.1. Ultrafiltration (UF)

The first commercial UF membranes were introduced in the mid-1960s by Millipore and Amicon. Initially, UF membranes were developed with goal of manufacturing RO membranes with higher fluxes[4]; however, they were later developed simultaneously with RO membranes for other applications. The typical pore diameter size for a UF membrane is 1-100 nm (2-20 nm for most applications). UF membranes are generally suitable for applications such as macromolecules, colloids and solutes with molecular weights (MW) larger than 10 kDa. The majority of UF membranes are prepared by phase inversion method and are structurally asymmetric (i.e. with non-uniform pore size). Asymmetric membranes have generally fast flow and low pressure drops. The first UF membranes were made from cellulose acetate [56]. Nowadays, different polymers such as polyamides (PA), polysulfone (PS), polyethersulfone (PES) and polyvinylidenefluoride (PVDF) are used for providing different range of temperature, pH and chemical resistance. There have been

[4] Flux= (Flow Rate)/(Membrane Area)

several applications in different industries for UF membranes but recovery of electrophoretic paints and dairy processing applications are the most famous ones [57–59].

### 2.1.2. Microfiltration (MF)

Microfiltration (MF) membranes with pore size range from 0.1 to 10 micron are typically used for separation of impurities such as particles, viruses, and bacteria from water, bio-products, etc. MF membranes were initially used during the Second World War for the biological examination of water as well as in pharmaceutical industries [60–62]. During the 1980s, this technology was used for water treatment as well. Following the cryptosporidium outbreak [63] in the United States in 1992, the more widespread use of MF was adopted for water treatment applications.

As stated earlier, membranes can be categorized based on various characteristics including the membrane material. Membranes are classified as either polymeric or inorganic categories. Because of their higher price, inorganic membranes are usually considered for some specific applications such as petrochemical applications (e.g. separation of $O_2$ from air for use in efficient combustion) [64]. On the other hand, polymeric membranes are widely used for different applications including water and wastewater treatment, food processing, and pharmaceutical industries [60,61]. These membranes can be prepared by methods such as phase inversion, interfacial reaction, coating, stretching, etc.

## 2.2. Membrane test formats

Since the introduction and development of membrane technologies a number of different test formats have been used in filtration processes such as Tangential Flow Filtration (TFF) cassettes, stirred cells and multi-well filter plates. In this section a conventional dead-end filtration test format (stirred cell with flat sheet membrane) and two HT dead-end filtration formats (syringe filter and 96-well filter plate) are introduced to choose the most appropriate format for HT studies and compare it with the conventional dead-end filtration format.

As outlined below, all three formats have been used widely in previous studies.

### 2.2.1. Stirred cell with flat sheet membrane

The stirred cell filtration device is used for conducting dead-end filtration studies. A membrane is located at the base of a cylindrical cell that is filled with solution. A magnetic stir bar is suspended just above the membrane surface and rotates at some angular velocity as determined by a magnetic stir plate on which the device sits. In certain setups a pressurized feed reservoir is used to deliver a continuous supply of solution to the device (e.g. [52,54]). This format is widely used for membrane testing given its ease of operation. The hydrodynamic conditions within the stirred cell are quite complex and thus a stagnant-film model is generally used to quantify the solute transport that occurs in the boundary layer above the membrane surface [65,66]. A number of previous studies [67,68] have also used CFD to model such systems. For example, a preliminary study by Darvishmanesh et al. [68] examined the effect of stirred cell module design and operating conditions on fluid patterns and flow profiles using CFD simulations; it appears that this area requires further attention to see the effect of different operational conditions on mass and momentum transfer as well as its scalability when using the stirred cell format.

Stirred cell devices are commercially available from a number of suppliers. Table 2.1 shows a list of stirred cell filtration modules available from Millipore and Advantec. According to Table 2.1**,** there are different sizes of stirred cells available with $\frac{\text{Volume, V (mL)}}{\text{Effective membrane area, A (cm}^2\text{)}}$ range between 2.4 $\frac{\text{mL}}{\text{cm}^2}$ -12.3 $\frac{\text{mL}}{\text{cm}^2}$ for the mentioned suppliers. V/A is proportional to size of the module and is used as a tool for investigating the geometric and dynamic similarities. Stirred cell filtration modules are inappropriate for HT testing since relatively large amount of time and sample is needed to run a single experiment while the parallelization of the experiments is not simple as well.

Table 2.1. Stirred cell filtration modules available from Advantec MFS (www.advantecmfs.com) and Millipore (www.emdmillipore.com).

| Model | | Volume (mL) | Membrane diameter (mm) | Effective membrane area ($cm^2$) | $\frac{\text{Volume (mL)}}{\text{Effective membrane area (cm}^2\text{)}}$ |
|---|---|---|---|---|---|
| Advantec MFS | UHP 25 | 10 | 25 | 3.5 | 2.8 |
| | UHP 43 | 70 | 43 | 6.2 | 11.3 |
| | UHP 62 | 200 | 62 | 27.0 | 7.4 |
| | UHP 76 | 450 | 76 | 38.5 | 11.7 |
| | UHP 90 | 600 | 90 | 54.5 | 11.0 |
| | UHP 150 | 2000 | 150 | 162 | 12.3 |
| Millipore | 8003 | 3 | 25 | 0.9 | 3.3 |
| | 8010 | 10 | 25 | 4.1 | 2.4 |
| | 8050 | 50 | 44.5 | 13.4 | 3.7 |
| | 8200 | 200 | 63.5 | 28.7 | 7.0 |
| | 8400 | 400 | 76 | 41.8 | 9.6 |

### 2.2.2. Syringe filter

The syringe filter is a miniature membrane filtration device which generally consists of a plastic cover with a membrane filter and it is connected to the end of a syringe via different types of connectors (e.g. Luer Lok$^{TM}$). Fig. 2.4 shows a typical syringe filter. The fluid can be either drawn or forced through the membrane via the action of the syringe plunger. They are commercially available from a number of suppliers with various MF membrane chemistries and properties. The typical pore sizes available for syringe filters range from 0.13 to 10 microns; the typical filter size is 10 to 25 mm in diameter. There are different applications for syringe filters such as using as a pre-filtration step for HPLC samples. Syringe filters may also be used to filter drugs prior to injection which is called harm reduction or harm minimization. They have also been used in HT microfiltration studies by Chandler and Zydney for microfiltration process of yeast cell harvesting [32]. However, there are a number of drawbacks associated with syringe filters; for example, the stirring cannot be performed during the filtration in this format because of the design compactness.

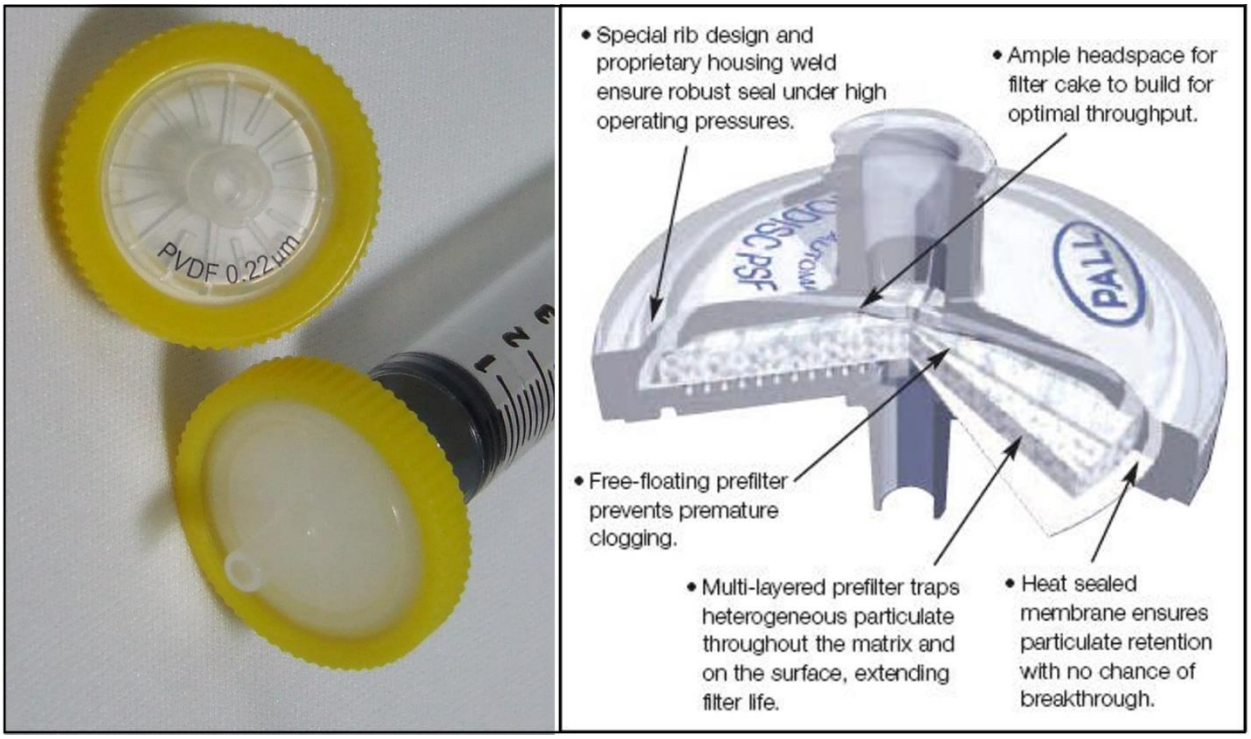


Figure 2.4. a. Picture demonstration of syringe filters (credits: Dot-red analytics); b. Schematic demonstration of AcroDisc syringe filter (credits: Pall life sciences).

### 2.2.3. 96-well filter plates

96-well filter plates are manufactured according to the standard American National Standards Institute (ANSI) dimensions of a micro-well plate and are available from various suppliers with a variety of filter media including UF, MF, and ion-exchange membranes (see Table 2.2). Fig. 2.5 shows a cut away graphic of a filter plate that shows with a single membrane disc at the bottom of each well. These plates are compatible with various sample collection and analysis formats. For example, AcroPrep™ 96-well filter plates from Pall are available with 350 µL and 1 mL capacities with MF and UF membranes.The ratio of membrane area to well volume are quite comparable to typical stirred cell devices (refer to Table 1 in [33]).

Various membrane materials are used with 96-well filter plate format including:

- Cellulose is a highly hydrophilic polysaccharide that is used for the production of dialysis and low-fouling MF, UF, and RO membranes in conventional formats. Cellulose membranes are poorly resistant to microbial attack and have a low pH (4-6.5) stability [61].
- Polyvinylidenefluoride (PVDF) is widely used as a high-quality material for MF and UF membranes. This membrane has a high thermal stability and chemical resistance. PVDF is resistant to most organic and inorganic acids and is a hydrophobic polymer which is commonly made by phase inversion method [69].
- Polycarbonate (PC) is a transparent thermoplastic with high dimensional stability. PC is generally used for production of porous membranes with a well-defined structure with high mechanical strength [61].
- Polyethersulfone (PES) and Polyethersulfone-based membranes are of the key polymeric materials which are widely used in separation fields because of outstanding oxidative, asymmetric structure, thermal and hydrolytic stability as well as good mechanical properties [70,71]. The main disadvantage of PES membranes is related to their relatively hydrophobic character which can greatly affect the membrane fouling. [71]. Modified PES membranes are also widely employed in biomedical fields (e.g. tissue engineering and dialysis devices) [71].

Polytetrafluoroethylene (PTFE), polypropylene (PP), glass fiber (GF), and polyether (PE) are some of the other membrane materials available in the 96-well filter plate format.

Considering the facts that 96-well filter plates are commercially available and inexpensive, are capable of performing 96 parallel experiments, are available with a variety of membranes, need relatively low sample size (~ 350 μL), are compatible with various sample collection and analysis formats, and have geometric and dynamic similarities with conventional formats such as stirred

cell filtration module, they have been selected to be used in this work for the HT development of membrane filtration process in stirred format.

Figure 2.5. Cut-away graphic of 96-well filter plate (Credits: Corning ®).

Table 2.2. Commercially available 96-well filter plates.

| **Company** | **Product** | **Membrane** |
|---|---|---|
| EMD Millipore | Multi-Screen | Durapore (PVDF) MF |
| | | Ultracel (Cellulose) UF |
| | | Immobilon-P (PVDF) MF |
| | | (PTFE) MF |
| | | (PC) MF |
| Pall | AcroPrep/Advance AcroPrep | Supor (PES) MF |
| | | GHP (PP) MF |
| | | Omega (PES) UF |
| Corning | FilterEX | (PVDF) MF |
| | | (PC) MF |
| Cole-Parmer | DispoDialyzer | (Cellulose) UF |
| Seahorse Bioscience | Filter Bottom Microplates | (PES) UF |
| | | (PP) MF |
| | | (PE) MF |
| | | (GF) MF |

## 2.3. Design of stirred well filtration (SWF) module

There are many challenges to be addressed in the design of a MSP system for membrane filtration studies. A summary of those that were assessed and resolved during the design phase of the stirred well filtration module is presented below.

### 2.3.1. Micro-plate mixing

Micro-plate mixing is one of the major issues in micro-scale processing development. According to a 2007 survey of HTStec (formerly HTS Technologies), 36% of the respondents have indicated that they understand that there are some problems with micro-plate mixing- but they are fine with it while 25% have found micro-plate mixing as a major issue and are actively investigating and/or implementing mixing technologies and 9% have responded that although they would accept it as a major issue, they are still wondering how to address it [72]. The overall survey findings suggest that efficient micro-plate mixing is still not among the top priorities of many laboratories.

There are four general strategies for micro-mixing: repeated aspiration and dispensing via either manual pipette or liquid handling equipment [20]; ultrasonic equipment [73]; magnetic stirrer [74,75]; orbital shakers [14]. For example, Bensch et al. [20] used repeated aspiration and dispensing for their study on aqueous two-phase systems (ATPS) using polymer-salt for protein partitioning while Maiser et al. [14] used orbital shaker for their study on the optimization of protein PEGylation reactions. Table 2.3 is adapted and modified from [72] to summarize the different styles of micro-plate mixing. The choice of an appropriate mixing system is a critical part of micro-scale bioprocessing development for the unit operations that require mixing.

Table 2.3. Micro-plate mixing formats (Adapted/Modified from [72])

| Vendor | Name | Technology |
|---|---|---|
| Advalytix | PlateBooster 96<br>PlateBooster384 | Surface acoustic waves (SAW), based on 96 and 384 well transducers, one per well |
| Covaris | L8 Acoustic Plate Mixer<br>L800 Acoustic Plate Mixer | Adaptive focused acoustics (AFA), based on an 80mm linear transducer |
| Eppendorf | MixMate® | Orbital shaker, up to 3,000 rpm in controlled in 2-D axis |
| Matrical | SonicMan™ | Variable sonication, via an interchangeable disposable pinned lid, matched to plate density. |
| Scientific Industries | Microplate Genie™ | Orbital shaker, up to 3,200 rpm, with small vortexing orbit of 1.0mm. |
| Tecan | Te-Shake | Up to 1500 rpm for microplates; up to 1200 rpm for deep-well plates |
| Thermo Fisher Scientific | iEMS® Incubator/Shaker | 400 to 1400 rpm in 250 rpm increments (5 speeds) |
| V&P Scientific | Alligator tumble stirrer | Magnetic stirrer based on encased neodymium iron boron with protective layers of PTFE and Parylene, U' shaped trapeze bar wire or raising and lowering of stainless steel balls in microplate wells. |

For membrane filtration tests, it was quickly concluded that it was not reasonable to use either an orbital shaker or repeated aspiration and dispensing system because of the challenges

involved in sealing and sample collection. However, a magnetic stirrer can be used in such processes if there is a compatible magnet with suitable size which can be moved in the desired directions by applying a strong enough magnetic field. It must be emphasized that the same stirring technique is used in conventional stirred cell filtration format. Among different techniques for multi-well plate mixing, many of them were not appropriate for this setup. For example, shaking was not considered to be used because of the continuous nature of the process which requires sample collection. Also, most shakers do not provide an optimum condition in terms of mixing profile. Furthermore, the ability to mix wells separately was another feature which was advised when designing the SWF module. Micro-motors were among the options which were initially considered to be used for developing the stirring technique. Miniature motors and micro-motors are found to be extremely versatile for various applications (e.g. medical devices). There are a number of companies which manufacture micro-motors such as Namiki Precision Jewel Ltd. and Hansen Corporation. However, the complexities incorporated with the motors themselves and their relatively high price cast doubt on their efficiency in terms of stirred well filtration module. Another potential problem with the usage of these micro-motors was the complications with manifold and the sealing. Sealing of micro-scale filtration process is a very challenging issue even without using the micro-motors (see next section). Hence, usage of magnetic stirring by micro-elements in a well by well manner was discovered as an effective method for stirring of the module. The Alligator Tumble Stirrer (V&P Scientific) was selected to be used with appropriate magnets for 96-well plate (~4.5-6.5 mm size). As stated by the manufacturer: "As opposed to using a spinning magnetic stirring bar, the Alligator Tumble Stirrer causes stirrers to tumble end over end inside each well, similar to the way alligators tumble their prey". This feature is different than what is obtained in a conventional stirred cell reactor or filtration module where the cylindrical stir

bar spins in a tangential direction on an axis that is perpendicular to the bottom surface or the membrane. This tumble stirrer is able to handle different multi-well plate formats including 6, 12, 24, 48, 96, 384, and 1536 well plates and other micro-scale vessels such as PCR (polymerase chain reaction) plates, microfuge tubes, test tubes, and bottles. The stirrer have been reported to be useful in several applications by the manufacturer, such as stirring genomic libraries as they are growing, stimulating the growth of aerobic organisms, suspending microorganisms, breaking up filamentous organisms, dissolving solids, mixing two or more compounds, mixing oil and water emulsions, scraping tissue culture monolayers and releasing DNA, and mixing and immobilizing reactions that use magnetic beads. The stirrer can be used in either horizontal or vertical orientation to gain different mixing regimes and the speed is controlled via a 120 volt 60 Hz controller. The tumble stirrer is shown in Fig. 2.6.

An immediate concern with the use of the tumble stirrer was the possibility of the stir element damaging the membrane at the bottom of the well. A number of strategies were explored including the use of a small cage or porous frit materials. However, the final design was quite simple and involved the use of a small washer that fit inside the well between the stirrer and the membrane. A number of different washers were tested in this regard including but not limited to low-friction Polytetrafluoroethylene (PTFE) flat washers, nylon general purpose flat washers, zinc-plated steel type A flat washers, and 18-8 stainless steel general purpose flat washers. The final design used a 9/32” OD, 9/64” ID washer made from Type 316 stainless steel. It was ideal for use with the AcroPrep 96-well filter plates (Pall). A picture demonstration of the micro-mixing system is presented in Fig. 2.7.


Figure 2.6. Pictures of tumble stirrer in vertical (a, b) and horizontal (c; credits: V&P Scientifics) orientations.

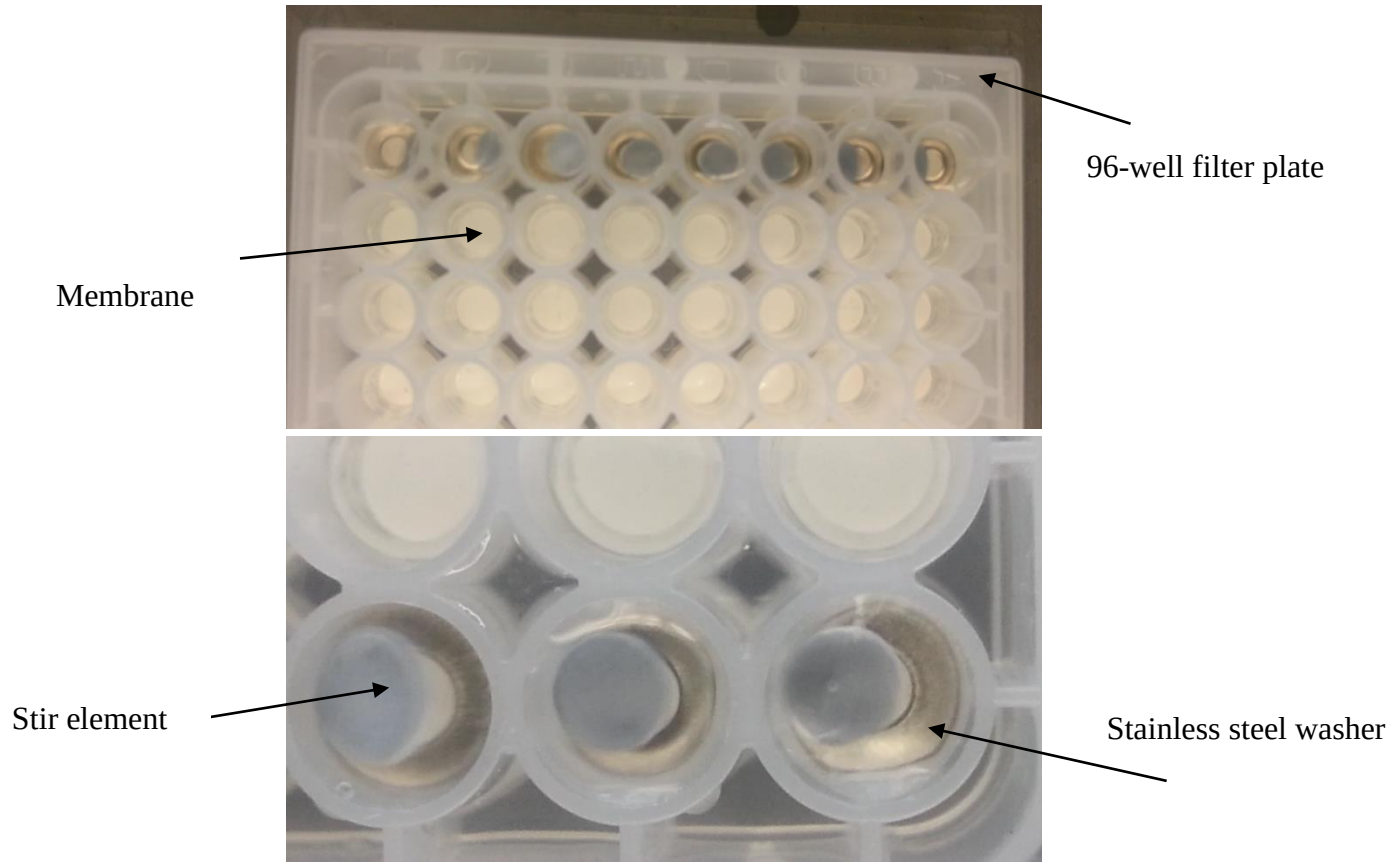


Figure 2.7. Picture of stir elements and washers in the wells of a 96-well AcroPrep filter plate.

### 2.3.2. Modes of operation

Membrane filtration processes are operated either in constant filtrate flux or constant pressure modes. In terms of the effect of concentration polarization and fouling, transmembrane pressure (TMP) increases when performing constant flux operation due to either the solute accumulation on membrane surface or different fouling mechanisms. On the other hand, performing constant pressure operation can lead to reduction of filtrate flux when having high extents of concentration polarization or fouling.

Modes of operation may have a significant effect on different stages of membrane processes; for example, the influence of modes of operation on cleaning process[5] of membranes after different types of fouling is demonstrated in Fig. 2.8. The solid lines show the cleaning procedure to restore the membrane permeability ($L_p$)[6] without chemical agents (i.e. backwashing) which results in a slight decrease in membrane permeability due to the hydraulically irreversible fouling. This type of cleaning is not efficient enough to restore the permeability after performing several filtration and cleaning steps. On the other hand, the dashed lines show the chemical membrane cleaning using chemical agents such as NaOH, $C_6H_8O_7$, NaOCl, and EDTA which are used when the backwashing is not strong enough to restore membrane performance. The main difference between Fig. 2.8.a and 2.8.b is the hydraulically and chemically irreversible flux declines in constant pressure mode against the hydraulically and chemically irreversible pressure increases in constant flux mode.

[5] Describing different cleaning procedures is beyond the scope of this work. For more information refer to [102–106].

[6] In membrane processes, the permeability is generally defined as $J = (\frac{\Delta P}{\mu}) \times L_p$ where J is the filtrate flux, ΔP is the transmembrane pressure and μ is the solution viscosity. More details are described in section 2.5.1.

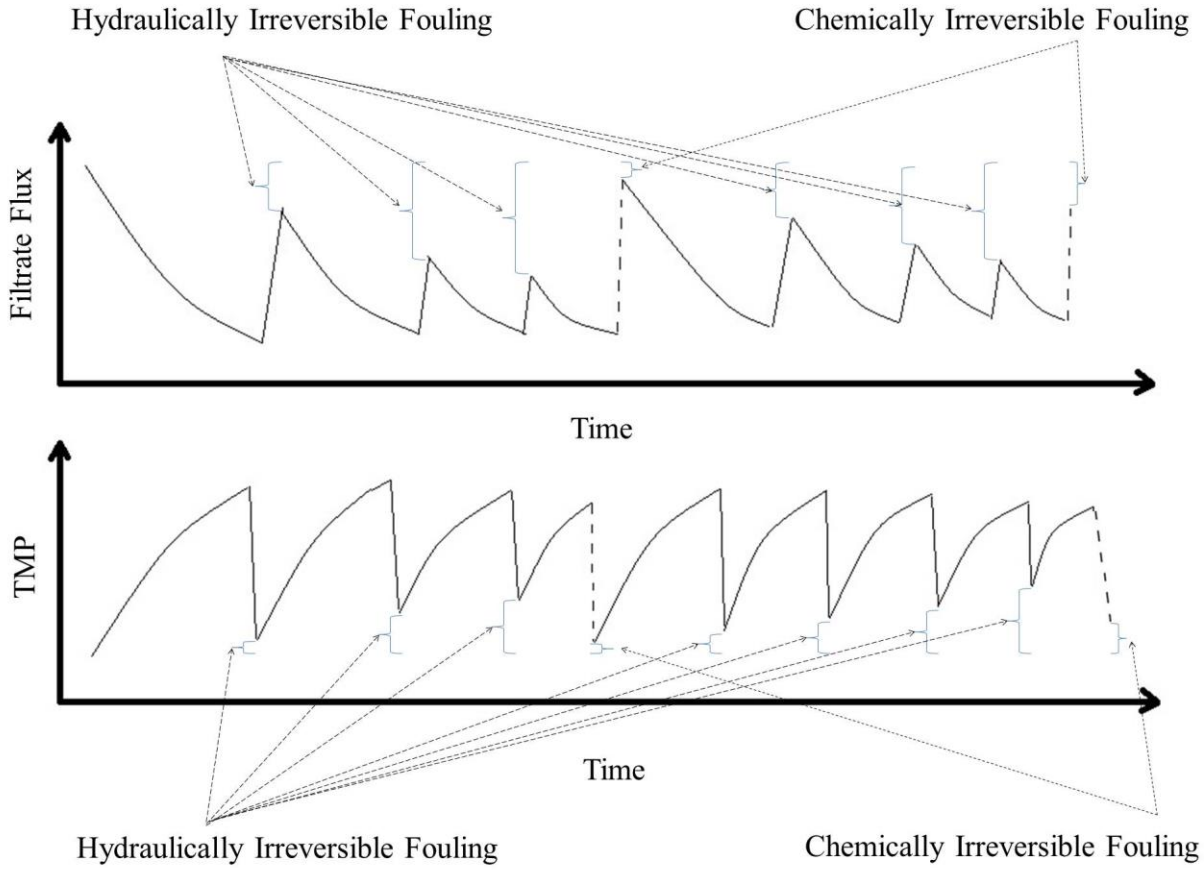


Figure 2.8. Hydraulically and chemically irreversible fouling demonstration: a. constant pressure; b. constant flux. Note that dashed lines represent chemical cleaning while solid lines show backwashing steps.

Although constant pressure processes are the workhorse of membrane filtration studies [50,76], there are a number of advantages in performing membrane filtration processes in constant flux. For example, constant flux operations are easier to study, characterize and model [50]. Constant flux filtration has been investigated earlier in a number of studies. Ghosh [76] developed a pulse injection method to study the fouling behavior of bovine serum albumin (BSA) protein using constant flux UF process. Kanani and Ghosh [50] developed a novel approach for modeling of permeate flux decline in constant pressure ultrafiltration of protein solutions. They assumed that

a constant pressure process is made up of numerous small, sequential, constant flux UF steps. Sun et al. [77] used a rapid characterization method to study the fouling behavior of protein using constant flux operation with cellulose acetate membranes. Two fouling phases were identified based on pressure-permeate volume profiles in this microfiltration process.

The SWF module was designed to conduct experiments in a continuous manner with constant flux using a high-precision, programmable, multi-channel syringe pump (general specifications are listed in Table A2 in Appendix D). Thus, it was important to find an inexpensive and appropriate technique to measure the TMP in each well during the runs. PC board mountable pressure transducers [32] from Omega (details described in the next sections) were found as an appropriate option in terms of size, application, pressure range, and cost for this process (general specifications are listed in Table A3 in Appendix D). To integrate the transducers with the syringe pump, a custom adapter was designed and fabricated. A key design feature was a low hold-up volume (approximately 500 μL). A picture and technical drawings (2D and 3D) of this adapter are presented in Appendix A.

### 2.3.3. Sealing

Proper sealing of the membrane filtration module is a critical feature of a HT filtration system in order to obtain reliable results. A number of options were considered and tested with a standard 96-well filter plate. The initial design used a relatively thick (0.2 cm) silicon rubber sheet with eight channels. However, early tests with various plates (Pall Acro-Prep, Millipore Multi-Screen, Seahorse filter plates) showed that the pressure provided from the manifold by the thumb screws was not effective to provide a tight sealing; this configuration was tested with different thicknesses as well. Thinner silicone rubber sheets provided some sealing at low flow rates (5

μL/min corresponds to approximately 12 LMH) but were ineffective at higher flow rates. The final design used multiple layers of Paraffin sheets (Parafilm) due to their high flexibility and strength. Two layers of Paraffin, each composed of five Parafilm sheets, with silicone o-rings (5/16" OD) sandwiched between the sheets were found to provide good sealing at all the flow rates tested. Eight small recesses were designed on the manifold plate to align with the o-rings that were used in the gasket. Furthermore, it was important to ensure proper sealing of the custom adapters which were designed to be connected to the syringes and pressure transducers. The appropriate connectors (18FTLL-1 from Value Plastic and f-332nx from IDEX Health & Science) as well as Epoxy were used to provide the proper sealing of this component. The sealing tests were conducted with water, phosphate buffered saline (PBS) solutions, and protein solutions. Fig. 2.9.a and 2.9.b show the silicon and custom gaskets respectively.


Figure 2.9. a. Leakage when using silicon rubber gasket. b. Custom made gasket composed of five Parafilm sheets, with silicone o-rings (5/16" OD) sandwiched between them.

### 2.3.4. Support and manifold plates

Two other important components which must be tested through the pre-design step were the support plate for the filter plate as well as the manifold plate. Both of these components should be manufactured with a very resistant material since the pressure applied from both the process and the screws designed to tight the setup are high enough to bend the manifold and the support plates. The initial design used Delrin plates which were found to deform under the high compressive strengths that were needed. Thus, the final design used aluminum 6061-T6 plates (see details below). Eight small recesses designed on the manifold plate to align with the o-rings that were used in the gasket (see section 2.3.3).

## 2.4. Stirred well filtration development

After testing different issues related to the SWF module, the design was finalized as shown in Fig. 2.10 includes the following major components:

- The manifold plate (thickness of 0.9 cm; aluminum 6061-T6.) was designed to direct the flow from the syringe pump to the SWF module by means of microfluidic connectors (f-332nx; IDEX Health & Science) and 1/16” OD high pressure polyether ether ketone (PEEK) green tubing. By using this configuration, up to eight filtration experiments can be run at the same time in the eight wells that form a single column on any 96-well filter plate.
- A liquid tight seal between the manifold plate and the 96-well filter plate was ensured by means of the custom gasket which was made using two layers of Paraffin, each composed of five Parafilm sheets, with silicone o-rings (5/16” OD) sandwiched between them. The

gasket was re-made and replaced after conducting each experiment to avoid any potential leakage.

- The support plate (thickness of 0.6 cm; aluminum 6061-T6) is designed with an outlet channel (0.35" × 2.9") which allows for the filtrate samples to drop from the filter plate directly into the collection plate.
- Unlike the manifold and the filter plate support units, the base support and side wall components were made from Delrin® and all of these components were assembled using six thumb screws with 1/4-20 UNC thread designation. The average amount of torque applied to each screw was approximately measured via a torque wrench (17 N.m).
- A 9/32" OD, 9/64" ID washer made from Type 316 stainless steel (McMaster-Carr) was located (pressed via a pin) inside each well on the small 'shoulder' feature of the AcroPrep™ filter plates to prevent any contact between the magnetic stirrers and the membrane. It should be emphasized that the well diameter in most of the 96-well filter plates (including Pall AcroPrep™) is not uniform such that the top of the well has a larger diameter comparing with the well bottom. This feature helps to ensure that the washer will not be displaced during the experiments. A single tumble stir disc (diameter of 6.4 mm and thickness of 0.73 mm; V&P Scientific) made from neodymium-iron-boron (48 MGO) coated with 0.05 mm layer of parylene, was positioned on top of the washer in each well of the filter plate. Fig. 2.11 is a drawing of the details in each well of the SWF setup. Technical drawings are presented in Appendix A.
- The simultaneous, well by well stirring action of the disc in each well was performed via the Alligator Tumble Stirrer (V&P Scientific). The stirrer was used in the horizontal orientation with the speed controlled via a 120 volt 60 Hz controller; the actual rotation

speed (rpm) in the wells was measured from playing multiple slow-speed videos of the stir elements. The mixing regime of the tumble stir discs within each well is considered as an 'end-over-end' stirring with the disc rotating around an axis that is parallel to the membrane surface which is different than that typically used in a conventional stirred cell filtration module which has a cylindrical stir bar spinning in a tangential direction on an axis normal to the membrane surface [42,78]. For example, the mixing behavior of the stirred cell modules can usually be modelled by means of axisymmetric model geometry; however, because of the asymmetric nature of the mixing behavior here, a 3D model is needed. The mixing and flow regime will certainly affect the mass and momentum transfer properties which are usually present in both empirical and analytical equations.

As mentioned in Section 2.3, a programmable multi-rack syringe pump was used to perform all the constant filtrate flux experiments. The TMP in each well was monitored via eight (for eight wells) PC board mountable pressure transducers (Omega Engineering PX26-030GV) with a custom adapter to connect the Luer-Lok™ syringes, pressure transducers, and 1/16" OD high pressure tubing by microfluidic connectors (f-332nx; IDEX Health & Science and 18FTLL-1; Value Plastics Inc.). A C Series analog input data acquisition (DAQ) board (National Instruments) was used to process the pressure signal from each pressure transducer. A compiled executable file which was written using the LabVIEW 2011 Runtime Engine and used to monitor and export the pressure data to a computer. Fig. 2.12 is a screenshot of the compiled file when running an experiment. Note that Fig. 2.12 shows the amplitude (TMP changes in psi) in y-axis and each transducer was given a unique starting amplitude number to be differentiated from the other measurements. To generate the standard TMP curve the data was exported into MS Excel

and the initial amplitude was subtracted from all the recorded values with the appropriate unit conversions from psi to kPa.

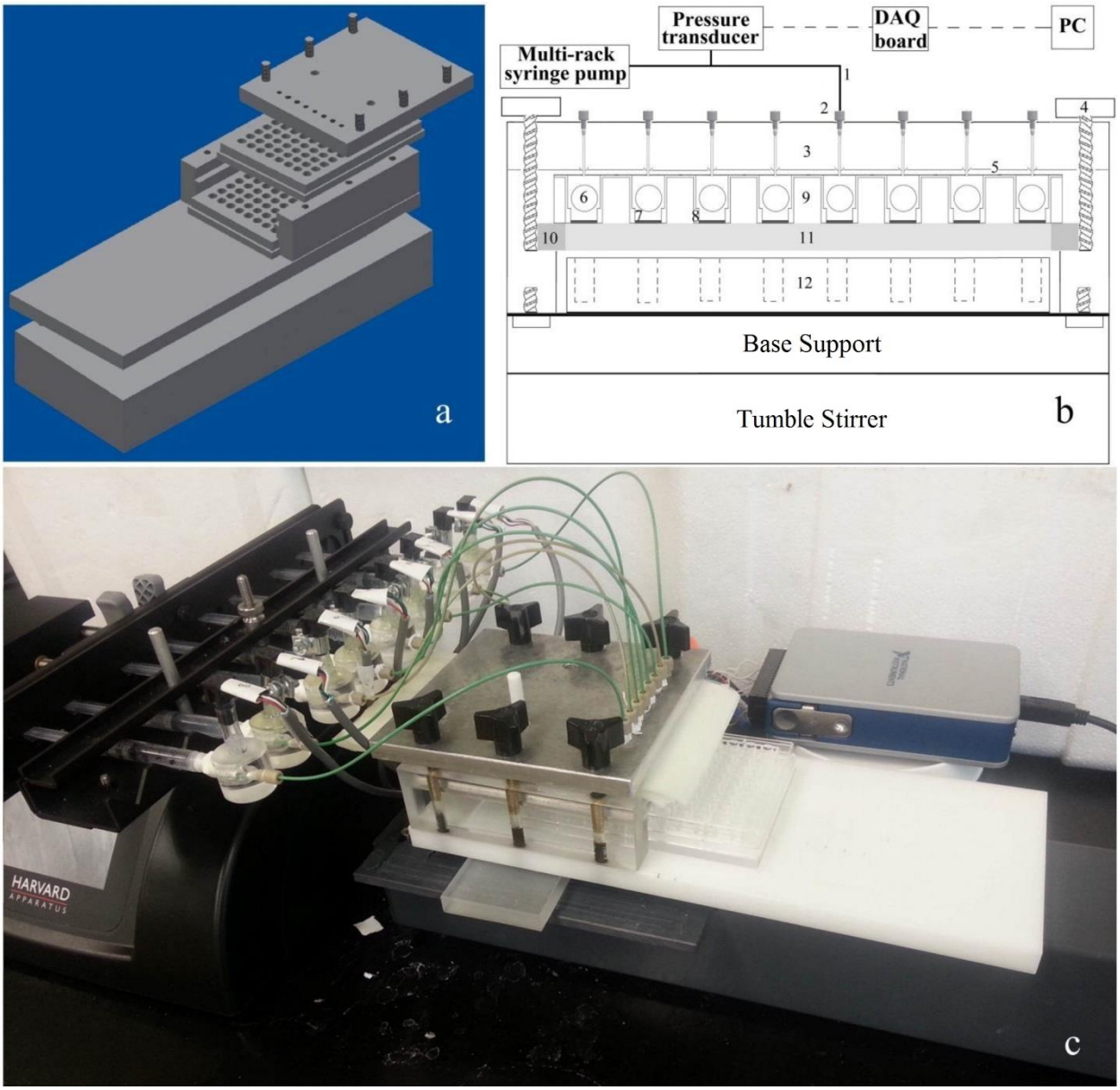


Figure 2.10. a. 3D image of the stirred well filtration (SWF) module. b. 2D diagram of the SWF module with the labeled components: 1. Tubing 2. Microfluidic connectors 3. Manifold plate 4. Thumb screw with fastener 5. Gasket 6. Magnetic tumble stir disc 7. Membrane 8. Stainless-steel washer 9. 96-well filter plate 10. Support plate 11. Support plate channel 12. 96-well collection plate. c. Picture view of the actual experimental setup with the SWF module integrated with the multi-rack syringe pump, custom adapters, pressure transducers, and DAQ board.

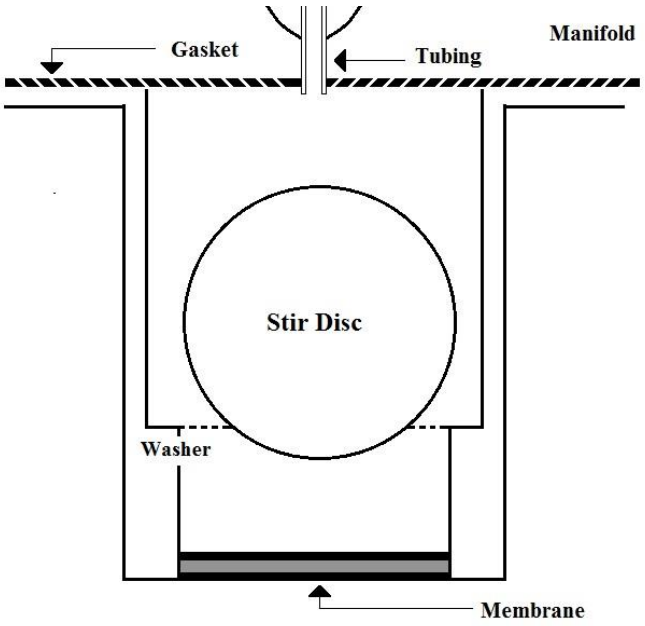


Figure 2.11. Schematic of a single well within the SWF module.

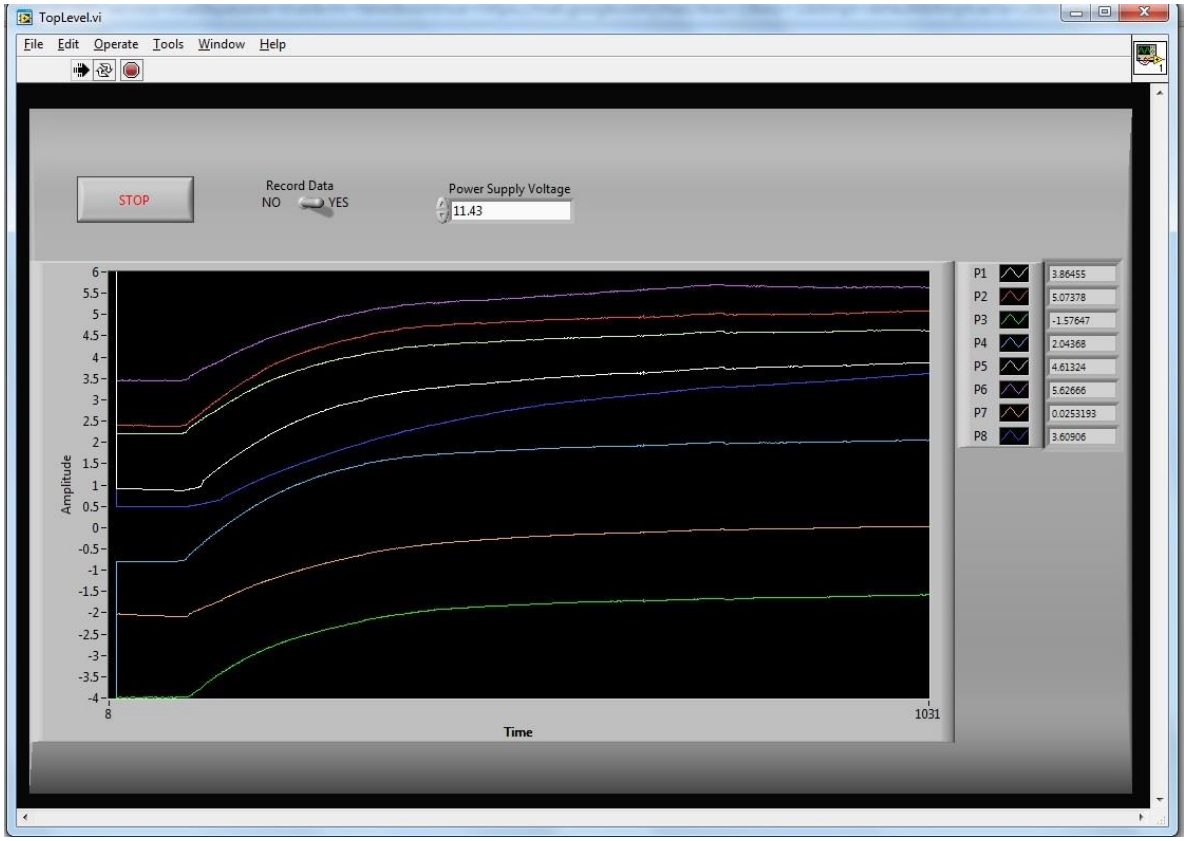


Figure 2.12. A screenshot of the compiled file when recording the amplitude (TMP in psi) data. The time unit recorded in x-axis is second.

## 2.5. Applications of SWF module to membrane filtration tests

The SWF module described above is ideally suited to conducting HT filtration studies. The application of this design to three membrane filtration goals/challenges is described below.

### 2.5.1. Standard filtration experiments

The features of the SWF module enable it conduct multiple number of standard membrane tests at once in a parallel fashion. For example, hydraulic permeability measurements can be used as one of the major membrane specifications [32,33]. As well, solute filtration experiments may be conducted and the results used to evaluate the effect of stirring conditions similar to conventional protein filtration studies [43,44]. The mentioned HT studies may assure the scalability, uniformity and reproducibility of the results obtained from SWF method. The developed module can also be used for the modeling of MF and UF processes using different mechanisms. Both MF and UF obey the basic mechanism of sieving with rejection of molecules whose size is greater than the membrane pore size. This mechanism is only valid for very dilute solutions. Darcy's law, which used permeability to relate the flux and applied pressure difference, can generally be used to describe the flux through an un-fouled membrane [55,61].The following is a modified version of Darcy's law where $L_p$ is the liquid permeability in m, J is the volumetric filtrate flux in m/s, $\Delta P$ is the transmembrane pressure in Pa and $\mu$ is the liquid viscosity in Pa.s:

$$J = \left(\frac{\Delta P}{\mu}\right) \times L_p \qquad (2.1)$$

The liquid permeability, $L_p$, is a function of pore size distribution and porosity of the membrane, in addition to viscosity of the permeate. There are two common approaches which could relate $L_p$ with the membrane structure. The Carman–Kozeny equation can be used when the membrane has an arrangement of near-spherical particles (like ceramic membranes) [55]. The Hagen–Poiseuille

equation on the other hand, is applied when the structure of the membrane can be assumed to be as uniform capillaries (e.g. track etched membranes). The flux can be described as the following using these equations:

$$J = \frac{\varepsilon^3}{K.\mu.A^2.(1-\varepsilon)^2}.\frac{\Delta P}{\delta} \qquad \text{Carman-Kozeny} \qquad (2.2)$$

$$J = \frac{\varepsilon.d_{pore}^2}{32.\mu.\tau}.\frac{\Delta P}{\delta} \qquad \text{Hagen–Poiseuille} \qquad (2.3)$$

where ε is membrane porosity, μ is dynamic viscosity of the filtrate, K is Carman-Kozeny equation constant, δ is the porous membrane thickness, A is specific area[7], τ and $d_{pore}$ are the tortuosity and the diameter of the capillaries.

### 2.5.2. Effect of concentration polarization and fouling

The HT features of the SWF module is ideal for studying membrane fouling behavior in stirred and unstirred conditions. The membrane surface can also be modified using conventional surface modification methods to investigate the effect of surface modification on fouling behaviour of the membrane as per the earlier studies by Zhou and colleagues [34,35]. A brief description on concentration polarization and fouling concepts is given below.

Concentration polarization is a natural result of the selective nature of membrane filtration processes. Hence, the particles or solutes are accumulated in a mass transfer boundary layer next to the membrane surface. This accumulation will reduce the thermodynamic activity of the solvents and the solvent flow through the membrane [55]. Although this phenomenon is inevitable,

[7] Surface area per unit of volume

it is possible to reduce its adverse effects on filtration performance (flux decline, permeability decrease, etc.) by using an appropriate method. Chudacek and Fane [44] have reported this phenomenon when performing an unstirred filtration experiment. They stated that the solute accumulation near the membrane surface and formation of an extra increasing barrier to the solvent flow is due to the fact that the solute is solely carried convectively. As a result, back diffusion phenomena happens which moderates this effect by decreasing the solute transport to the membrane surface. This is identical with what have been specified as concentration polarization layer in the previous part. However, the extent of concentration polarization layer in the bulk solution can be reduced by using a feasible method like mixing [79]. This results in higher solute transport when using constant pressure or lower TMP when using constant flux versus unstirred case.

Fig 2.13 shows the schematic demonstration of concentration polarization phenomenon in the boundary layer.

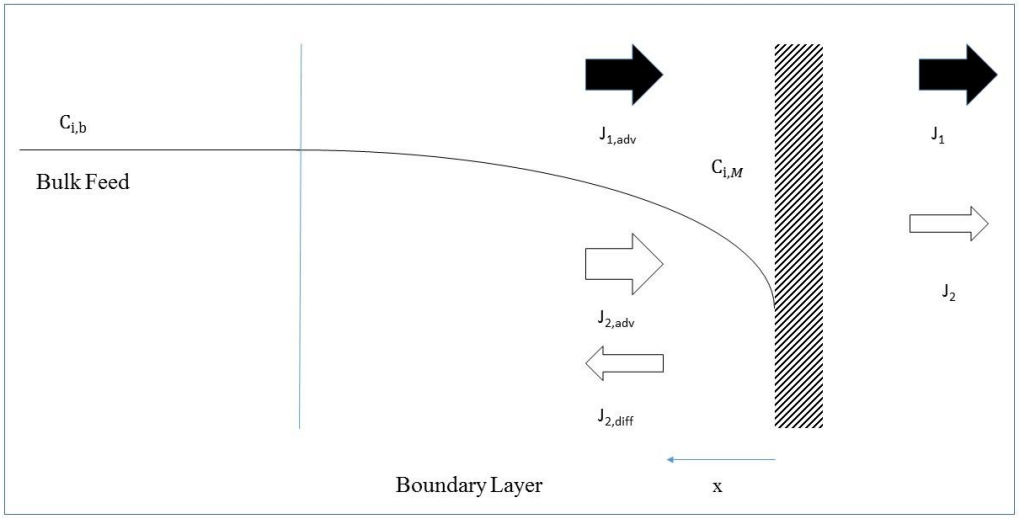


Figure 2.13. Demonstration of concentration polarization phenomenon in the boundary layer. Note that particle 2 is the considered as the particle which is mainly retained.

Under steady-state conditions the following relationships describe the relevant molar fluxes (in kmol/($m^2$s)).

$$j_{1,adv} = j_1 \quad (2.4)$$

$$j_{2,adv} = j_{2,diff} + j_2 \quad (2.5)$$

A number of assumptions are required in order to obtain an appropriate mass balance for this system:

- Steady state
- Diffusion obeys Fick's law.
- Negligible concentration gradient parallel to the membrane.
- No chemical reaction.
- Constant diffusion coefficient and density.

Considering these assumptions, the following expression can be written:

$$J.C_i = J.C_{i,P} - D_{ji}\frac{dC_i}{dx} \quad (2.6)$$

Considering the boundary conditions:

$$x = 0 \rightarrow C_i = C_{i,M} \quad (2.7)$$

$$x = L \rightarrow C_i = C_{i,b} \quad (2.8)$$

where $C_{i,M}$, $C_{i,b}$and $C_{i,P}$ are the membrane surface, bulk and permeate concentrations respectively. Solving Equation (2.6) gives the following:

$$J = \left(\frac{D_{ji}}{L}\right).\ln\left(\frac{C_{i,M}-C_{i,P}}{C_{i,b}-C_{i,P}}\right) \rightarrow C_{i,M} = \left(C_{i,b} - C_{i,P}\right).\exp\left(\frac{J.L}{D_{ji}}\right) \quad (2.9)$$

where L is the mass transfer boundary layer thickness. The term $\left(\frac{D_{ji}}{L}\right)$ is usually simplified as $k_{i,b}$, the mass transfer coefficient. The word concentration polarization is used for describing the higher average concentration of the mass transfer boundary layer which has an exponential relationship. Due to this higher concentration, the polarization is occurred in the bulk. For a fully rejected solute the equation becomes:

$$J = k_{i,b}.\ln\left(\frac{C_{i,M}}{C_{i,b}}\right) \qquad (2.10)$$

Fouling, on the other hand, can be defined as buildup of material on or in the membrane surface. In other words, foulants can simply be explained as non-dissolved materials which are either deposited on the membrane surface, on layers adhered to membrane surface, in the pore mouths or on walls, or a mixture of these conditions. There are several fouling formats including adsorption, pore blockage, deposition and gel formation. Adsorption occurs due to the specific interactions between the solute and the membrane which can lead to an additional hydraulic resistance. Extent of adsorption may be dependent on concentration which means that concentration polarization is a very decisive factor in such cases. Pore blockage on the other hand, can lead to flux reduction due to the partial or complete closure of membrane pores. A deposit of particles can form as in form of multi-layers on membrane leading to an increase in membrane resistance which is denoted as cake resistance. In case of concentrated solutions of macromolecules (e.g. proteins), a gel layer can be formed very close to the membrane surface [55]**.** In general, membrane fouling can be either hydraulically reversible or irreversible. Hydraulically reversible fouling can be cleaned using methods such as back washing; however, hydraulically irreversible fouling requires chemical cleaning. In some cases the fouling has a permanent effect

on membrane resistance and cannot be cleaned by chemical methods. This type of fouling is called chemically irreversible fouling [62].

The key influences of fouling can be categorized as two groups at this point: those that damage the membrane and those solely foul the membrane. However, a fouled membrane may be damaged if cleaning is not conducted with an extra care. Fouling itself can affect the filtration performance significantly during the operation especially on process permeability and selectivity. The extent of fouling can be influenced by many parameters including nature of solutes and solvents, concentration, membrane type, pore-size distribution, and hydrodynamics of the module. There are several types of foulants in various membrane processes such as inorganic precipitates, colloids, biological substances, macromolecules, proteins, and particulates [55].

Several methods have been proposed to reduce or eliminate the adverse effects of fouling on filtration performance. These methods are usually known as fouling prevention methods. Membrane cleaning, surface modification of the membrane, preparation of anti-fouling and self-cleaning membranes, and mixing are among the fouling prevention methods. It is well-known that one of the simplest and most common techniques to control the effects of concentration polarization phenomenon and membrane fouling is to introduce mixing near the membrane surface. Thus, SWF method can be very appropriate for performing fouling studies not only for its HT nature but also for the ability to perform stirred filtration in micro-scale format.

### 2.5.3. Membrane filtration process optimization

It is believed that membrane filtration pore size is not the only factor which is decisive in these processes [48,80]. In fact, membrane separation –especially ultrafiltration– is usually

considered as a complicated process depending on both hydrodynamic and physicochemical operational factors. To illustrate, changing physicochemical conditions can affect key parameters of the process such as concentration polarization, sieving coefficient and membrane fouling significantly [48,51,52,54,76,81]. A number of studies related to effect of physicochemical conditions on membrane filtration are presented in the following paragraphs.

pH and ionic strength are usually considered as two key physicochemical factors affecting membrane filtration performance by affecting the particle-particle and particle-membrane interactions. Some phenomena like a minimum in flux at the isoelectric point and the effect of salt on filtration performance are common as showed by different authors [48–51,53,54,82]. In terms of fouling, particle-membrane interactions influence the filtration behavior in the initial stages of the process and particle-particle interactions have an effect during the entire process. Typically, fouling is more extensive when the solute (e.g. protein) in the feed solution is uncharged[8] (pH=isoelectric point). Moreover, very low salt concentration can contribute to severe membrane fouling. Additionally, very high concentration of salt can cause protein precipitation and enhance hydrophobic membrane-protein interactions and increase the extent of fouling [48].

Regarding the sieving coefficient, the highest sieving coefficient of a protein, for example, is observed at pH close to its isoelectric point when it is uncharged. In pH other than protein isoelectric point an electrostatic double layer is formed around the protein molecule in the solution. The electric double layer increases the protein size. This factor is one of the reasons why the sieving coefficient is at its optimum in pH close to protein isoelectric point. Another reason why protein isoelectric point has the highest sieving coefficient is the membrane charge which can be

[8] Positive and negative charges neutralize each other.

affected by pH change as well. When the membrane has the same charge as the protein, presence of repulsion forces can cause reduction in sieving coefficient. If the membrane carries an opposite charge comparing with the protein, a protein layer is formed due to the charge adsorption which has the same charge as the protein has and it decreases the sieving coefficient because of the repulsion force between adsorbed layer and the protein. The salt concentration effect on sieving coefficient is generally considerable when the protein is charged. However, salt concentration has no significant effect on sieving coefficient when the protein is uncharged. As expected, pH and ionic strength have a substantial effect on protein fractionation when using mixture solutions [48,83,84]

Fane et al. [82] have observed that increase of ionic strength in isoelectric point has a different effect comparing with other pHs when doing BSA ultrafiltration experiments. At isoelectric point, increase of ionic strength from 0 M to 0.2 M increased the permeability rapidly while an increase from 0.2 to 0.8 had a little effect. In the meantime, ionic strength increase in higher and lower pHs (2 and 10) have resulted in decrease of permeability. They have also reported that increasing the pH to 10 has increased the flux itself. The flux-pH plot have suggested that there is a distinct minimum in the absence of salt while there is no minimum present when salt is present and the flux rises monotonically from pH 2. It was also observed that protein adsorption plays an important role in variation of flux with ionic environment. For example, BSA adsorption is reported to be the highest under ultrafiltration condition at pH 5 and will be increased when salts present.

IgG and BSA were used by Saksena and Zydney [54] to prove that it is feasible to obtain an effective separation even for proteins with comparable molecular weights by adjusting the pH and ionic strength. By using pH 4.8 IgG was excluded from the membrane pores since it has a

positive charge which resulted in a low sieving coefficient for IgG and an effective separation. It has also been reported that the BSA flux is strongly reduced when using low salt concentration at pH 7.4 which could be due to the strong electrostatic exclusion of the negatively charged BSA from the membrane pores under the mentioned conditions. Extent of protein adsorption, bulk mass transfer coefficients and actual membrane transport properties were all reported to be functions of ionic strength and pH. For example, the extent of adsorption in single protein filtration and the free solution diffusivity are maximum and minimum respectively in protein's isoelectric point**.**

Ghosh and Cui [51,52] have also reported that the fractionation of BSA and lysozyme are highly dependent on pH of the solution and the highest protein transmission occurs near the isoelectric point of the protein. They have reported a wide range for BSA-lysozyme separation with selectivities from 3.3 at pH 5.2 to 220.0 at pH 8.8. This phenomenon has been considered to be due to the positive charge existing on lysozyme in higher pH.

It should be noted that protein filtration process is not the sole filtration process which depends on physicochemical conditions. For example, NOM behavior in filtration process is believed to be highly dependent on pH, ionic strength, presence of divalent metal cations and chelating agents [85] as well as membrane pre-treatment and surface modification [34,35].

Therefore, membrane filtration operations are complicated processes which need optimization considering several operational factors. As a result, usage of statistical methodologies such as design of experiments (DOE), response surface modeling (RSM) and genetic algorithm (GA) is required in order to find the optimum operational conditions. SWF technique is compatible with such methodologies since it is capable of performing up to 8 parallel experiments in a short period using insignificant amount of sample. Similar optimization approaches have been used in

earlier HT studies with for other downstream processes such as chromatography as reported by Chhatre and Titchener-Hooker [26].

# Chapter 3: Materials and methods

## 3.1. Materials

### 3.1.1. Buffers

A phosphate buffered saline (PBS) solution that was made by diluting a 10× concentrated buffer solution (Sigma Aldrich) with distilled, deionized water from a Millipore Milli-Q system was used as buffer to prepare the majority of solutions. The solution pH (7.4 ± 0.1) was measured using a sympHony™ SB20 meter (VWR). A limited number of experiments (refer to section 4.4) were performed in altered buffer conditions to assess the effect of solution pH and ionic strength on membrane filtration performance. The 'high' salt buffer included the following: 137 mM NaCl, 2.7 mM KCl, 10 mM $Na_2HPO_4$ and 2 mM $KH_2PO_4$ in Milli-Q water [86]. The 'low' salt buffer included the following: 10 mM $Na_2HPO_4$ and 2 mM $KH_2PO_4$ in Milli-Q water. Where necessary the solution pH was adjusted by the addition of a small amount of concentrated HCl solution [54].

### 3.1.2. Protein solutions

Various protein concentrations were used through different experiments of this work. The majority of the experiments were performed using protein solution that was made by diluting BSA (Sigma Aldrich) to a final concentration of 125 µg/ml in PBS solution. All protein solutions were pre-filtered using 0.2 µm Supor® membrane syringe filters (Pall 4612) to eliminate any protein aggregates. Protein solutions were prepared at least 1 day prior to each experiment, and then stored at 4 °C overnight, in order to ensure that there was not any foam present in the final solution. A limited number of solutions were prepared to perform experiments with higher concentrations of protein solutions (0.25 mg/mL and 1 mg/mL as described in sections 4.3 and 4.4 respectively) and in altered buffer conditions.

### 3.1.3. Pall 96-well filter plate with Omega™ membrane

The AcroPrep™ 96-well filter plate from Pall with an Omega™ UF membrane with a nominal molecular weight cut off (MWCO)[9] of 30 kDa (Pall 5035) was selected for this work. Previous studies have used the same membranes in the conventional stirred cell device for protein [53,66,87] and virus [88] filtration applications. Table 3.1 shows the general specifications of 96-well filter plates; a picture of the plate is shown in Fig. 3.1.a. For the 350 µL plate, the ratio of well volume to membrane area is comparable to the values reported in Table 2.1 for the stirred cell device. The Omega™ membrane is a modified version of PES membrane with an ultrathin functional PES skin layer to control the sieving properties of the membrane, a porous PES substructure and a porous support matrix [89]. The PES chemical structure is shown in Fig. 3.1.b. This membrane is available in four different MWCO values: 3 kDa, 10 kDa, 30 kDa, and 100 kDa. According to the manufacturer, it exhibits low protein binding, high flux, high selectivity and high stability to biological and physical degradation. It has been used by many researchers in previous membrane studies in various formats (membrane discs, membrane sheets, and filter plates); these studies are described in Chapter 4.

PES and PES-based membranes are one of the key polymeric materials and are commonly used in various filtration processes because of outstanding oxidative, thermal and hydrolytic stability as well as good mechanical properties [70,71]. These membranes which are prepared with phase inversion method have normally an asymmetric structure. The final membrane structure is influenced by various factors including temperature, concentration, solvent and additives of PES solution. The main disadvantage of PES membranes is related to their relatively hydrophobic

[9] Molecular weight cut-off or MWCO is defined as the lowest molecular weight solute (in kilodaltons) in which more than 90% of the solute is retained by the membrane.

character which can greatly affect the membrane fouling. Adsorption of nonpolar solutes and hydrophobic particles are widely reported as the main cause of membrane fouling which can result in poor separation performance, higher energy demand and shorter membrane lifetime [71].

PES membranes are also widely employed in biomedical fields (e.g. tissue engineering and dialysis devices). However, blood proteins will rapidly adsorb onto the surface of the PES membrane and the adsorbed protein layer can cause further undesirable results. Therefore, the blood compatibility of PES membrane is not adequate [71,90,91] Furthermore, PES membrane is stable in water and is an inert membrane, and acts only as a barrier in separation process, thus not fitted to the complex separation processes when not modified. The current trend is to develop new modification methods of common polymers or membranes, such as PES and PES-based membranes to increase the antifouling property, biocompatibility and other specific functions [71].

Table 3.1. AcroPrep Pall 96-well filter plate specifications

| **Well Bottom Area ($cm^2$)** | **Max Well volume (µL)** | **$\frac{\text{Max Well volume (mL)}}{\text{Well Bottom Area } (cm^2)}$** | **Dimensions (cm;H/L/W)** | **Max Well Diameter (cm)** | **General Applications** |
|---|---|---|---|---|---|
| 0.25 | 350 | 1.4 | 1.4/12.8/8.6 | 0.75 | Pre-filtration, Particulate removal, and Cell harvesting |
| 0.25 | 1000 | 4 | 3.3/12.8/8.6 | 0.75 | |

a

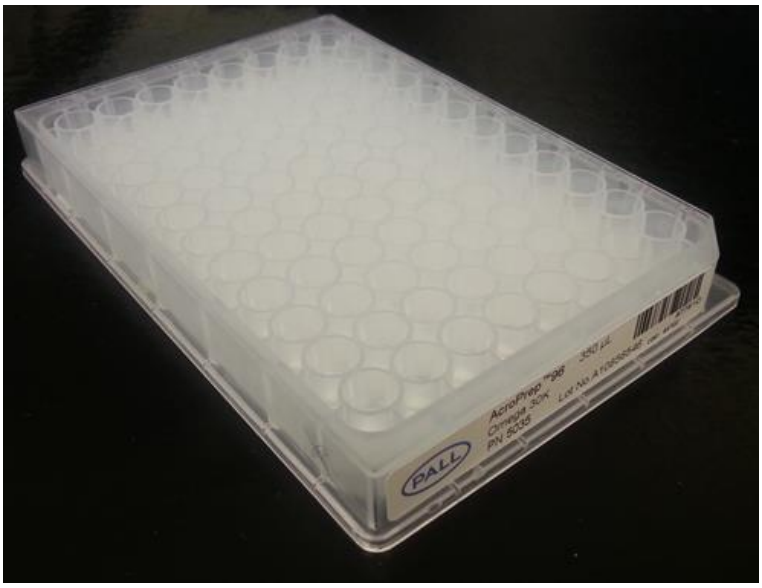

b

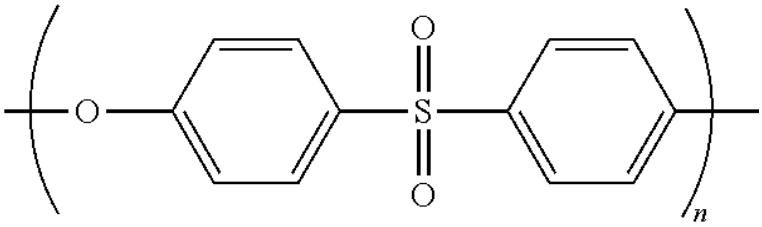


Polyethersulfone (PES)

Figure. 3.1. a. AcroPrep Pall 96-well filter plate with 30 kDa Omega$^{TM}$ membrane. b. Polyethersulfone (PES) structure (credits [92]).

## 3.2. Methods

### 3.2.1. Hydraulic permeability and volume measurement

The hydraulic permeability ($L_p$) of the membrane discs in the individual wells of the 96-well filter plate was determined according to Equation 2.1. Experiments were performed using a PHD multi-rack syringe pump (Harvard Apparatus) to set the flow rate simultaneously in up to eight different wells. The filtrate flux was calculated by dividing the flow rate by the membrane surface area (0.25 $cm^2$) using the appropriate unit conversions. The actual filtrate flux (J) was verified by timed collection of the PBS solution from each well with the amount of solution measured from absorbance readings at 977 nm [35] using a PowerWave XS microplate reader

(from BioTek). This method has been used earlier to measure the liquid volume in multi-well format [35]. The calibration curve (Fig. 3.2**)** was prepared by plotting absorbance at 977 nm against different volumes of water using transparent half area (Corning® Costar® 3695) or regular 96 well plates (Corning® Costar® 3596) plates. Residuals plot for Fig. 3.2 is available in Appendix B. Although the model plot (Fig. 3.2) presents a fairly linear trend in both regular and half-area plate cases, a slight non-linearity was observed according to residuals plot for the half-area plate which shows some type of trend in its residuals plot (Fig. A5). The applicability of this method for protein samples has been verified in earlier studies [35] and it was reported that proteins do not absorb at this wavelength, while water shows an absorbance peak. The actual filtrate flux (J) was also verified by weighing the collection plate before and after the runs as well as weighing pre-filled and used syringes before and after the experiments. The flow rates set by the syringe pump were within 5% of those measured in the collection plate using the micro-plate reader (977 nm) and syringe/plate weighing methods using balance (Fig. 3.3). The solution viscosity (μ) was evaluated using literature data. The hydraulic permeability experiments were conducted in an unstirred format. All the permeability and protein filtration experiments (as described in the next sections) were conducted at room temperature.

As mentioned in chapter 2, eight PC board mountable pressure transducers (Omega Engineering PX26-030GV) were used to monitor the pressure in each well during the filtration experiments. The typical data for TMP measurement is shown in Fig. 3.4. Note that the pressure increases initially when changing the flux (adjusted by syringe pump) and then it plateaus rapidly (between 150 seconds to 450 seconds depending on the flux) and remains properly constant. The delay in pressure reading is believed to be due to the pressure transducer nature. The average pressure in the final 15 seconds was used as the TMP in hydraulic permeability analysis.

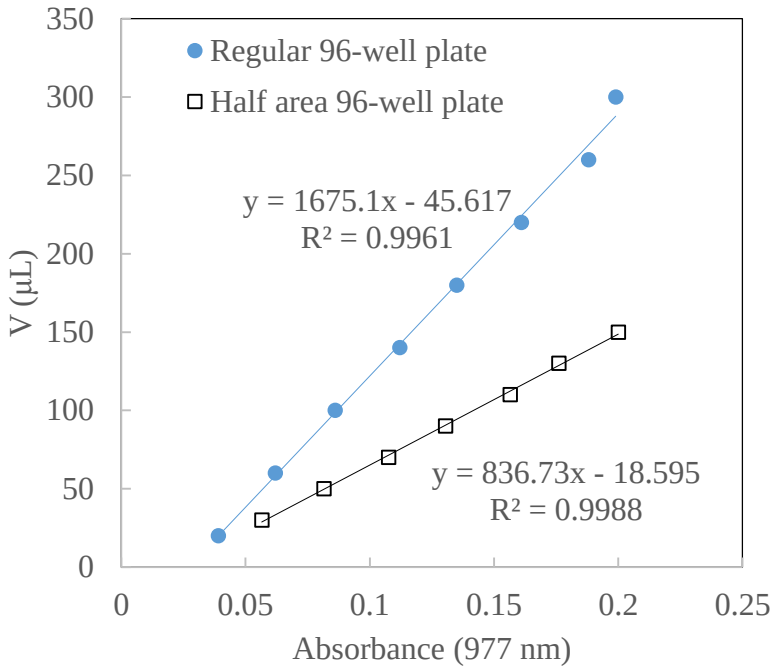


Figure 3.2. Volume calibration curve at 977 nm using: regular and half area 96-well plate.

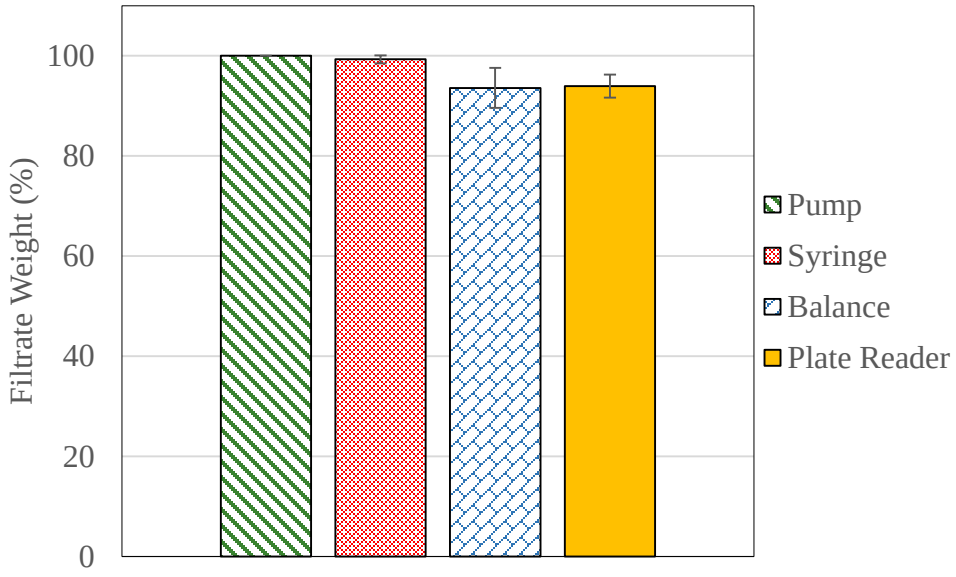


Figure 3.3. Flux verification of the operation via balance and 977 nm absorbance.

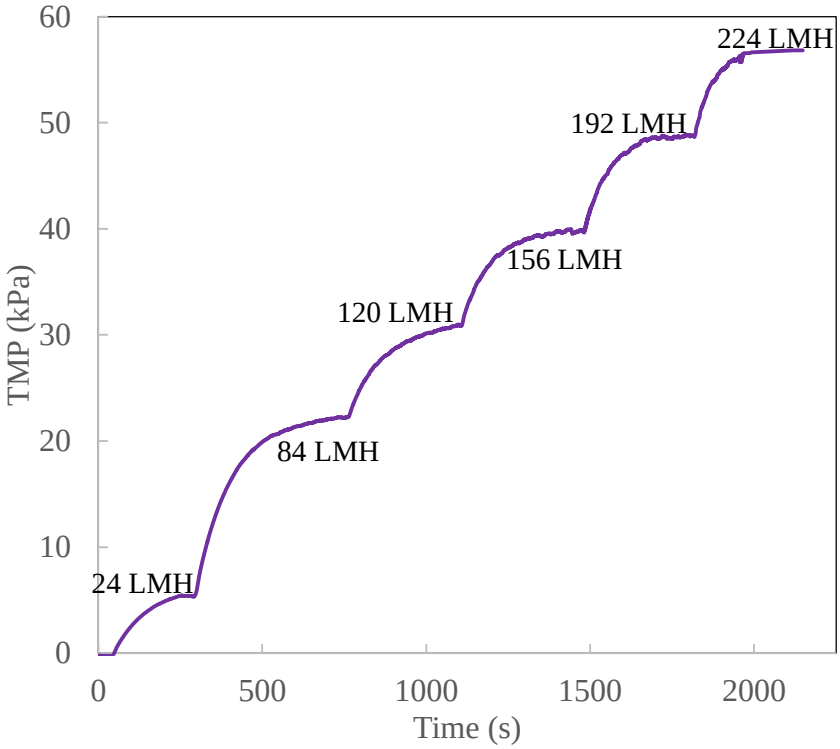


Figure 3.4. Typical data for TMP profile for a single well on 96-well filter plate. The step changes in filtrate flux settings are displayed for comparison on the end of each profile.

### 3.2.2. Protein filtration experiments

After preparing the BSA solutions, they were loaded into 3 mL Luer-Lok™ syringes (BD Biosciences) and connected to the pressure transducers by a custom adapter described in Section 2.4. The same protein solution was used for pre-filling of all of the tubing and wells before starting any experiment to prevent the adverse effect of the introduction of any air bubbles. A feed solution sample was taken from each well before starting each experiment. For the stirred experiments, the magnetic stir elements were also added to each well when filling it with the protein solution. The SWF module was assembled and then the tumble stirrer and the syringe pump were turned on. The protein filtration experiments were performed at filtrate flow rates of 5, 15, and 25 µL/min (corresponded to flux values of 12, 36 and 60 LMH). Transparent half area (Corning® Costar® 3695; maximum volume = 180 µL) or regular 96 well plates (Corning® Costar® 3596; maximum

volume = 350 μL) were used as the collection plates depending on the collection volume. Collection of multiple samples from each well was done by manually moving the collection plate in an orthogonal direction such that up to eight filtrate samples were collected at the same time from eight wells. The samples were temporarily stored at 4 $^{o}$C prior to disassembling the SWF module and then post-filtration samples of the bulk solutions were collected. The individual wells were washed out with PBS buffer and Milli-Q water before reassembling the module for another sieving experiment or hydraulic permeability test.

The membrane filtration performance is presented using sieving coefficient results. In membrane processes, either the observed sieving coefficient ($S_o$) or actual sieving coefficient ($S_a$) are used to quantify the filtration performance. The former is defined as the ratio of filtrate concentration to bulk concentration and thus ranges from zero to one for fully rejected and fully transmitted solutes respectively. The latter is defined as the ratio of filtrate concentration to wall concentration and it depends on hydrodynamic conditions, the membrane properties, physicochemical conditions, and particle-particle and particle-membrane interactions. In most membrane filtration processes the two values are different and they are often used for modelling of the complex hydrodynamics in case of stirred cell filtration modules. In such processes, a stagnant film model is used to explain the protein concentration profile above the membrane. A full description of the stagnant film model is beyond of the scope of this work; more information can be found in Blatt et al. [93]. Note that all the reported results for sieving coefficients in this work are related to the observed sieving coefficient ($S_o$).

### 3.2.3. Protein content quantification

The Pierce™ BCA protein assay kit (Thermo Scientific) was used to quantify the BSA concentration in the feed and filtrate samples. According to the kit instructions, 25 µL of sample and 200 µL of BCA working reagent (WR) were gently mixed in a UV-transparent 96-well microplate by repeated aspiration and dispensing (Costar® 3596, Corning Inc.) and then incubated at 37 $^{o}$C for 30 minutes. The WR itself was made by mixing reagents A and B in a 50:1 ratio. As shown in Fig 3.5, the protein concentration is exhibited by a color change of the WR from green to purple in proportion to the protein concentration. The solution absorbance was measured at 562 nm via the PowerWave XS microplate reader (BioTek). Actual BSA concentrations were determined by comparison with a standard calibration curve – see Fig. 3.6 for typical results. Final feed samples were analyzed in triplicate. BCA assay was found to be more appropriate comparing with other protein quantification assays such as Bradford in terms of concentration ranges, accuracy, and linearity. Appropriate regression analysis was performed to determine the linearity. Residuals plot for Fig. 3.6 is available in Appendix B. Although the model plot (Fig. 3.6) shows a reasonably linear trend in both low and high concentrations, a slight non-linearity was observed according to residuals plot for the high BSA concentrations which shows some type of trend in its residuals plot.

The BCA assay principally relies on two reactions: first, reduction of $Cu^{2+}$ ions (in form of cupric sulfate) to $Cu^{+}$ by the peptide bonds in protein. The amount of $Cu^{2+}$ reduced is proportional to the amount of protein present in the solution; second, two molecules of bicinchoninic acid (BCA) chelate with each $Cu^{+}$ ion to form a purple solution which significantly absorbs light at a wavelength of 562 nm. This assay can be modified using lower or higher temperatures (e.g. room

temperature) and WR-sample ratio (in case enough sample is not present); however, these modifications could affect the assay sensitivity.

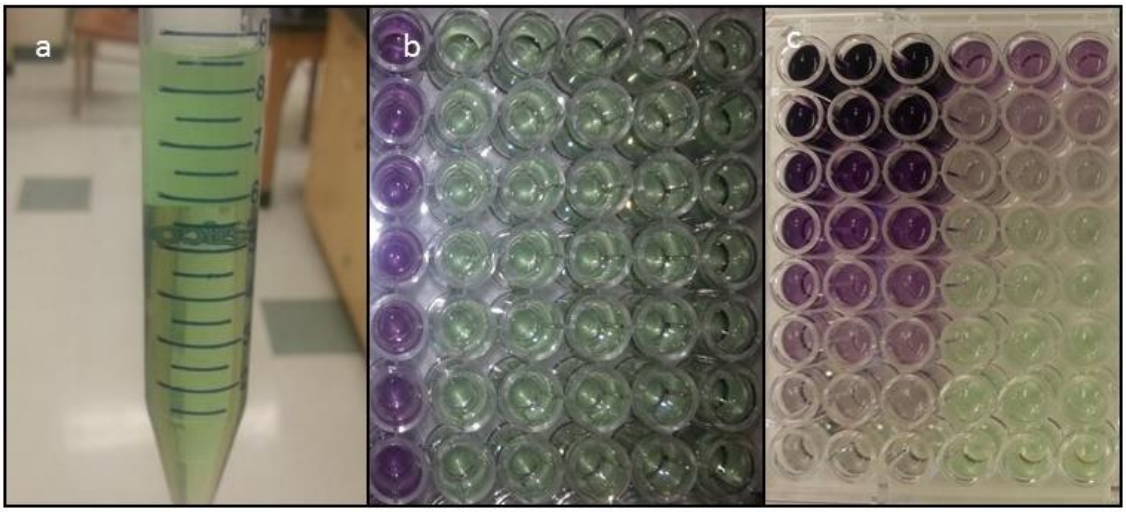


Figure 3.5. a. BCA working reagent. b. BCA assay unknowns. c. BCA assay calibrations.

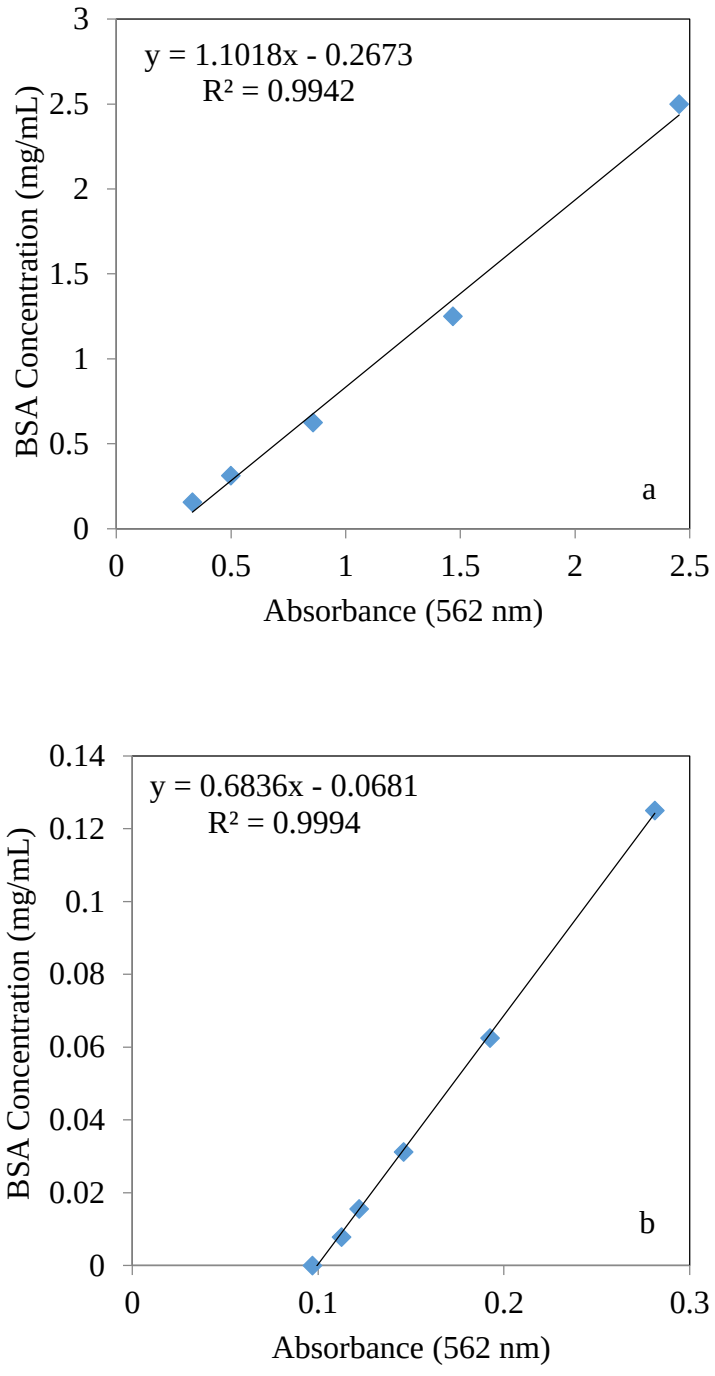


Figure 3.6. BCA assay calibration curves using BSA in a. high concentration range; and b. low concentration range.

### 3.2.4. High-throughput membrane fouling test

The effect of stirring on membrane fouling during protein filtration experiments was evaluated by designing and developing a five step high-throughput test as described below. The permeability of the native (i.e. un-tested) membrane ($L_{p0}$) in multiple wells was measured using the method described in section 3.2.1. Then a subset of the wells was used for stirred BSA filtration experiments and the remaining wells were used for unstirred BSA filtration experiments. These experiments were conducted with a higher BSA concentration (0.25 µg/ml) at a filtrate flux of 60 LMH to make fouling assessment more feasible. After collecting the final feed samples, a membrane washing procedure was performed such that each membrane was rinsed thoroughly about 10 times using Milli-Q water and PBS buffer. Next, an intermediate permeability measurement was performed on each well to evaluate any effects due to the protein fouling in both stirred and unstirred conditions. Subsequently, a second BSA filtration run was conducted but the wells which were previously designated for unstirred filtration were now assigned for stirred filtration and vice versa. Lastly, the membrane cleaning procedure was done once more according to the method described above and the final membrane permeability was measured.

# Chapter 4: Results and discussions

## 4.1.Multi-well measurements of hydraulic permeability

The dependence of filtrate flux of buffer solution on TMP is shown in Fig. 4.1.a and Fig. 4.1.b for the sixteen wells in two columns (eight wells, labeled A through H, per column) of the Omega™ 30 kDa membrane AcroPrep filter plate. All of the results for one column were collected simultaneously in a single experiment. Although the experiments were done by altering the filtrate flux, via the syringe pump settings, and recording the required TMP by means of eight pressure transducers, according to the standard convention in the field of membrane processing, Fig. 4.1.a and Fig. 4.1.b are shown as filtrate flux versus TMP. The results in Fig. 4.1 were collected from step-wise increases in the filtrate flux from the lowest value, 24 LMH (10 µl/min), to the highest value, 228 LMH (95 µl/min). As stated in section 3.2.1, the flow rates set by the syringe pump were approximately within 5% of those measured in the collection plate using the micro-plate reader (977 nm) and syringe/plate weighing methods using balance (Fig. 3.3**)**. This issue may be result of minor sample evaporation and measurement errors.

The observed linearity between the filtrate flux and TMP values was encouraging for all sixteen wells; the linear line of best fit for each well (i.e. membrane) is shown in Fig. 4.1 for comparison. Table A1 in Appendix C summarizes all of the hydraulic permeability results along with R-squared values for the filtrate flux vs TMP plots. Fig. 4.2 is plotted using Equation 2.1 in order to calculate the hydraulic permeability of each membrane disc at the bottom of a well. As seen in Fig. 4.2, there was not any observed trend between the hydraulic permeability values and well position of each set of the experiment within the column on the 96-well filter plate. Hence, the hydraulic permeability results using SWF setup seem to be independent of the well assignment. A previous study using a 96-well filter plate with MF membranes found that the variation in

hydraulic permeability was greater within a column (numbered 1–12) compared to along a row (labeled A–H) [33]. The 95% confidence intervals of the slope of flux versus TMP results are shown as error bars in Fig. 4.2. In general the results in Fig. 4.2 were fairly consistent across all the wells with an average permeability (shown as horizontal line) of $1.19\times10^{-12}$ m. The data presented here are in good agreement with the literature and manufacturer's technical information. According to the manufacturer, the hydraulic permeability of the Omega™ 30 kDa membrane discs ranges from $0.86\times10^{-12}$ to $1.80\times10^{-12}$ m depending on the size of the actual disc. Furthermore, a value of $1.05\times10^{-12}$ m was reported by Yuan and Zydney [94] for the hydraulic permeability of 25 mm diameter Omega™ 30 kDa membranes. The coefficient of variation for the permeability results in Fig. 4.2 was 10.7%. This value is in good agreement with previous studies that reported a range from 4% to 16% for measurements using MF [32,33] and UF [35] membranes.

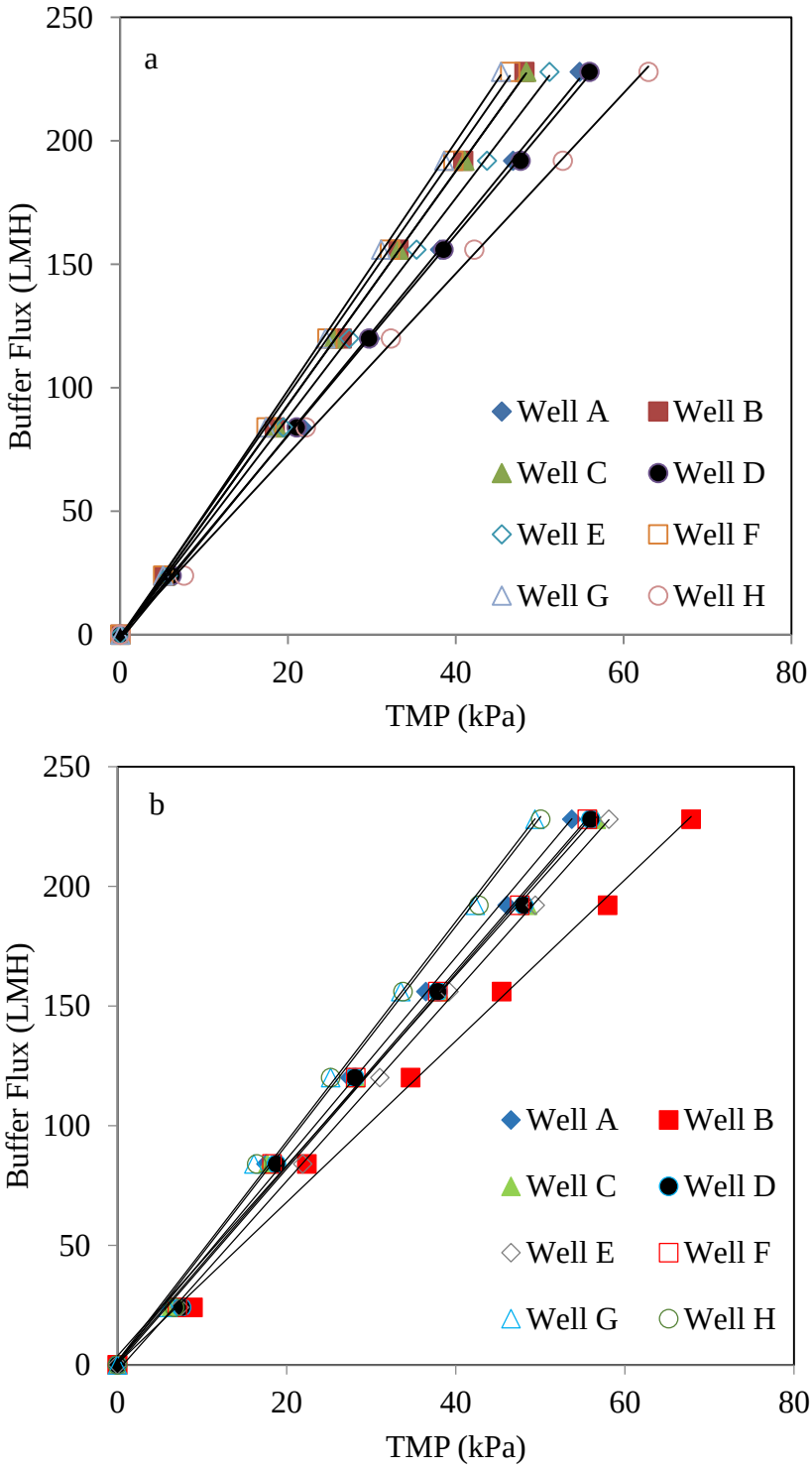


Figure 4.1. a. Filtrate flux as a function of applied pressure for 30 kDa Omega™ membranes in the eight wells of a single column (column 1) on the 96-well AcroPrep filter plate. The linear model of best fit of the data for each membrane is shown for comparison. b. Filtrate flux as a function of applied pressure for 30 kDa Omega™ membranes in eight wells of column 2 (identical to panel a).

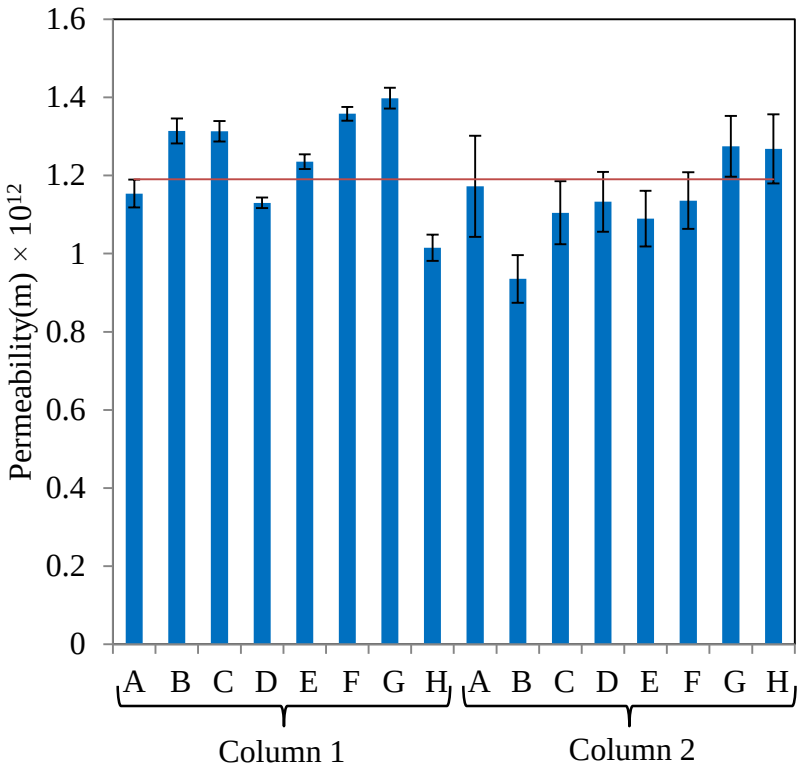


Figure 4.2. Hydraulic permeability results using the SWF module for the same sixteen wells of the 30 kDa Omega™ membranes from Figure 4.1. The horizontal line represents the average permeability for all sixteen membranes.

## 4.2.Multi-well evaluation of protein filtration

In order to determine if the stirring conditions are a critical process parameter for HT screening of filtration processes, a series of constant flux filtration experiments with dilute BSA solution (125 μg/ml) were conducted using the SWF module. Previous studies have used a similar approach with conventional stirred cell devices. For example, Chaudacek and Fane [44] studied the effects of concentration polarization on the filtration performance of a UF membrane for both stirred and unstirred conditions. Ghosh and Cui [51] optimized the separation of BSA and another model protein in a UF process by varying the solution pH and membrane properties. Typical TMP

profiles for processing of the BSA solution through the 30 kDa Omega™ membrane are shown as a function of filtrate volume in Fig. 4.3. The three panels on the left-hand side were done without stirring; each panel is for a different filtrate flux value and shows the TMP profiles for the eight individual wells in one column of the AcroPrep filter plate. The uniformity and reproducibility of the results across all eight wells is quite apparent – the only exception was a single well at the lowest filtrate flux of 12 LMH (5 μl/min). The reason for this single inconsistency is not clear, however it could simply reflect an obstruction in the tubing between the transducer and the SWF module. The LabVIEW program records the TMP immediately from when the syringe pump is turned on, at the desired flow rate, and thus each profile starts at zero pressure for zero filtrate volume. For all three filtrate flux values, the TMP increased in a fairly uniform fashion with increasing amount of total filtrate volume. For example at 36 LMH (15 μl/min), the average TMP (± coefficient of variation) for the eight wells increased from 10.0 (± 9.0%) kPa at 200 μl to 37.8 (± 11.6%) kPa at 1000 μl. In order to compare the different experimental conditions, we chose to report the average final TMP value. The greatest increase in TMP with filtrate volume was seen at the highest filtrate flux (60 LMH) where the average final TMP was 64.2 (± 6.4%) kPa. The slight discontinuities within some of the TMP profiles of Fig. 4.3 are simply caused by a brief pause of the syringe pump in order to move the 96-well collection plate ahead one position. A progressive increase in TMP during constant flux filtration is a well-known phenomenon and is attributed to the effects of concentration polarization and fouling [48,50,76]. The molecular weight of the BSA protein (66.5 kDa) is more than double the MWCO of the membrane used in this study and thus this pair is ideally suited to probe the effects of concentration polarization on membrane filtration performance.

The three panels on the right-hand side of Fig. 4.3 show TMP profiles for processing the same BSA solution through the 30 kDa Omega™ membrane at the same three filtrate flux values but with stirring in each well of the SWF module. The rotational speed of the magnetic stir discs was set to approximately 350 rpm via the tumble stirrer speed controller. Again, the uniformity and reproducibility across the eight wells of the filter plate for each filtrate flux is quite good. At the highest filtrate flux (60 LMH) there is slightly more variation in the TMP profile compared to the lower ones. It is readily apparent that the TMP profiles depend quite strongly on the stirring conditions within the individual wells of the filter plate. At 12 and 36 LMH, the TMP profile with stirring exhibits an initial increase but then plateaus at a constant TMP value out to the highest filtrate volume collected. At 60 LMH, the TMP profile increased with filtrate volume to an average final TMP value (± coefficient of variation) of 24.6 (± 38.5%) kPa but at a much lower rate compared to that shown in the left-hand side panels that were conducted without stirring. The high coefficient of variation at this filtrate flux is primarily due to the results that were collected for one well; the coefficient of variation decreased to 23.6% when this well was excluded. A similar comparison at the lower filtrate flux values revealed that the average final TMP without stirring was approximately 3.8 and 7.5 times higher than that with stirring at 36 and 12 LMH respectively.

The results obtained with the SWF module are consistent with previous studies that used the conventional stirred format. For example, Chudacek and Fane [44] observed an increase in membrane resistance during BSA filtration through 10 kDa membranes in unstirred conditions. They also reported a progressive membrane fouling and attributed this behavior to membrane-solute interaction. Fane [43] compared the membrane performance of colloidal silica solutions in both stirred and un-stirred conditions during constant pressure filtration (Fig. 4.4 is adapted and modified from that study). The incorporation of stirring above the membrane surface resulted in

higher filtrate fluxes. Ghosh [76] has reported that the fouling in constant flux filtration is more rapid and non-linear during the initial filtration period due to the combined effects of rapid initial fouling and concentration polarization. However, the pressure increase was reported to be linear and slower after the initial rapid increase. The combined effects of rapid initial fouling and concentration polarization were observed in most panels of Fig. 4.3 of this study as well. Also, it has been reported that the increase in TMP and the slope of the linear region both raise by increasing the flux which is the case in filtration experiments in this work [48,76].

From the same experiments that gave the TMP vs filtrate flux results in Fig. 4.3, a comparison of BSA transmission through the Omega 30 kDa membranes was made as described below. For each individual well, the observed sieving coefficient ($S_o$) was evaluated as the ratio of the BSA concentration in the first 200 µl of filtrate solution to the feed concentration in the well. The feed concentration was determined from an average of the initial concentration and feed concentration after filtering 200 µl[10]. The average sieving coefficient from the eight experiments that were conducted for a given filtrate flux and stirring condition are displayed in Fig. 4.5. At each filtrate flux, the standard deviation of the sieving coefficient values for the stirred experiments is significantly smaller than that for the unstirred experiments. If it is assumed that the sieving coefficient results for both tests follow the t-distribution, the Student's *t*-test revealed that there is no statistical difference between the stirred and unstirred filtration results at both 12 and 36 LMH; the 95% confidence interval of the difference of the sample means includes zero. However, at 60 LMH the average sieving coefficient from the stirred experiments (7.1% ± 0.8) is statistically different than that for the unstirred experiments (4.6% ± 1.7); the 95% confidence interval for the

[10] Note that since it was not possible to take a feed sample after 200 µl, this concentration was found by interpolation of initial and final concentrations of the retentate solutions.

difference of the sample means does not include zero. Additional details on the statistics are provided in Table 4.1**.**

Overall, the results from Fig. 4.3 and Fig. 4.5 prove that the stirring conditions in HT filtration tests have a significant effect on the membrane process performance. Previous studies have used experimental data from sieving experiments to find the mass transfer properties and actual sieving coefficient using a stagnant film model [66,95]. However, given the unique mixing profile of the stir discs in each well (as discussed before), it was considered that it is not appropriate to use the conventional expressions for mass transfer coefficients in stirred cell modules in case of the SWF module. A complementary study using computational fluid dynamics is required to evaluate the fluid patterns and flow profiles in each well to be able to model the system and calculate the appropriate mass and momentum transfer properties.

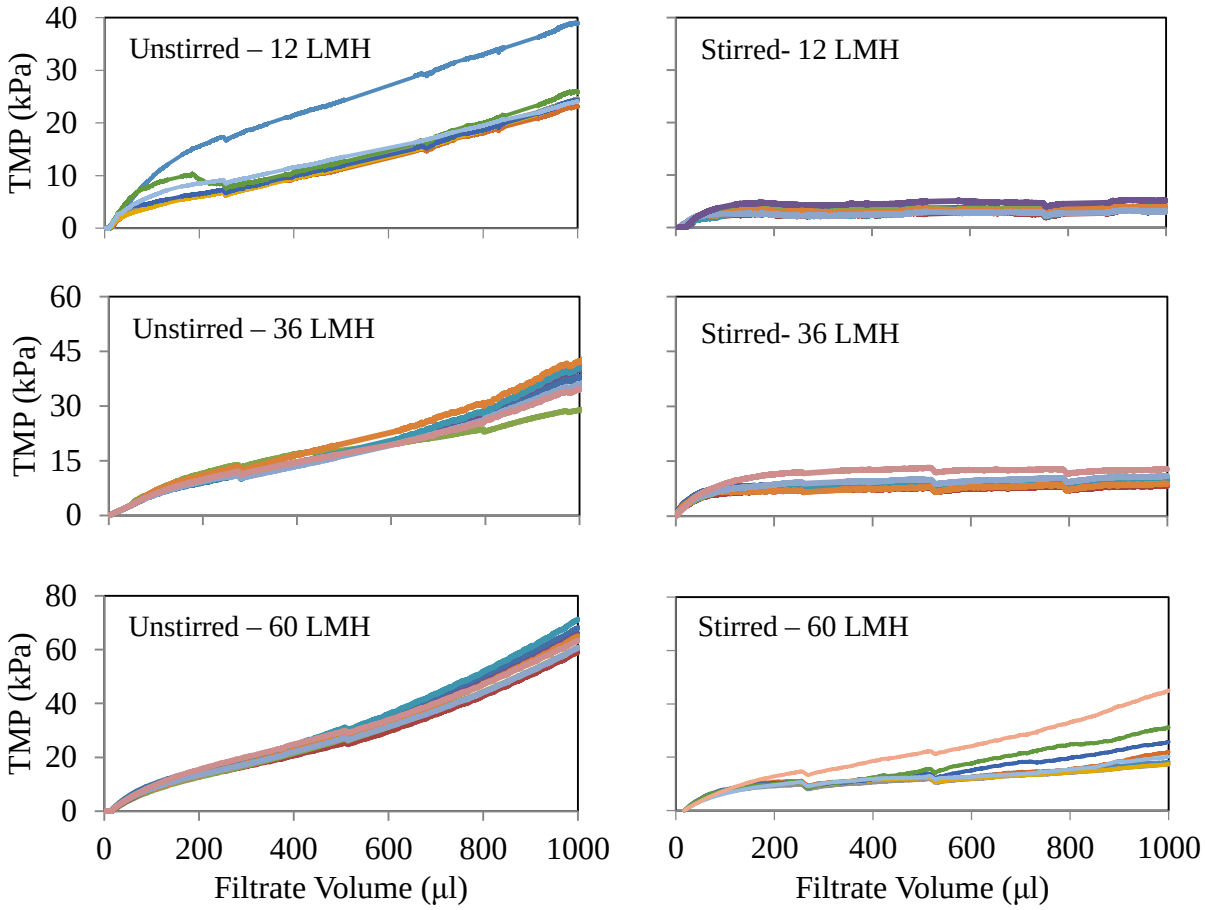


Figure 4.3. TMP profiles during constant flux filtration experiments (12, 36, and 60 LMH) with BSA solution (125 µg/ml) and 30 kDa Omega™ membrane for both stirred and unstirred conditions. The eight profiles in each panel were collected simultaneously using the SWF module and thus correspond to the eight wells in one column of the 96-well filter plate. The results in each panel correspond to a different set of eight wells (i.e. one column) on the 96-well AcroPrep filter plate. For each filtrate flux pair of panels, the same y-axis scale applies to both the unstirred and stirred experiments.

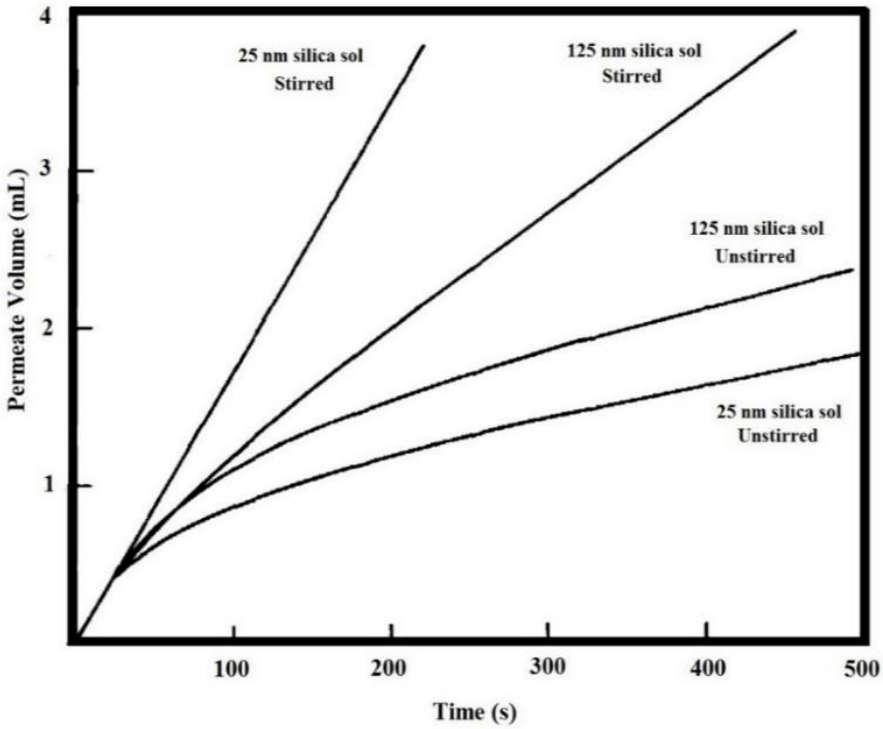


Figure 4.4. Effect of stirring on membrane filtration performance of colloid silica suspensions (credits: Fane [43]).

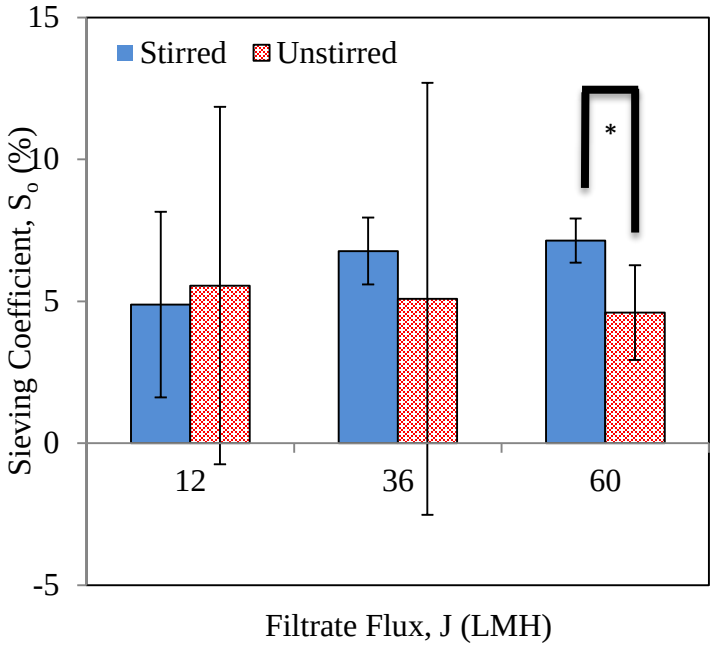


Figure 4.5. A comparison of the average sieving coefficient of BSA through the Omega™ 30 kDa membrane for different filtrate flux with both stirred and unstirred conditions. The error bars represent plus/minus one standard deviation for the eight filtration experiments that were conducted simultaneously using the SWF module. *Denotes a statistically significant difference between stirred and unstirred conditions, Student's t-test, $p < 0.05$.

Table 4.1. Summary of statistical analyses for the observed sieving coefficient results in Fig. 4.5. S and U subscripts denote stirred and unstirred conditions respectively. Note that J is the filtrate flux in LMH, μ and $\bar{x}$ are the mean of the population and samples respectively, S is the standard deviation (error bars on Fig. 4.5), n is the sample size, and $\mu_S - \mu_U$ is calculated using $(\bar{x}_S - \bar{x}_U) - c_t\sqrt{S_P^2\left(\frac{1}{n_S} + \frac{1}{n_U}\right)} \leq \mu_S - \mu_U \leq (\bar{x}_S - \bar{x}_U) + c_t\sqrt{S_P^2\left(\frac{1}{n_S} + \frac{1}{n_U}\right)}$ where $S_P^2$ is the weighted sum of the sampled variances $S_P^2 = \frac{(n_U-1)S_U^2+(n_S-1)S_S^2}{n_U-1+n_S-1}$ and $c_t = 2.365$ for $n = 8$.

| J (LMH) | Stirring? | $\bar{x}$ (%) | S | $\mu_S - \mu_U$ |
|---|---|---|---|---|
| 12 | Yes | 4.89 | 3.27 | (-6.05, 4.72) |
| | No | 5.55 | 6.30 | |
| 36 | Yes | 6.77 | 1.17 | (-4.18, 7.54) |
| | No | 5.09 | 7.61 | |
| 60 | Yes | 7.14 | 0.78 | (1.22, 4.10) |
| | No | 4.60 | 1.67 | |

### 4.3.High-throughput membrane fouling test

A high-throughput test strategy was developed to assess the membrane fouling behavior during the protein filtration experiments in case of stirred and unstirred conditions. Six protein filtration experiments were conducted simultaneously in six wells of the AcroPrep filter plate in order to demonstrate the usefulness of this strategy. Each well was tested for both stirred and un-stirred conditions. As shown in Table 4.2, only three of those six wells contained the magnetic stir disc that is required to create the stirring conditions. For the membranes in wells B, D, and F, the first filtration experiment was conducted with stirring while the second run was done without stirring; the opposite order was used for the membranes in Wells C, E, and G. Typical TMP profiles for the processing of BSA solution (250 μg/ml) through the Omega 30 kDa membrane are

shown as Fig. 4.6.a and Fig. 4.6.b for Wells B and C respectively. The TMP profiles are similar to those shown in Fig. 4.3 for the same filtrate flux (60 LMH); the profiles increased by increasing filtrate volume for both experiments, however at a much lower rate for the stirred well conditions. Also, the variation between different wells for the same stirring condition is apparent. Similar results were obtained for the other four wells D, E, F, and G (results not shown). It was also found that the effect of the stirring conditions on the TMP profile was independent of the order in which the filtration experiments were performed. Note that for each profile, the slight changes in TMP that occurred at approximately 75 and 150 μl were caused by a brief pause of the syringe pump in order to move the 96-well collection plate ahead one position each time to allow for the collection of multiple filtrate samples.

Table 4.2 compares the post-filtration feed concentration ($C_{final}$) values that were obtained from two different experimental approaches. The measured values correspond to the results from the BCA assay on the feed samples taken directly from each well at the end of each filtration test. The calculated values correspond to those obtained from a simple mass balance on each well that accounted for the volume of filtrate collected, the pre-filtration feed concentration, and the concentration of filtrate samples with the latter two being determined by the BCA assay. The variation between these two values was determined according to equation (4.1):

$$\frac{\left|C_{final\_calculated} - C_{final\_measured}\right|}{C_{final\_measured}} \times 100\% \qquad (4.1)$$

Calculated and measured values of final bulk concentration had a good agreement in case of the six filtration tests in Table 4.2 which were conducted with stirring. The average variation was less than 10% with the individual values ranging from 4% to 17%. On the other hand, for the six experiments without stirring, the average variation was four times higher (43%) with the individual

values ranging from 17% to 70%. These numbers suggest that there was an accumulation of proteins at the membrane surface which causes a reduction in the protein transmission when performing unstirred experiments. A similar analysis has been previously used to estimate the deposited mass of various solutes on retentive UF membranes for stirred and unstirred conditions [44].

The three hydraulic permeability measurements that were made on each membrane (before the first filtration experiment, in between the two filtration experiments, and after the second filtration experiment) were employed to assess for any changes in membrane properties due to irreversible fouling effects. For the six wells in Table 4.2, the results are compared in Fig. 4.6.c by plotting the normalized hydraulic permeability $L_p/L_{p0}$ where $L_{p0}$ is the hydraulic permeability of the native membrane. All of the wells showed approximately the same percent permeability reduction following the two filtration experiments. Moreover, it was found that the order in which the filtration experiments were done had no significant effect on the membrane performance (either stirred-unstirred or unstirred-stirred). Thus no conclusions can be made about the effect of stirring on membrane fouling. It is likely that this result is due to the washing step that was done after each filtration test. These results suggest that majority of the fouling due to unstirred BSA filtration is hydraulically reversible. Further work is needed to verify this hypothesis.

Table 4.2. Comparison of the filtration test results for the six membranes (Wells B through G) used for the high-throughput membrane fouling test. The post-filtration feed concentrations ($C_{final}$) were measured using the BCA assay (S: Standard Deviation). The same value was also calculated from the measurements of the initial bulk and filtrate concentrations for each stirred well according to a simple mass balance. The sequence and timing of the three hydraulic permeability measurements are also shown.

| | | Well B | Well C | Well D | Well E | Well F | Well G |
|---|---|---|---|---|---|---|---|
| | | Initial hydraulic permeability ($L_{p0}$) measurement | | | | | |
| Filtration Experiment #1 | Stirring? | Yes | No | Yes | No | Yes | No |
| | Measured $C_{final}$ (±S) (mg/ml) | 0.410 (±0.016) | 0.250 (±0.008) | 0.515 (±0.018) | 0.270 (±0.010) | 0.487 (±0.010) | 0.275 (±0.009) |
| | Calculated $C_{final}$ (mg/ml) | 0.436 | 0.373 | 0.434 | 0.317 | 0.429 | 0.351 |
| | | Intermediate hydraulic permeability measurement | | | | | |
| Filtration Experiment #2 | Stirring? | No | Yes | No | Yes | No | Yes |
| | Measured $C_{final}$ (±S) (mg/ml) | 0.238 (±0.009) | 0.473 (±0.021) | 0.272 (±0.007) | 0.417 (±0.013) | 0.263 (±0.012) | 0.350 (±0.014) |
| | Calculated $C_{final}$ (mg/ml) | 0.405 | 0.440 | 0.421 | 0.432 | 0.371 | 0.410 |
| | | Final hydraulic permeability measurement | | | | | |

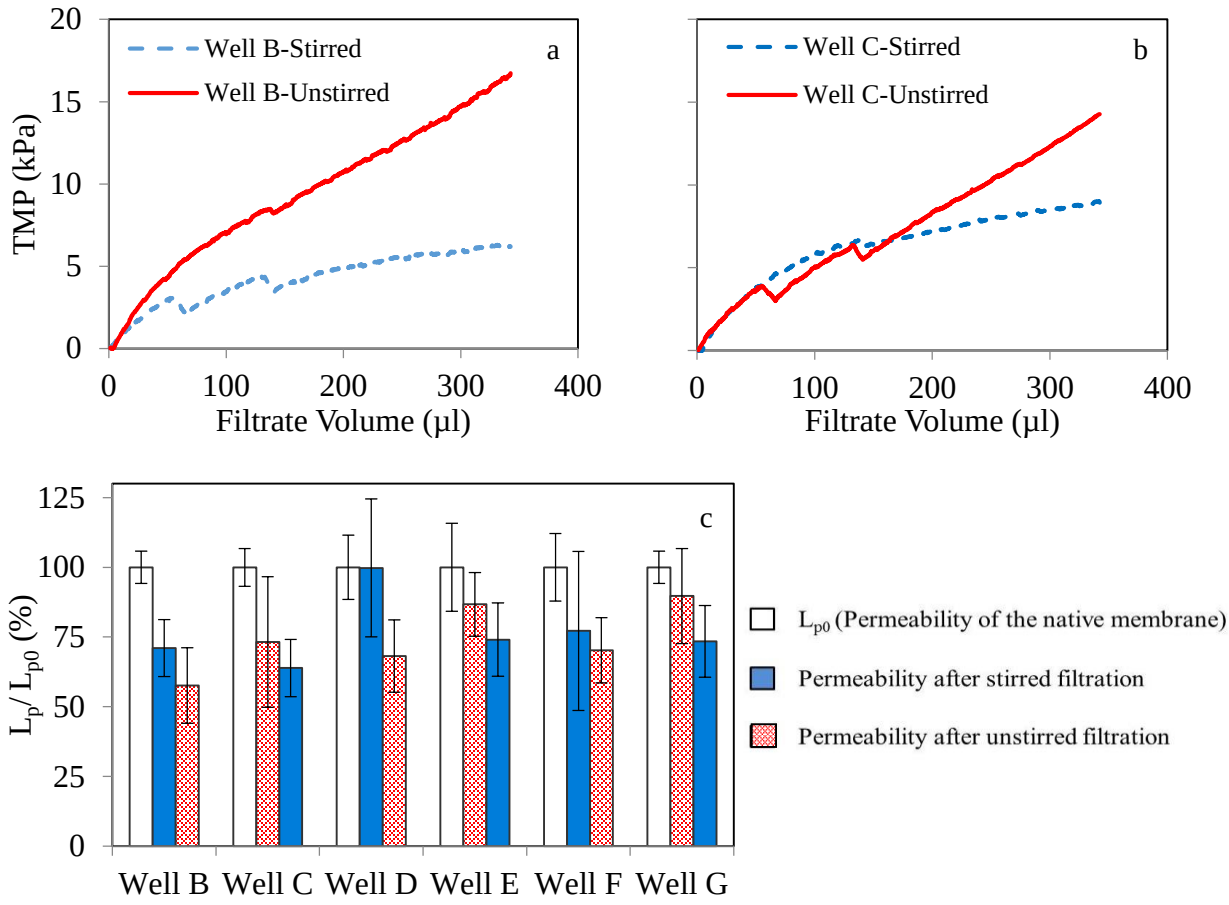


Figure 4.6. Fouling test filtration experiments. a. TMP profiles for 'Well B' during constant flux filtration experiments (60 LMH) with BSA solution (250 µg/ml) and 30 kDa Omega™ membrane. As per the details in Table 4.2, the stirred filtration experiment (dashed line) was completed first (followed by a hydraulic permeability measurement) and then the un-stirred filtration experiment (solid line) was completed. b. TMP profiles for 'Well C' during the same constant flux filtration experiments described for panel a except that the un-stirred filtration experiment was completed first and then the stirred filtration experiment was completed. c. Comparison of changes in hydraulic permeability following the protein filtration experiments for the six membranes in Wells B through G. The results were normalized by the hydraulic permeability of the native membrane ($L_{p0}$) and are presented in the order that they were conducted. The error bars correspond to the uncertainty in $L_p/L_{p0}$ as determined from the 95% confidence interval of the slope of flux versus TMP for each hydraulic permeability measurement and standard propagation of error analysis.

### 4.4.Process optimization using design of experiments methodology

The importance of optimizing the performance of membrane filtration processes was first outlined in section 2.5.3. In order to demonstrate the practicality of the SWF technique for filtration process optimization, a set of protein solutions were prepared from different buffer solutions and then tested simultaneously in the multiple wells of the 96-well filter plate. The optimization was planned according to a design of experiments (DOE) methodology.

Factorial design is an approach in DOE in which more than a single factor affects the response variable. Factorial design is the opposite of ideal conditions where only a single variable changes at time. It is generally considered that for the majority of factorial experiments, each factor has only two levels (low and high) and k factors. Thus, a full factorial design requires $2^k$ data points (experiments) to cover all the existing combinations of the different factors. In a full factorial design, none of the interactions among the different factors is neglected. Hence, $2^k$ data points are used to separately calculate and interpret the $2^k$ slope coefficients in the model. However in the real experimental systems, when there are numerous factors that are identified as being potentially significant, then the $2^k$ experiments needed for a full factorial can become too large and expensive. Furthermore, it should be noted that in most processes only the main factors and a number of the factor interactions are decisive. Therefore, performing a full factorial design to calculate all the probable factors is too laborious and inefficient (e.g. $2^6$=64 experiments for 6 factors). Fractional factorial design, on the other hand, is defined as an experimental design consisting of a chosen subset of the experimental runs of a full factorial design to find the effect of the most important factors and their interactions. Fractional factorial designs are denoted using the notation $2^{k-p}$ where p is the size of the fraction  For example, a $2^{6-2}$ design is a quarter of a two level, six factor factorial design [96,97].

The effects of solution pH and solution ionic strength were selected in accordance with previous studies that used the conventional stirred cell device to evaluate their effects on protein sieving behaviour [82,98] and protein mixture fractionation [51,54]. As a proof of principle, a simple $2^2$ factorial design was used with 'low' and 'high' levels of solution pH and salt concentration. Four separate solutions were made to perform the experiments in this section as shown in Table 4.3. The pH was adjusted using a few drops of HCl (1 N) in order to have both lower and higher levels of pH (5 and 7). Lower and higher levels of the salt concentration (C=0 mM and C=139.7 mM) were provided by preparing phosphate buffered saline (PBS) and phosphate buffer (PB) solutions. The PBS was prepared by dissolving 137 mM NaCl, 2.7 mM KCl, 10 mM $Na_2HPO_4$ and 2.0 mM $KH_2PO_4$ in Milli-Q water. Phosphate buffer has been prepared by dissolving the same concentrations of $Na_2HPO_4$ and $KH_2PO_4$ (without using KCl and NaCl) in Milli-Q water.

A higher BSA solution concentration (1 mg/ml) and filtrate flux of 30 LMH were used for these experiments. Fig. 4.7 shows a summary of the DOE considering the maximum TMP as the response variable as an example while Table 4.3 shows how the experiments were designed according to DOE standards. Each experiment was randomly designated to a single well to prevent any potential effects of the well order on the results. Note that the DOE experiments were repeated in order to verify the reproducibility of the results.

Table 4.3. Design of experiment table. (–) sign demonstrates low level for each factor (C=0 mM and pH=5 for salt concentration and pH respectively) while (+) sign shows the high level for the factors (C=139.7 mM and pH=7 for salt concentration and pH respectively). The wells were designated randomly for two sets of experiments.

| Factor<br>Number of Experiment | Well Assignment (Run1, Run2) | A (pH) | B (salt concentration) | AB |
|---|---|---|---|---|
| 1 | E, C | – | – | + |
| 2 | D, D | + | – | – |
| 3 | C, F | – | + | + |
| 4 | F, E | + | + | – |

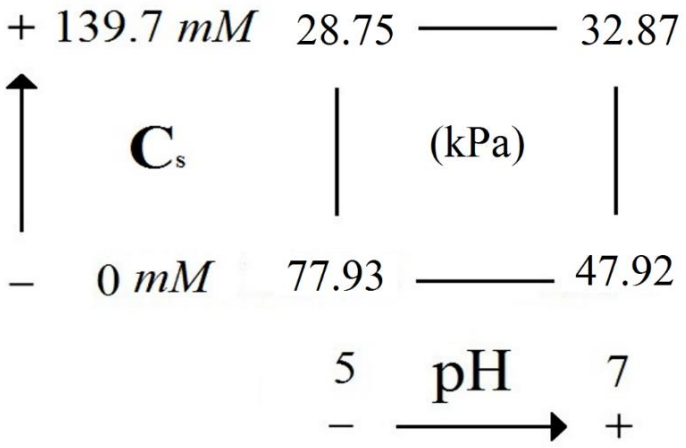


Figure 4.7. Design of experiments summary. Maximum TMP is considered as an example response variable.

Fig. 4.8 shows the TMP profiles for the filtration of BSA solution at 30 LMH through the Omega 30 kDa membrane for the four different solution conditions. All the experiments were conducted in the stirred mode[11] with the rotational speed of the magnetic stir discs set to approximately 350 rpm. The four TMP profiles are remarkably similar at filtrate volumes up to approximately 200 µl. However, at higher filtrate volumes there are considerable differences. The highest TMP was required for the 'low pH – low salt' BSA solution. As previously described in

[11] The key idea is that in absence of mixing, the results are not representative of what is normally done in stirred cell formats.

section 2.5.3, previous studies have reported similar observations during protein filtration experiments conducted close to the protein isoelectric point (pH 4.8) [51,54,82,98]. The lowest TMP was required for the 'high salt' solution irrespective of the solution pH. Thus at the low pH condition, an increase in salt concentration resulted in a significant drop in TMP. Fane et al. [82] conducted constant pressure filtration experiments of BSA through UF membranes and reported similar results in that at solution pH near the protein isoelectric point, an increase in salt concentration resulted in a dramatic increase in filtrate flux. The consistency and uniformity of the results in Fig. 4.8 were verified by repeating the same set of experiments in another set of four wells on the same filter plate – those results are shown as the bottom panel of Fig. 4.8.

Table 4.4 shows the sieving coefficient data related to the $2^2$ factorial design with the repeat experiment (two sets of experiments) at three different filtrate volumes of 50 μL, 250 μL, and 450 μL. Sieving coefficient has been reported to be affected by changes in solution conditions in previous studies as described in section 2.5.3. For example, Saksena and Zydney [54] have used a protein mixture of IgG and BSA to verify that it is possible to achieve an effective separation even for proteins with comparable molecular weights by adjusting the solution environment. It was reported that by using pH 4.8, IgG was excluded from the membrane pores since it has a positive charge which resulted in a low sieving coefficient for IgG and an effective separation [54] It was also stated that the changes in salt concentration did not affect the sieving coefficients of BSA and IgG when conducting experiments at their isoelectric points (BSA:4.8 and IgG:7.4) since the proteins are uncharged at their isoelectric point. However, this change had a significant effect on the sieving coefficient of the protein which has a different isoelectric point than the pH of the solution when performing experiments with protein mixtures.

As described in section 2.3.5 and according to the previous works [48,51,54,82], it is widely believed that the highest sieving coefficient of a protein, for example, is observed at pH close to its isoelectric point when it is uncharged because of the absence of the electrostatic double layer which is formed around the protein molecule and increases the protein size in the solution with the pH other than the isoelectric point. Furthermore, the membrane charge can also be affected by pH change which typically decrease the sieving coefficient in pH other than the isoelectric point. Salt concentration has no significant effect on sieving coefficient when the protein is uncharged while its effect is normally considerable when the protein is charged. [48,83,84]

As mentioned earlier, the molecular weight of the BSA protein (66.5 kDa) is more than double the MWCO of the membrane used in this study and as a result is not ideally suited to investigate the physicochemical effects on sieving coefficient. Thus, the results from sieving coefficient were not clearly comparable with earlier studies. Despite this limitation, the reproducibility and uniformity of the data is quite satisfactory.

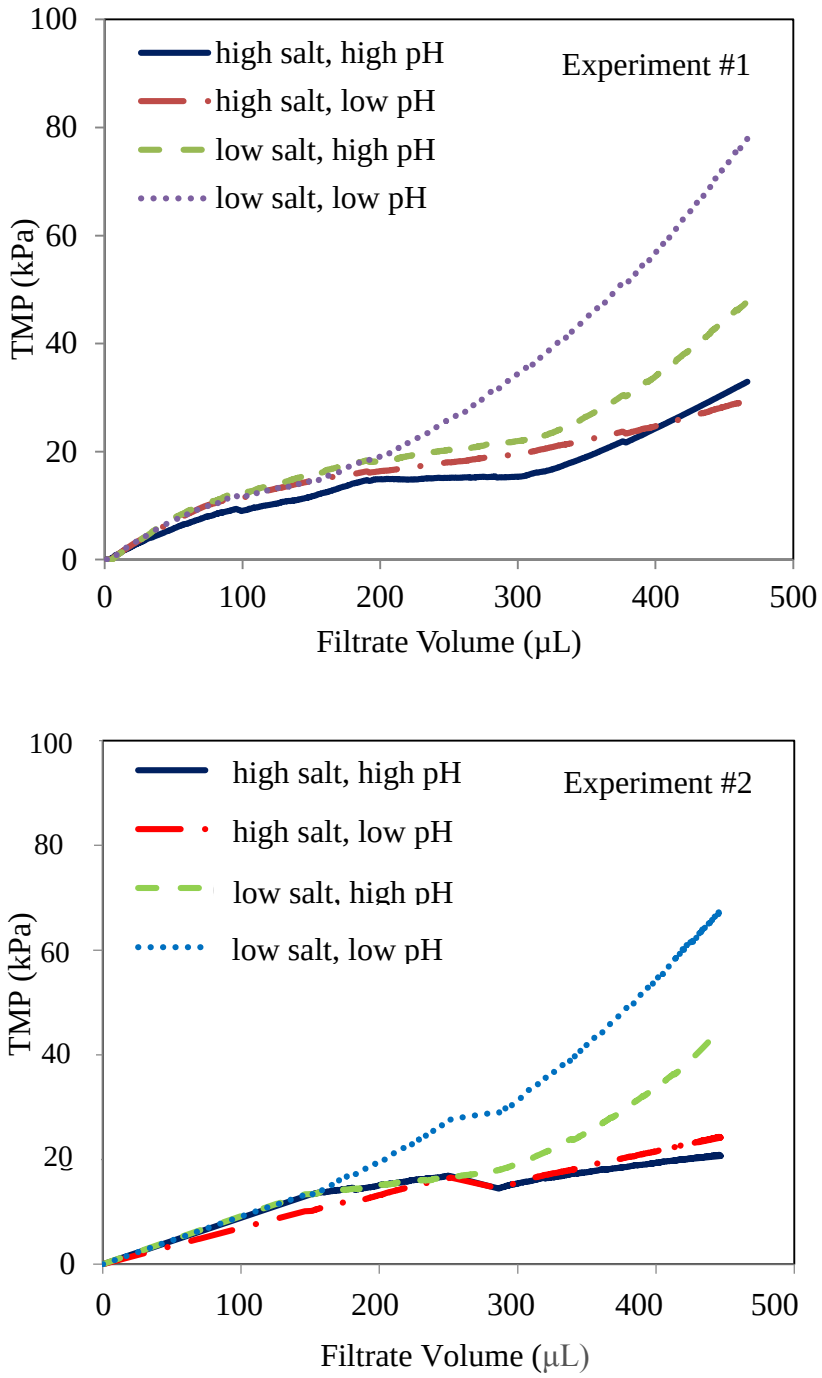


Figure 4.8. TMP profiles for constant flux filtration experiments (30 LMH) with BSA solution (1000 µg/ml) and 30 kDa Omega™ membrane; 'high' solution pH = 7, 'low' solution pH = 5, 'high' salt concentration = 137 mM NaCl, 2.7 mM KCl, 10 mM $Na_2HPO_4$ and 2 mM $KH_2PO_4$ in Milli-Q water, 'low' salt concentration = 10 mM $Na_2HPO_4$ and 2 mM $KH_2PO_4$ in Milli-Q water. The bottom panel corresponds to another experiment conducted at the exact same conditions as the top panel to evaluate the repeatability of the results.

Table 4.4. Sieving coefficient results according to design of experiments (DOE). The second column for each filtrate volume shows the results from the repeated experiment.

| Filtrate Volume (μL) | 50 | | 250 | | 450 | |
|---|---|---|---|---|---|---|
| | Observed Sieving Coefficient, $S_o$ (%) | | | | | |
| Experiment | Exp. #1 | Exp. #2 | Exp. #1 | Exp. #2 | Exp. #1 | Exp. #2 |
| Low pH-Low salt | 15.3 | 13.8 | 7.2 | 7.3 | 9.7 | 9.3 |
| High pH-Low salt | 12.3 | 13.2 | 5.9 | 4.9 | 4.9 | 8.1 |
| Low pH-High salt | 11.6 | 12.1 | 4.2 | 4.6 | 3.0 | 3.3 |
| High pH-High Salt | 11.6 | 12.0 | 3.8 | 4.3 | 2.3 | 3.3 |

The capacity to run eight filtration experiments simultaneously is fairly amenable to the incorporation of DOE methodologies for process optimization. For example, all of the eight experiments in a $2^3$ full factorial design or fractional factorial design (e.g. $2^{4-1}$, $2^{5-2}$) can be run at once using our SWF experimental setup. There are just two restrictions with the current SWF experimental setup. The first is that all eight experiments must be conducted at the same filtrate flux due to the nature of the multi-rack syringe pump. The second is that the same membrane, that is common across all 96-wells of a filter plate, must be used. However, the first restriction can be mitigated using more advanced fluid delivery systems which are able to provide various flow rates while different surface modification strategies which are included as part of the process optimization [34,35] can be used in order to resolve the latter limitation. The combination of the unique characteristics of the SWF module along with the simplicity of analysis in the DOE methodology produces an excellent strategy for analyzing the effects of various operational factors on membrane filtration performance.

# Chapter 5: Conclusions and future works

## 5.1. Conclusions

The SWF module that was developed in this work allows for the capacity to parallelize and thus speed up the filtration experiments and also process miniaturization to reduce the amount of materials needed for an experiment. The use of commercially available 96-well filter plates, fairly inexpensive laboratory equipment, and custom parts that can be readily fabricated in-house will enable other researchers to build similar systems. The key features of the design are the ability to control the stirring conditions above the membrane surface and to simultaneously monitor the TMP during constant flux filtration experiments. These characteristics allow for a direct comparison to conventional filtration experiments that are conducted using the standard stirred cell device and thus must be done in a sequential fashion. A review of the key findings from this work are summarized below:

- ✓ Omega$^{TM}$ 30 kDa membrane hydraulic permeability measurements were uniform and reproducible across sixteen wells with an average value of $1.19\times10^{-12}$ m and coefficient of variation of 10.7%. The results are in good agreement with both the literature and the technical information from the membrane manufacturer.
- ✓ The filtration of BSA solution (125 μg/ml) through the Omega$^{TM}$ 30 kDa membrane showed the stirring conditions within each well had a significant effect on the TMP profile for a given filtrate flux value. The maximum TMP in the stirred wells were on average 7.5, 3.8, and 2.6 times lower than those in the stirred wells at fluxes of 12, 36, and 60 LMH respectively. Also, at the highest filtrate flux (60 LMH), the average sieving coefficient for stirred conditions was statistically different than that for unstirred conditions and the sieving coefficient results from stirred filtration were found to be more reproducible than

that of unstirred filtration. For the 68 different TMP profiles shown in this work, there were just two or three (less than 5%) outliers that deviated significantly from the general trend. It is believed that the productivity gained by running multiple tests at once in a simple manner far outweighs such slight errors.

- ✓ A five step HT membrane fouling test was conducted to assess the effect of the stirring conditions on UF membrane fouling during protein filtration experiments. From those tests, it was hypothesized that for the unstirred condition, the accumulation and adsorption of proteins at the membrane surface caused a reduction in protein transmission. However, the hydraulic permeability results were not conclusive enough to indicate that the stirring conditions had a significant effect on the fouling tendency of the membrane. This could suggest that stirring has most significantly affected the hydraulically irreversible fouling in those tests.
- ✓ The opportunity to perform eight filtration experiments simultaneously is quite amenable to the incorporation of optimization methodologies for process optimization. As a proof of principle, the effects of solution pH and salt concentration on TMP profiles were studied during constant flux filtration of BSA solution through the Omega$^{TM}$ 30 kDa membrane. This approach could be extended to more sophisticated strategies that are used for the complex mixtures that are frequently encountered in biopharmaceutical and environmental applications.

## 5.2. Future works

- Design and development of a second generation SWF system that uses a multichannel microfluidic flow control (MMFC) system (from ELVEFLOW microfluidics) to conduct constant pressure experiments. The MMFC system has individual flow controllers for each flow channel. Also, the individual channels of the MMFC system will allow for filtrate flux experiments to be conducted simultaneously at different flux values. This feature is a considerable advantage over the existing design that relies on the multi-rack syringe pump.
- Adapt the stagnant film model to SWF data in order to determine mass transfer coefficient and actual sieving coefficient.
- Perform experiments with various combinations of single solute and mixed solute pairs which can be helpful in order to obtain more conclusive results related to sieving coefficient. For example, IgG, BSA, ovalbumin, GFP, myoglobin, lysozyme, β-lactoglobulin, α-lactalbumin, casein, gamma globulin, or any of their paired solutes can be used with the appropriate MF and UF membrane to perform future studies. Also, alternative studies can be conducted on pDNA recovery using UF membranes (e.g. pDNA/RNA separation) and MF of various fermentation broths. The results of previous studies can be compared with current setup in this manner.
- Apply mathematical models to results from SWF technique to analyze fouling behavior with more details. Mass and momentum transfer models must be developed according to the unique end-over-end mixing profile using both experimental data and CFD. In this way, the mixing profile of the SWF module can be compared with mixing profiles in

conventional stirred cell filtration setups. Furthermore, such investigations could help scale-up studies using this HT technique.

- Assess the effect of module design and operating conditions on flow velocity profiles and mass transfer characteristics using CFD simulations to determine how accurately the micro-scale systems reflect the performance of larger scale systems.
- Evaluate the potential of using membrane pre-treatment and surface modification methods including chemical, photochemical, and/or enzyme grafting to overcome the limitation of 96-well filter plate format which requires 'same' membrane be used in all experiments. It is anticipated that combining SWF with these methods could offer an exceptional opportunity for HT fouling test as well as filtration process optimization with larger design-spaces.
- Combine stimuli-responsive membranes such as membranes with magnetically activated micro-mixers [99] with SWF module for environmental and biological fouling prevention applications. Mixing can be induced using the tumble stirrer for HT experiments instead of conventional oscillating magnetic field used for regular filtration setups.
- Employ SWF technique for HT development of environmental engineering processes. For example, fouling behavior of natural organic matter has been found to be a very complex process depending on several operational factors such as ionic strength, pH, presence of cations and anions, membrane pre-treatment, etc.
- Perform experiments with complex real biological solutions in order to see the performance of SWF module in practice for applications in pharmaceutical industries. MF and UF have wide applications in food industries (e.g. in diary processing, whey fractionation, and juice production process). Food industry processes are generally

identical with biological processes in terms of complexity and sensitivity. As a result, SWF technique may provide an exceptional opportunities in this field as well.

## References

[1] N.J. Titchener-Hooker, P. Dunnill, M. Hoare, Micro biochemical engineering to accelerate the design of industrial-scale downstream processes for biopharmaceutical proteins., Biotechnol. Bioeng. 100 (2008) 473–487.

[2] S. Chhatre, N.J. Titchener-hooker, Micro-biochemical engineering: using small-scale devices to predict industry-scale downstream performance Compr. Biotechnol. 2 (2011), 891–903.

[3] W.-T. Hsu, R.P.S. Aulakh, D.L. Traul, I.H. Yuk, Advanced microscale bioreactor system: a representative scale-down model for bench-top bioreactors. Cytotechnology. 64 (2012) 667–678.

[4] M. Micheletti, G.J. Lye, Microscale bioprocess optimisation., Curr. Opin. Biotechnol. 17 (2006) 611–618.

[5] M. Brivio, W. Verboom, D.N. Reinhoudt, Miniaturized continuous flow reaction vessels: influence on chemical reactions., Lab Chip. 6 (2006) 329–344.

[6] A. Zanzotto, N. Szita, P. Boccazzi, P. Lessard, A.J. Sinskey, K.F. Jensen, Membrane-aerated microbioreactor for high-throughput bioprocessing., Biotechnol. Bioeng. 87 (2004) 243–254.

[7] N. Szita, P. Boccazzi, Z. Zhang, P. Boyle, A.J. Sinskey, K.F. Jensen, Development of a multiplexed microbioreactor system for high-throughput bioprocessing. Lab Chip. 5 (2005) 819–826.

[8] Z. Zhang, P. Boccazzi, H.-G. Choi, G. Perozziello, A.J. Sinskey, K.F. Jensen, Microchemostat-microbial continuous culture in a polymer-based. instrumented microbioreactor. Lab Chip. 6 (2006) 906–913.

[9] A. Khademhosseini, R. Langer, J. Borenstein, J.P. Vacanti, Microscale technologies for tissue engineering and biology. Proc. Natl. Acad. Sci. U. S. A. 103 (2006) 2480–2487.

[10] P. Fernandes, J.M.S. Cabral, Microlitre/millilitre shaken bioreactors in fermentative and biotransformation processes – a review, Biocatal. Biotransform. 24 (2006) 237–252.

[11] A.S. Tait, J.P. Aucamp, A. Bugeon, M. Hoare, Ultra scale-down prediction using microwell technology of the industrial scale clarification characteristics by centrifugation of mammalian cell broths. Biotechnol. Bioeng. 104 (2009) 321–331.

[12] T.A. Barrett, A. Wu, H. Zhang, M.S. Levy, G.J. Lye, Microwell engineering characterization for mammalian cell culture process development. Biotechnol. Bioeng. 105 (2010) 260–275.

[13] G.J. Lye, P. Ayazi-Shamlou, F. Baganz, P.A. Dalby, J.M. Woodley, Accelerated design of bioconversion processes using automated microscale processing techniques, Trends Biotechnol. 21 (2003) 29–37.

[14] B. Maiser, F. Dismer, J. Hubbuch, Optimization of random PEGylation reactions by means of high throughput screening., Biotechnol. Bioeng. 111 (2014) 104–114.

[15] G. Molineux, Pegylation: engineering improved pharmaceuticals for enhanced therapy, Cancer Treat. Rev. 28 (2002) 13–16.

[16] F.M. Veronese, Peptide and protein PEGylation, Biomaterials. 22 (2001) 405–417.

[17] F. Veronese, J. M. Harris, Introduction and overview of peptide and protein pegylation, Adv. Drug Deliv. Rev. 54 (2002) 453–456.

[18] S.M. Cramer, M.A. Holstein, Downstream bioprocessing: recent advances and future promise, Curr. Opin. Chem. Eng. 1 (2011) 27–37.

[19] G.J. Lye, J. Hubbuch, T. Schroeder, E. Willimann, Shrinking the Costs of Bioprocess Development - Case Study - Bioprocess Int. (2009) 18–22.

[20] M. Bensch, B. Selbach, J. Hubbuch, High throughput screening techniques in downstream processing: Preparation, characterization and optimization of aqueous two-phase systems. Chem. Eng. Sci. 62 (2007) 2011–2021.

[21] S.A. Oelmeier, F. Dismer, J. Hubbuch, Application of an aqueous two-phase systems high-throughput screening method to evaluate mAb HCP separation. Biotechnol. Bioeng. 108 (2011) 69–81.

[22] M. Wiendahl, S.A. Oelmeier, F. Dismer, J. Hubbuch, High-throughput screening-based selection and scale-up of aqueous two-phase systems for pDNA purification. J. Sep. Sci. 35 (2012) 3197–3207.

[23] C.J. Welch, M. Shaimi, M. Biba, J.R. Chilenski, R.H. Szumigala, U. Dolling, D.J. Mathre, P.J. Reider, Microplate evaluation of process adsorbents. J. Sep. Sci. 25 (2002) 847–850.

[24] C.J. Welch, J. Albaneze-Walker, W.R. Leonard, M. Biba, J. DaSilva, D. Henderson, B. Laing, D.J. Mathre, S. Spencer, X. Bu, T. Wang, Adsorbent screening for metal impurity removal in pharmaceutical process research, Org. Process Res. Dev. 9 (2005) 198–205.

[25] M. Bensch, P. Schulze Wierling, E. von Lieres, J. Hubbuch, High throughput screening of chromatographic phases for rapid process development. Chem. Eng. Technol. 28 (2005) 1274–1284.

[26] S. Chhatre, N.J. Titchener-Hooker, Review: Microscale methods for high-throughput chromatography development in the pharmaceutical industry. J. Chem. Technol. Biotechnol. 84 (2009) 927–940.

[27] J.L. Coffman, J.F. Kramarczyk, B.D. Kelley, High-throughput screening of chromatographic separations: I. Method development and column modeling. Biotechnol. Bioeng. 100 (2008) 605–618.

[28] M.D. Wenger, P. Dephillips, C.E. Price, D.G. Bracewell, An automated microscale chromatographic purification of virus-like particles as a strategy for process development. Biotechnol. Appl. Biochem. 47 (2007) 131–139.

[29] L. Britsch, T. Schroeder, J. Friedle, Automated, high-throughput chromatographic separation of biological compounds, Am Biotechnol Lab. 26 (2008) 20–23.

[30] T. Bergander, K. Nilsson-Välimaa, K. Oberg, K.M. Lacki, High-throughput process development: determination of dynamic binding capacity using microtiter filter plates filled with chromatography resin. Biotechnol. Prog. 24 (n.d.) 632–639.

[31] S. Chhatre, D.G. Bracewell, N.J. Titchener-Hooker, A microscale approach for predicting the performance of chromatography columns used to recover therapeutic polyclonal antibodies. J. Chromatogr. A. 1216 (2009) 7806–7815.

[32] M. Chandler, A. Zydney, High throughput screening for membrane process development. J. Membr. Sci. 237 (2004) 181–188.

[33] N.B. Jackson, J.M. Liddell, G.J. Lye, An automated microscale technique for the quantitative and parallel analysis of microfiltration operations, J. Membr. Sci. 276 (2006) 31–41.

[34] M. Zhou, H. Liu, J.E. Kilduff, R. Langer, D.G. Anderson, G. Belfort, High-throughput membrane surface modification to control NOM fouling., Environ. Sci. Technol. 43 (2009) 3865–3871.

[35] M. Zhou, H. Liu, J.E. Kilduff, R. Langer, D.G. Anderson, G. Belfort, High throughput synthesis and screening of new protein resistant surfaces for membrane filtration, 56 (2010) 1932–1945.

[36] J. Pieracci, J. V Crivello, G. Belfort, Photochemical modification of 10 kDa polyethersulfone ultrafiltration membranes for reduction of biofouling. 156 (1999). 223–240.

[37] H. Yamagishi, J. V. Crivello, G. Belfort, Development of a novel photochemical technique for modifying poly (arylsulfone) ultrafiltration membranes. J. Membr. Sci. 105 (1995) 237–247.

[38] S. Kong, J. Aucamp, N.J. Titchener-Hooker, Studies on membrane sterile filtration of plasmid DNA using an automated multiwell technique. J. Membr. Sci. 353 (2010) 144–150.

[39] A.L. Khan, S. Basu, A. Cano-Odena, I.F.J. Vankelecom, Novel high throughput equipment for membrane-based gas separations. J. Membr. Sci. 354 (2010) 32–39.

[40] M.R. Bilad, P. Declerck, A. Piasecka, L. Vanysacker, X. Yan, I.F.J. Vankelecom, Development and validation of a high-throughput membrane bioreactor (HT-MBR), J. Membr. Sci. 379 (2011) 146–153.

[41] P. Vandezande, L. Gevers, J. Paul, I. Vankelecom, P. Jacobs, High throughput screening for rapid development of membranes and membrane processes. J. Membr. Sci. 250 (2005) 305–310.

[42] S.T. Johnston, K.A. Smith, W.M. Deen, Concentration polarization in stirred ultrafiltration cells. AIChE J. 47 (2001) 1115–1125.

[43] A.G. Fane, Ultrafiltration of suspensions. J. Membr. Sci. 20 (1984) 249–259.

[44] M. Chudacek, A.G. Fane, The dynamics of polarisation in unstirred and stirred ultrafiltration. J. Membr. Sci. 21 (1984) 145–160.

[45] K. Katsoufidou, S.G. Yiantsios, A.J. Karabelas, Experimental study of ultrafiltration membrane fouling by sodium alginate and flux recovery by backwashing. J. Membr. Sci. 300 (2007) 137–146.

[46] Chhaya, C. Sharma, S. Mondal, G.C. Majumdar, S. De, Clarification of Stevia extract by ultrafiltration: Selection criteria of the membrane and effects of operating conditions. Food Bioprod. Process. 90 (2012) 525–532.

[47] R.R. Bhave, Fermentation and Biochemical Engineering Handbook, Elsevier, 1996.

[48] R. Ghosh, Protein Bioseparation Using Ultrafiltration: Theory, Applications and New Developments, Imperial College Press, 2003.

[49] Q. Li, R. Ghosh, S. Bellara, Z. Cui, D. Pepper, Enhancement of ultrafiltration by gas sparging with flat sheet membrane modules. Sep. Purif. Technol. 14 (1998) 79–83.

[50] D.M. Kanani, R. Ghosh, A constant flux based mathematical model for predicting permeate flux decline in constant pressure protein ultrafiltration. J. Membr. Sci. 290 (2007) 207–215.

[51] R. Ghosh, Z.F. Cui, Fractionation of BSA and lysozyme using ultrafiltration: effect of pH and membrane pretreatment. J. Membr. Sci. 139 (1998) 17–28.

[52] R. Ghosh, Q. Li, Z.F. Cui, Fractionation of BSA and lysozyme using ultrafiltration: Effect of gas sparging. AIChE J. 44 (1998) 61–67.

[53] Y. Wan, R. Ghosh, Z. Cui, High-resolution plasma protein fractionation using ultrafiltration. Desalination. 144 (2002) 301–306.

[54] S. Saksena, A.L. Zydney, Effect of solution pH and ionic strength on the separation of albumin from immunoglobulins (IgG) by selective filtration. Biotechnol. Bioeng. 43 (1994) 960–968.

[55] R. Field, Fundamentals of Fouling, in Membrane Technology: Membranes for Water Treatment, Wiley, Volume 4, 2010.

[56] H.S. Ramaswamy, M. Marcotte, Food Processing: Principles and Applications, CRC Press, 2005.

[57] A. Kołtuniewicz, The history and state of arts in membrane technologies, VIII Spring Membrane School "Membrane, membrane processes and their application", Opole-Turawa, 23–26 April 2006.

[58] K. Scott, Membrane Separation Technology: Industrial Applications and Markets, Scientific & Technical Information, 1990.

[59] A. Mawson, Membrane Separation Technologies: Current and Potential Applications, IPENZ Annual Conference February 1995, Palmerston North.

[60] Membrane Technology Workshop Summary, Final Report, (2012): http://energy.gov/sites/prod/files/2013/11/f4/membrane_tech_workshop_summary.pdf

[61] L.J. Zeman, A.L. Zydney, Microfiltration and Ultrafiltration: Principles and Applications, CRC Press, 1996.

[62] M.M. Benjamin, D.F. Lawler, Water Quality Engineering: Physical / Chemical Treatment Processes, John Wiley & Sons, 2013.

[63] J.E. Aldom, A.M. Chagla, Recovery of Cryptosporidium oocysts from water by a membrane filter dissolution method, Lett. Appl. Microbiol. 20 (1995) 186–187.

[64] H. Verweij, Inorganic membranes, Curr. Opin. Chem. Eng. 1 (2012) 156–162.

[65] B.D. Mitchell, W.M. Deen, Effect of concentration on the rejection coefficients of rigid macromolecules in track-etch membranes, J. Colloid Interface Sci. 113 (1986) 132–142.

[66] W.S. Opong, A.L. Zydney, Diffusive and convective protein transport through asymmetric membranes, AIChE J. 37 (1991) 1497–1510.

[67] R. Ghidossi, D. Veyret, P. Moulin, Computational fluid dynamics applied to membranes: State of the art and opportunities, Chem. Eng. Process. Process Intensif. 45 (2006) 437–454.

[68] S. Darvishmanesh, J. Vanneste, J. Degrève, B. Van Der Bruggen, Computational fluid dynamic simulation of the membrane filtration module, in: Proceedings of the 20th European Symposium on Computer Aided Process Engineering – ESCAPE20, 2010.

[69] Norman N. Li, Advanced Membrane Technology. New York: New York Academy of Sciences, 2003.

[70] N. Nady, M.C.R. Franssen, H. Zuilhof, M.S.M. Eldin, R. Boom, K. Schroën, Modification methods for poly(arylsulfone) membranes: A mini-review focusing on surface modification, Desalination. 275 (2011) 1–9.

[71] C. Zhao, J. Xue, F. Ran, S. Sun, Modification of polyethersulfone membranes – A review of methods, Prog. Mater. Sci. 58 (2013) 76–150.

[72] J. Comley, Microplate Mixing Trends 2007 Report, published by HTStec Limited, Cambridge, UK, September 2007.

[73] S. Kirby, P. Robinson, J. Curtis, J. Laugharn, C. Wark, Benefits of Covaris AFA ultrasonication on the HTS process from compound master to HTS assay plate, ELRIG-SBS Meeting, Nottingham, UK, 2007.

[74] B. Pscheidt, Z. Liu, R. Gaisberger, M. Avi, W. Skranc, K. Gruber, H. Griengl, A. Glieder, Efficient Biocatalytic Synthesis of ( R )-Pantolactone. Adv. Synth. Catal. 350 (2008) 1943–1948.

[75] Y.W. Alelyunas, L. Pelosi-Kilby, P. Turcotte, M.-B. Kary, R.C. Spreen, A high throughput dried DMSO LogD lipophilicity measurement based on 96-well shake-flask and atmospheric pressure photoionization mass spectrometry detection., J. Chromatogr. A. 1217 (2010) 1950–1955.

[76] R. Ghosh, Study of membrane fouling by BSA using pulsed injection technique, J. Membr. Sci. 195 (2002) 115–123.

[77] X. Sun, D.M. Kanani, R. Ghosh, Characterization and theoretical analysis of protein fouling of cellulose acetate membrane during constant flux dead-end microfiltration, J. Membr. Sci. 320 (2008) 372–380.

[78] S. Saksena, A.L. Zydney, Influence of protein–protein interactions on bulk mass transport during ultrafiltration, J. Membr. Sci. 125 (1997) 93–108.

[79] M. Bakhshayeshi, D.M. Kanani, A. Mehta, R. van Reis, R. Kuriyel, N. Jackson, A.L. Zydney, Dextran sieving test for characterization of virus filtration membranes, J. Membr. Sci. 379 (2011) 239–248.

[80] A.S. Bhadouria, M. Sorci, M. Gu, G. Belfort, J. Hahn, Optimization of Membrane Separation Processes for Protein Fractionation, Ind. Eng. Chem. Res. 53 (2014) 5103–5109.

[81] R. Ghosh, Z.. Cui, Protein purification by ultrafiltration with pre-treated membrane. J. Membr. Sci. 167 (2000) 47–53.

[82] A.G. Fane, C.J.D. Fell, A. Suki, The effect of ph and ionic environment on the ultrafiltration of protein solutions with retentive membranes. J. Membr. Sci. 16 (1983) 195–210.

[83] R. G. Harrison, Bioseparations science and engineering. New York: Oxford University Press, 2003.

[84] W.K. Wang, Membrane separations in biotechnology (2nd ed., rev. and expanded.). New York: M. Dekker, 2001.

[85] S. Hong, M. Elimelech, Chemical and physical aspects of natural organic matter (NOM) fouling of nanofiltration membranes. J. Membr. Sci. 132 (1997) 159–181.

[86] S. Morais, Á. Maquieira, R. Puchades, Selection and characterisation of membranes by means of an immunofiltration assay. Application to the rapid and sensitive determination of the insecticide carbaryl. J. Immunol. Methods. 224 (1999) 101–109.

[87] M. Feins, K.K. Sirkar, Novel internally staged ultrafiltration for protein purification. J. Membr. Sci. 248 (2005) 137–148.

[88] S.R. Wickramasinghe, E.D. Stump, D.L. Grzenia, S.M. Husson, J. Pellegrino, Understanding virus filtration membrane performance. J. Membr. Sci. 365 (2010) 160–169.

[89] S. Mochizuki, A.L. Zydney, Dextran transport through asymmetric ultrafiltration membranes: Comparison with hydrodynamic models. J. Membr. Sci. 68 (1992) 21–41.

[90] Z. Liu, X. Deng, M. Wang, J. Chen, A. Zhang, Z. Gu, C. Zhao, BSA-modified polyethersulfone membrane: preparation, characterization and biocompatibility. J. Biomater. Sci. Polym. Ed. 20 (2009) 377–397.

[91] B. Fang, Q. Ling, W. Zhao, Y. Ma, P. Bai, Q. Wei, H. Li, C. Zhao, Modification of polyethersulfone membrane by grafting bovine serum albumin on the surface of polyethersulfone/poly(acrylonitrile-co-acrylic acid) blended membrane. J. Membr. Sci. 329 (2009) 46–55.

[92] E.M.V. Hoek, F. Peng, W. Jinwen, Oil-tolerant polymer membranes for oil-water separations. U.S. Patent Application 13/697,277.

[93] W. Blatt, A. Darvid, A. Michaels, L. Nelsen, Solute polarization and cake formation in membrane ultrafiltration: causes, consequences, and control techniques. Membr. Sci. Technol. (1970) 47-97.

[94] W.E.I. Yuan, A.L. Zydney, Humic acid fouling during ultrafiltration, Environ. Sci. Technol., 2000, 34 (23), 5043–5050.

[95] K.A. Smith, C.K. Colton, E.W. Merrill, L.B. Evans, Convective transport in a batch dialyzer: determination of true membrane permeability from a single measurement. Chem. Eng. Prog. Symp. Ser., 64 (1968) 45–58.

[96] G.E.P. Box, W.G. Hunter, The 2k − p fractional factorial designs, parts I and II. J. Technometr. 3 (1961) 311–458.

[97] K. Dunn, Process Improvement Using Data, Version 294-34b8, McMaster University, 2014: http://learnche.mcmaster.ca/pid/PID.pdf

[98] S.P. Palecek, A.L. Zydney, Hydraulic permeability of protein deposits formed during microfiltration: effect of solution pH and ionic strength. J. Membr. Sci. 95 (1994) 71–81.

[99] H.H. Himstedt, Q. Yang, L.P. Dasi, X. Qian, S.R. Wickramasinghe, M. Ulbricht, Magnetically activated micromixers for separation membranes. Langmuir. 27 (2011) 5574–5581.

[100] J.A. Asenjo, B.A. Andrews, Aqueous two-phase systems for protein separation: phase separation and applications. J. Chromatogr. A. 1238 (2012) 1–10.

[101] D.M. Czajkowsky, J. Hu, Z. Shao, R.J. Pleass, Fc-fusion proteins: new developments and future perspectives. EMBO Mol. Med. 4 (2012) 1015–1028.

[102] S. Ebrahim, Cleaning and regeneration of membranes in desalination and wastewater applications: State-of-the-art. Desalination. 96 (1994) 225–238.

[103] A. Lim, Membrane fouling and cleaning in microfiltration of activated sludge wastewater, J. Membr. Sci. 216 (2003) 279–290.

[104] N. Porcelli, S. Judd, Chemical cleaning of potable water membranes: A review, Sep. Purif. Technol. 71 (2010) 137–143.

[105] S. Siavash Madaeni, T. Mohamamdi, M. Kazemi Moghadam, Chemical cleaning of reverse osmosis membranes, Desalination. 134 (2001) 77–82.

[106] G. Trägårdh, Membrane cleaning, Desalination. 71 (1989) 325–335.

# Appendices

## Appendix A – Technical drawings

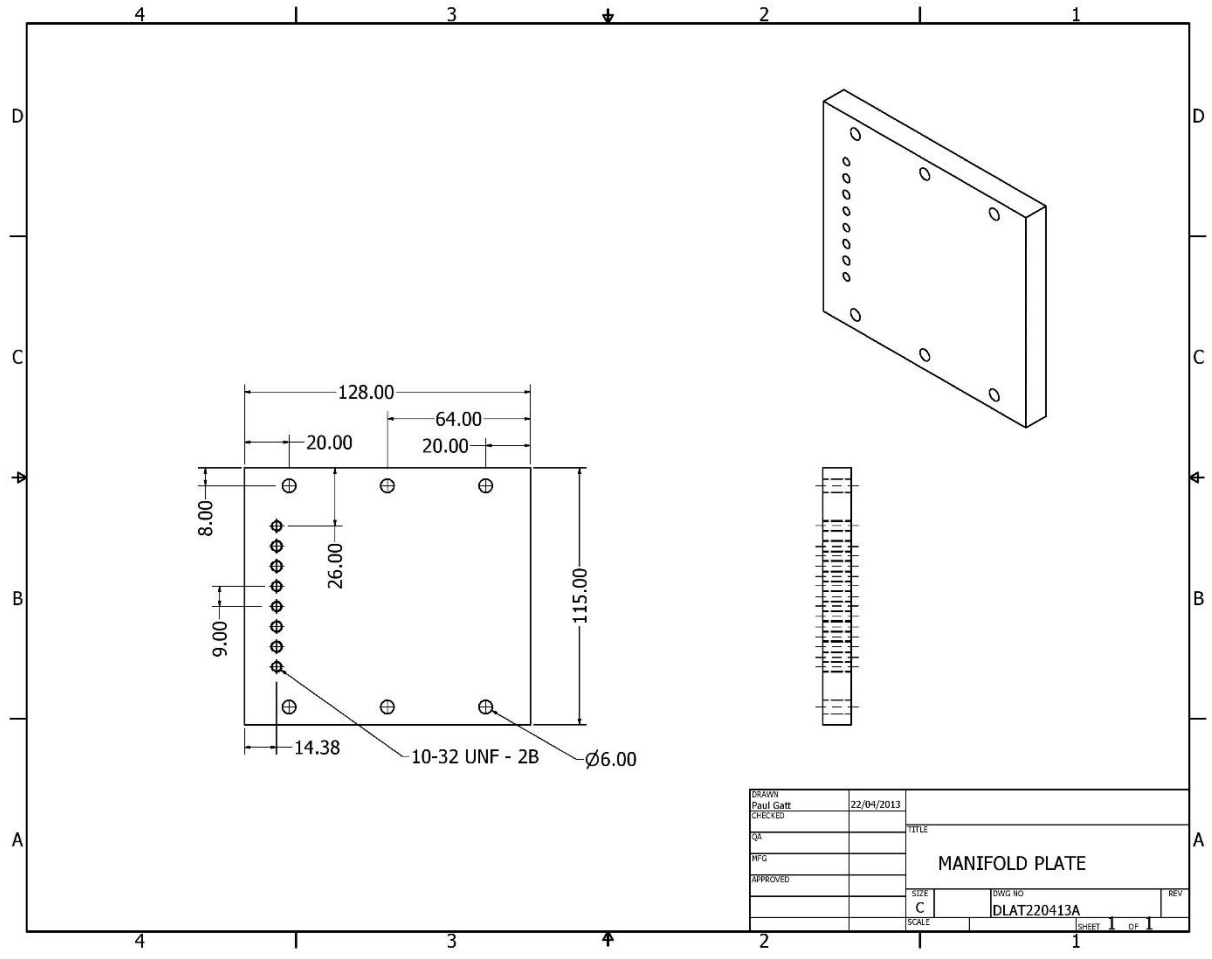


Figure A1. 2D demonstration of the manifold plate.

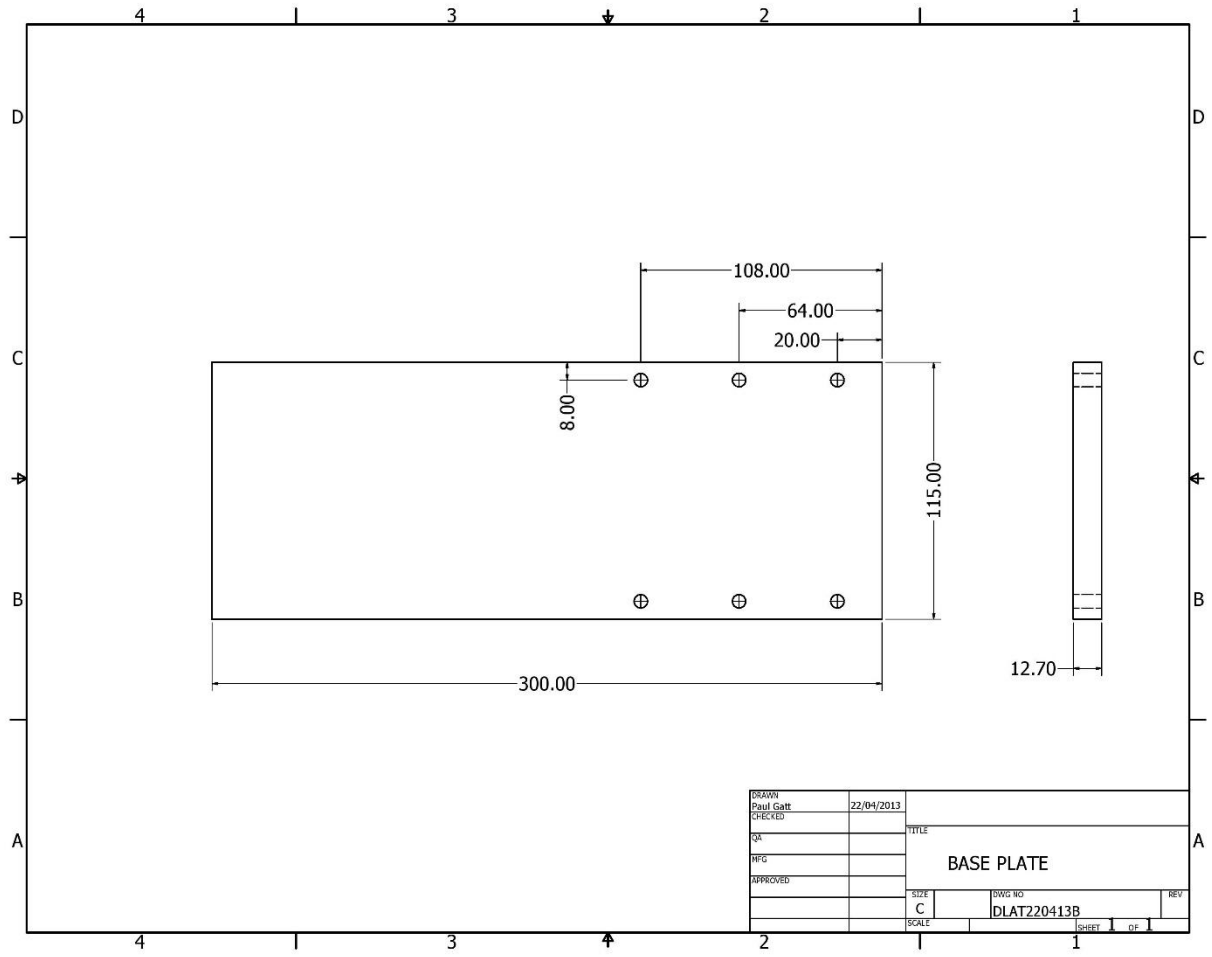


Figure A2. 2D demonstration of the base support of the unit.

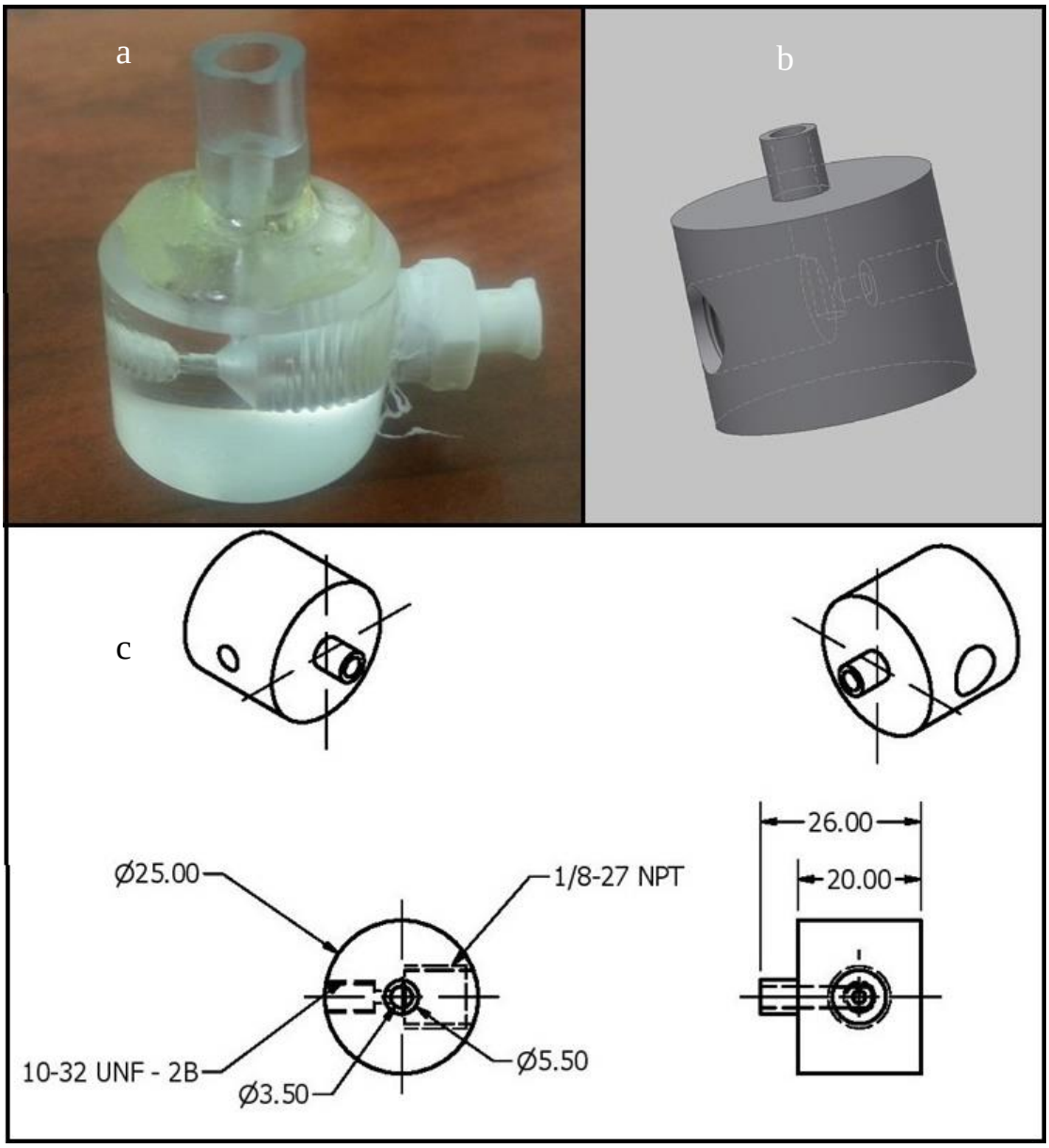


Figure A3. Pressure transducer microfluidic adapter a. Picture demonstration. b. 3D schematic; c. Technical drawing.

**Appendix B – Statistical analysis for 977 nm volume measurement and BCA assays.**

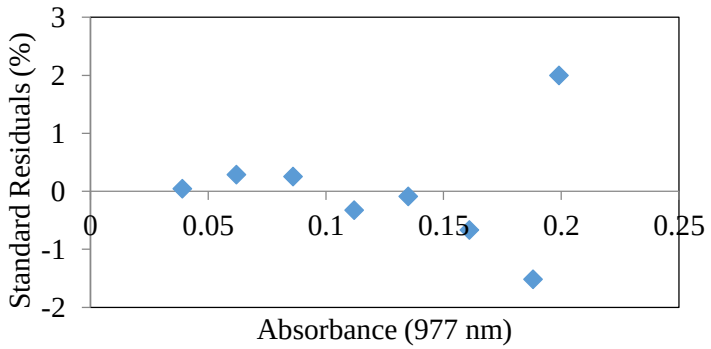


Figure A4. Standard residuals for 977 nm volume measurement assay in regular 96-well plate.

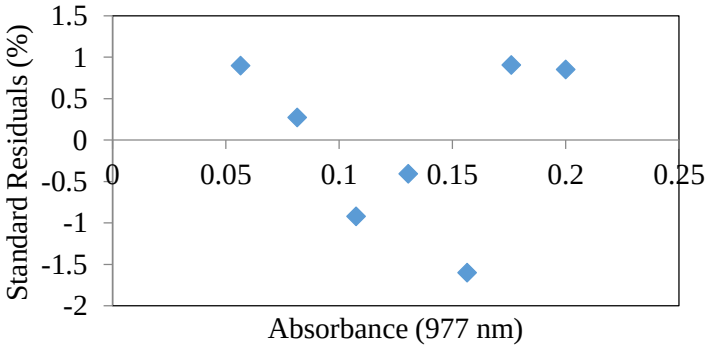


Figure A5. Standard residuals for 977 nm volume measurement assay in half-area 96-well plate.

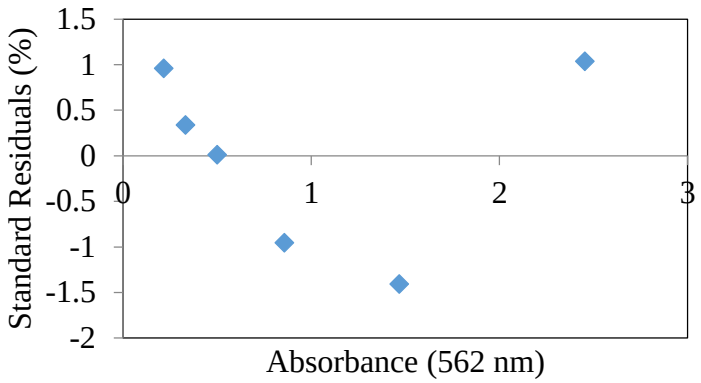


Figure A6. Standard residuals for BCA assay in 96-well plate for high concentrations of BSA protein.

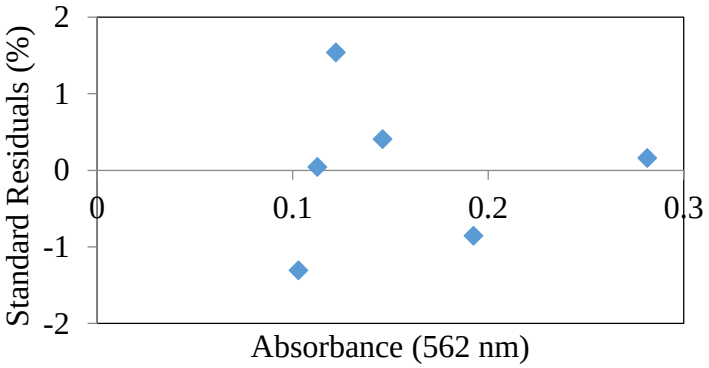


Figure A7. Standard residuals for BCA assay in 96-well plate for low concentrations of BSA protein.

## Appendix C – Summary of hydraulic permeability results

Table A1. Summary of hydraulic permeability results. The slope confidence interval (CI) is used as a measure of the reliability of the slope and it means that there is 95% probability that the real slope value be included in calculated slope ± CI span.

| Well # | Flux/TMP (LMH/kPa) | Permeability ($m \times 10^{12}$) | Slope confidence interval ($m \times 10^{14}$) | $R^2$ |
|---|---|---|---|---|
| 1 | 4.1535 | 1.15375 | 1.234 | 0.9968 |
| 2 | 4.7315 | 1.31431 | 1.118 | 0.9960 |
| 3 | 4.728 | 1.31333 | 0.915 | 0.9966 |
| 4 | 4.0674 | 1.12983 | 0.473 | 0.9968 |
| 5 | 4.4466 | 1.23517 | 0.649 | 0.9969 |
| 6 | 4.8886 | 1.35794 | 0.610 | 0.9972 |
| 7 | 5.0321 | 1.39781 | 0.929 | 0.9963 |
| 8 | 3.6545 | 1.01514 | 1.174 | 0.9993 |
| 9 | 4.2166 | 1.17238 | 4.326 | 0.9972 |
| 10 | 3.3671 | 0.93531 | 2.130 | 0.9996 |
| 11 | 3.9764 | 1.10455 | 2.813 | 0.9997 |
| 12 | 4.0781 | 1.13281 | 2.671 | 0.9999 |
| 13 | 3.9223 | 1.08953 | 2.494 | 0.9998 |
| 14 | 4.0884 | 1.13567 | 2.533 | 0.9999 |
| 15 | 4.5881 | 1.27447 | 2.710 | 0.9997 |
| 16 | 4.5642 | 1.26783 | 3.076 | 0.9992 |

## Appendix D – Technical specifications of syringe pump and pressure transducer

Table A2. PHD ULTRA™ syringe pump specifications.

| | |
|---|---|
| Accuracy | ± 0.35% |
| Reproducibility | ± 0.05% |
| Syringes (Min./Max.) | 0.5 µl / 140 ml |
| Minimum Flow Rate (0.5 µl syringe) | 1.56 pl/min |
| Maximum Flow Rate (140 ml syringe) | 220.97 ml/min |
| Linear Force (Max): | 34 kg (75 lbs) @ 100% Force Selection |
| Drive Motor | 0.9° Stepper Motor |
| Motor Drive Control | Microprocessor with 1/16 microstepping |
| Number of Microsteps per one rev. of Lead Screw | 12,800 |
| Minimum Step Rate | 27.5 sec/µstep |
| Maximum Step Rate | 26 µsec/µstep |
| Minimum Pusher Travel Rate | 0.18 µm/min |
| Maximum Pusher Travel Rate | 190.80 mm/min |
| Mode of Operation | Continuous |

Table A3. Omega PX26-030GV pressure transducer specifications

| | |
|---|---|
| Accuracy | 1% FS[12] |
| Linearity | 1.0% FS BFSL[13] |
| Hysteresis & Repeatability | 0.2% FS |
| Zero Balance | ±1.5 mV |
| Span Tolerance | ±3.0 mV |
| Pressure Range | 0-30 psi |
| Proof Pressure | 60 psi |
| Response Time | 1 millisecond |
| Gage Type | Silicon sensor |
| Wetted Parts | Polyester, Silicon, fluorosilicone |

[12] Full Scale
[13] Best Fit Line